

A GENERAL PSEUDOSPECTRAL FORMULATION OF A CLASS OF
STURM-LIOUVILLE SYSTEMS

A THESIS SUBMITTED TO
THE GRADUATE SCHOOL OF NATURAL AND APPLIED SCIENCES
OF
MIDDLE EAST TECHNICAL UNIVERSITY

BY

HAYDAR ALICI

IN PARTIAL FULFILLMENT OF THE REQUIREMENTS
FOR
THE DEGREE OF DOCTOR OF PHILOSOPHY
IN
MATHEMATICS

SEPTEMBER 2010

Approval of the thesis:

**A GENERAL PSEUDOSPECTRAL FORMULATION OF A CLASS OF
STURM-LIOUVILLE SYSTEMS**

submitted by **HAYDAR ALICI** in partial fulfillment of the requirements for the degree of
Doctor of Philosophy in Mathematics Department, Middle East Technical University
by,

Prof. Dr. Canan Özgen
Dean, Graduate School of **Natural and Applied Sciences**

Prof. Dr. Zafer Nurlu
Head of Department, **Mathematics**

Prof. Dr. Hasan Taşeli
Supervisor, **Mathematics, METU**

Examining Committee Members:

Prof. Dr. Marat U. Akhmet
Mathematics Dept., METU

Prof. Dr. Hasan Taşeli
Mathematics Dept., METU

Prof. Dr. Tanıl Ergenç
Mathematics Dept., Atılım University

Assoc. Prof. Dr. Hakan I. Tarman
Eng. Sci. Dept., METU

Assoc. Prof. Dr. Ömür Uğur
Institute of Applied Mathematics, METU

Date:

I hereby declare that all information in this document has been obtained and presented in accordance with academic rules and ethical conduct. I also declare that, as required by these rules and conduct, I have fully cited and referenced all material and results that are not original to this work.

Name, Last Name: HAYDAR ALICI

Signature :

ABSTRACT

A GENERAL PSEUDOSPECTRAL FORMULATION OF A CLASS OF STURM-LIOUVILLE SYSTEMS

Alici, Haydar

Ph. D., Department of Mathematics

Supervisor : Prof. Dr. Hasan Taşeli

September 2010, 83 pages

In this thesis, a general pseudospectral formulation for a class of Sturm-Liouville eigenvalue problems is constructed. It is shown that almost all, regular or singular, Sturm-Liouville eigenvalue problems in the Schrödinger form may be transformed into a more tractable form. This tractable form will be called here a *weighted equation of hypergeometric type with a perturbation* (WEHTP) since the non-weighted and unperturbed part of it is known as the equation of hypergeometric type (EHT). It is well known that the EHT has polynomial solutions which form a basis for the Hilbert space of square integrable functions. Pseudospectral methods based on this natural expansion basis are constructed to approximate the eigenvalues of WEHTP, and hence the energy eigenvalues of the Schrödinger equation. Exemplary computations are performed to support the convergence numerically.

Keywords: Schrödinger operator, regular and singular Sturm-Liouville eigenvalue problems, pseudospectral methods, equation of hypergeometric type, classical orthogonal polynomials.

ÖZ

STURM-LIOUVILLE SİSTEMLERİNİN BİR SINIFI İÇİN GENEL BİR SANKİ-SPEKTRAL FORMÜLASYON

Alıcı, Haydar

Doktora, Matematik Bölümü

Tez Yöneticisi : Prof. Dr. Hasan Taşeli

Eylül 2010, 83 sayfa

Bu tezde, Sturm-Liouville özdeğer problemlerinin bir sınıfı için genel bir sanki-spektral formülasyon verildi. Schrödinger formundaki neredeyse bütün düzgün ya da tekil Sturm - Liouville özdeğer problemlerinin daha uygun bir forma dönüştürülebileceği gösterildi. Bu formun yalın hali hipergeometrik tip denklem (EHT) olarak bilindiği için yeni form burada perturbe edilmiş ağırlıklı hipergeometrik tip denklem (WEHTP) olarak adlandırılacaktır. Hipergeometrik tip denklemin, karesi integrallenebilir fonksiyonların oluşturduğu Hilbert uzayına baz teşkil eden polinom çözümlerinin olduğu biliniyor. Yeni formun, dolayısı ile orijinal Schrödinger denkleminin, özdeğerlerini sayısal olarak hesaplamak için bu polinom bazları esas alan sanki-spektral metodlar inşa edildi. Metodun yakınsaklığını destekleyen örnek hesaplamalar yapıldı.

Anahtar Kelimeler: Schrödinger operatörü, tekil ve tekil olmayan Sturm-Liouville özdeğer problemleri, sanki-spektral yöntemler, hipergeometrik tipte denklem, klasik dik polinomlar.

To my lovely wife and sweet son

ACKNOWLEDGMENTS

I would like to express my sincere gratitude to my supervisor, Prof. Dr. Hasan Taşeli, for his constant support, precious guidance and encouragement throughout the research. I have always valued his ideas, comments and suggestions.

Next, I would like to thank Assoc. Prof. Dr. Hakan I. Tarman who called my attention to the method by providing the course on “Spectral Methods”.

A special thank goes to Ömür Uğur for editing the manuscript and directioning me in improving the thesis.

I also would like to thank Celalettin Kaya, İbrahim Erkan, Dr. Faruk Polat, Dr. Abdullah Özbekler, Dr. Erdal Karapınar and all my friends who have been helpful, considerate and supporters. Nevertheless, I offer a special thank to Dr. Halil İbrahim Çetin for his valuable helps on the computer implementation of the method, Dr. Ali Sait Demir for his precious friendship throughout my university life, Hüseyin Altundağ for sharing his office, tea, ideas, etc., Rezan Sevinik for accompanying me during the congress held in abroad where I found the chance of presenting my thesis.

I would like to express my appreciation to my wife Yasemin. In the absence of her support and encouragement, this thesis would never have been completed.

I will also never forget the unending support and love my family has provided me all my life.

This research has been supported by a grant from TÜBİTAK, the Scientific and Technical Research Council of Turkey.

TABLE OF CONTENTS

ABSTRACT	iv
ÖZ	v
ACKNOWLEDGMENTS	vii
TABLE OF CONTENTS	viii
LIST OF TABLES	x
LIST OF FIGURES	xii
CHAPTERS	
1 INTRODUCTION	1
2 POLYNOMIALS OF HYPERGEOMETRIC TYPE	12
2.1 Some basic properties of polynomials of hypergeometric type	12
2.1.1 Zeros of polynomials of hypergeometric type	13
2.2 Classical orthogonal polynomials (COPs)	16
2.2.1 Jacobi polynomials	16
2.2.2 Laguerre polynomials	17
2.2.3 Hermite polynomials	18
3 PSEUDOSPECTRAL METHODS	20
3.1 Differentiation matrices	20
3.2 Gauss quadrature rule of integration	22
3.3 Pseudospectral formulation of the WEHTP	24
3.4 Error estimates for spectral methods	27
4 APPLICATION TO THE SCHRÖDINGER EQUATION	34
4.1 The Schrödinger equation over the real line	34
4.2 The Schrödinger equation over the half line	48
4.3 The Schrödinger equation over a finite interval	60

5	CONCLUSION	73
	REFERENCES	77
	VITAE	81

LIST OF TABLES

TABLES

Table 4.1 Several eigenvalues of ADWP for $a_1 = 100$, as a function of a_2 [3].	39
Table 4.2 The effect of c on the accuracy E_0 of an ADWP with $a_1 = 100$ and $a_2 = 0.25$ when $N = 69$ [3].	39
Table 4.3 First few eigenvalues of the MP when $a = 0.02$ and all discrete eigenvalues when $a = 0.2$. The last column includes exact eigenvalues.	41
Table 4.4 First few nearly degenerate states of SDWP by using HPM with $N_{HPM} =$ 140 and optimization parameter $c = 2.05$	42
Table 4.5 First few nearly degenerate states of SDWP by using LPM with $N_{LPM} = 70$ and optimization parameter $c = 2.05$	42
Table 4.6 Improvement of accuracy for E_{100} of the SDWP with respect to N , where $c = 2.6$ [3].	42
Table 4.7 Discrete states of modified Pöschl-Teller potential hole with $m = 10$ by using HPM where $N_{HPM} = 400$ and optimization parameter $c = 1.3$	44
Table 4.8 Discrete states of modified Pöschl-Teller potential hole with $m = 10$ by using LPM where $N_{LPM} = 200$ and optimization parameter $c = 1.3$	44
Table 4.9 Ground state energies of the quartic oscillator $V(x) = x^2 + v_4x^4$, as a function of v_4 [78].	45
Table 4.10 Ground state energies of the sextic oscillator $V(x) = x^2 + v_6x^6$, as a function of v_6 [78].	45
Table 4.11 The effect of parameter c on the truncation size N to calculate the ground state eigenvalue of the sextic oscillator, as v_6 varies, within quadruple precision arithmetic.	46
Table 4.12 Even discrete states of the Gaussian potential $V(x) = -e^{-\delta x^2}$ as δ varies. . .	47

Table 4.13 Odd discrete states of the Gaussian potential $V(x) = -e^{-\delta x^2}$ as δ varies. . . .	48
Table 4.14 The energy eigenvalues $E_{n,\ell}^{(3)}$ of the potential, $V(r) = r^2 + v_4 r^4$, as a function of v_4	52
Table 4.15 Discrete states of the Gaussian potential $V(x) = -e^{-\delta r^2}$ in three-dimension when $l = 0$ as δ varies.	53
Table 4.16 Several eigenvalues of the Airy equation. The last column includes the negatives of first ten zeros of Airy function $\text{Ai}(x)$	54
Table 4.17 Bound states $E_{n,0}^{(3)}$ of Woods-Saxon potential in 3-dimensions when $\ell = 0$ with $N_{wLPM} = 200$ and $c = 30$	55
Table 4.18 Several states of the ECPSC potential in three-dimensions when $Z = 50$, $Z_{as} = 1$ and $\lambda = \mu = 0.025$ as ℓ varies.	57
Table 4.19 Bound energy eigenvalues of the ECSC potential in three-dimensions when $Z = 1$ and $\lambda = 0.05$, as μ varies. The case, $\mu = 0$ corresponds to the Yukawa potential.	58
Table 4.20 Several states of the pure attractive Coulomb potential in three-dimensions when $Z = Z_{as} = 1$ as ℓ varies.	58
Table 4.21 Bound states of the Hulthén screening potential in three-dimensions when $Z = 50$ and $\lambda = 0.025$, as ℓ varies.	60
Table 4.22 Convergence rate of eigenvalues $E_{2n}(0, 10)$ of spheroidal wave equation as n varies [3].	65
Table 4.23 Eigenvalue $E_{101}(m, C^2)$ of spheroidal wave equation while m and C^2 vary.	66
Table 4.24 Several even states of (4.99) as a function of μ	67
Table 4.25 Several eigenvalues of Mathieu differential equation with $q = 1$ [3].	69
Table 4.26 Triple eigenvalues of Coffey-Evans equation with $\nu = 50$, $N = 72$ [3].	69
Table 4.27 Several eigenvalues of (4.115) when $w(x) = 3 + \cos x$	71
Table 4.28 Several eigenvalues of (4.115) when $w(x) = 1 + \cos x$	71
Table 5.1 Comparison with standard CPM for the first eigenvalue of Mathieu equation with $q = 1$ [3].	75

LIST OF FIGURES

FIGURES

Figure 4.1 Ground state and fifth excited state eigenfunctions of the ADWP with $a_1 = 100$ and $a_2 = 0.5$	40
Figure 4.2 Several eigenfunctions of the SDWP by using LPM.	43
Figure 4.3 The eigenfunction $\Psi_2(x)$ of quartic anharmonic oscillator with $v_4 = 0.01$ and $c = 2.1$. Solid line is obtained by spline approximation.	46
Figure 4.4 The eigenfunction $\mathcal{R}_1(r)$ of woods-Saxon potential computed by using $N = 120$ collocation points with several c values.	56
Figure 4.5 ground state eigenfunction of spheroidal wave equation while $m = 1$ and C^2 varies (left) and $C^2 = 10$ and m varies (right).	66
Figure 4.6 Eight eigenfunction of Coffey-Evans equation when $\nu = 50$	70
Figure 4.7 First two eigenfunctions of the Collatz equation in (4.115).	72
Figure 5.1 Number of correct digits versus matrix size N for E_{100} of Mathieu potential in (4.113) with $q=1$, and SDWP in (4.33) [3].	75

CHAPTER 1

INTRODUCTION

Mathematical models of many problems in physics and applied sciences lead to differential eigenvalue problems. The most frequently encountered problem of this type is the celebrated Sturm-Liouville eigenvalue problem

$$Lu(x) = \lambda u(x), \quad x \in (a, b) \quad (1.1)$$

described by the second-order linear formally self-adjoint differential operator

$$L = \frac{1}{w(x)} \left[-\frac{d}{dx} \left(p(x) \frac{d}{dx} \right) + q(x) \right] \quad (1.2)$$

where $p > 0$, p' , q and $w > 0$ are assumed to be real and continuous on the closed interval $[a, b]$. If a and b are finite, boundary conditions are imposed in the form

$$\begin{aligned} \cos \alpha u(a) + \sin \alpha p(a) u'(a) &= 0 \\ \cos \beta u(b) + \sin \beta p(b) u'(b) &= 0 \end{aligned} \quad (1.3)$$

where $\alpha, \beta \in [0, \frac{\pi}{2}]$. In this case, equation (1.1) together with the above boundary conditions comprises the regular Sturm-Liouville system. On the other hand, the problem is called singular, if either the interval (a, b) is unbounded or the functions p , q and w satisfy the conditions stated above on the open interval (a, b) , but at least one of these functions fails to satisfy them at one or both end points.

A scalar λ , for which (1.1) has a nontrivial solution $u(x)$ satisfying the boundary conditions, is called an eigenvalue and $u(x)$ is the corresponding eigenfunction of the problem. Their properties may be summarized in the following proposition whose proof can be found in [20].

Proposition 1.1 *For a regular Sturm-Liouville problem,*

(i) Eigenvalues are real, simple (there is no two linearly independent eigenfunction having the same eigenvalue) and constitute an increasing sequence $\lambda_0 < \lambda_1 < \dots < \lambda_n < \dots$ which tends to ∞ .

(ii) The eigenfunctions u_m and u_n associated with the eigenvalues $\lambda_m \neq \lambda_n$ are orthogonal over the interval (a, b) in the sense that

$$\int_a^b u_m(x)u_n(x)w(x)dx = h_n^2\delta_{mn}$$

where h_n is called normalization constant and δ_{mn} is the Kronocker delta. Moreover, they form a complete orthogonal set of functions. In other words, they form an orthogonal basis in the Hilbert space $L_w^2(a, b)$. Thus, any reasonable function can be expanded into a Fourier series in terms of the set $\{u_m\}_{m=0}^\infty$.

(iii) The eigenfunction u_m has exactly m zeros in the open interval (a, b) . Moreover, the zeros of u_m and u_{m+1} are interlaced, that is, there exist exactly one zero of u_m between two consecutive zeros of u_{m+1} .

Many of these problems can not be solved explicitly, and hence requires well designed, i.e., accurate, cheap and efficient numerical algorithms to obtain approximate solutions. Most commonly used numerical schemes may be classified into two main groups, namely, shooting and matrix methods.

Basic idea behind the shooting method is to reduce the boundary value problem (1.1) to an initial value problem and solve it over the interval (a, b) for a sequence of trial λ values which are adjusted until the boundary conditions at both ends can be satisfied simultaneously, at which point there is an eigenvalue [61]. The simplest such method is shooting from one end point to the other, say a to b . This means that one chooses initial conditions, for instance,

$$u(a) = -\sin \alpha, \quad p(a)u'(a) = \cos \alpha \tag{1.4}$$

which satisfy the boundary condition at a . Then the solution $u_a(x; \lambda)$ of the resulting initial value problem is used to construct the so-called *mis-distance* or *mis-match* function which measures the deviation of $u_a(b; \lambda)$ from the boundary condition at b . Thus, the natural choice for the mis-match function is

$$D(\lambda) = \cos \beta u_a(b; \lambda) + \sin \beta p(b)u'_a(b; \lambda) \tag{1.5}$$

whose zeros are the eigenvalues of the original problem which may be found by standard methods [61].

Another alternative is to shoot from two ends to some interior matching point $c \in (a, b)$. In this case, in addition to the left-hand solution $u_a(x; \lambda)$, similarly, one constructs right-hand solution $u_b(x; \lambda)$ by using the boundary condition at b and looks for a constant $\lambda := \lambda_0$ for which $u_a(c; \lambda_0) = u_b(c; \lambda_0)$. However, it is possible for some other λ values to have $u_a(c; \lambda) = u_b(c; \lambda)$ by rescaling the right-hand solution. But in this case, the obtained first order derivatives of the left- and right-hand solutions do not agree at the matching point any more. Thus, for λ to be an eigenvalue of the problem, the derivative values u' should match at c , as well as the function values u [49]. Therefore, the suitable mis-match function appears to be the Wronskian of u_a and u_b at the matching point c

$$D(\lambda) = \begin{vmatrix} u_a(c; \lambda) & u_b(c; \lambda) \\ u'_a(c; \lambda) & u'_b(c; \lambda) \end{vmatrix} \quad (1.6)$$

which is zero only when λ is an eigenvalue [61].

It is pointed out in [61] that, numerically, for some choices of c , computation of $D(\lambda)$ may be more complicated than the others. There are also some other disadvantages of the shooting methods, for instance, oscillating character of the mis-distance function makes it difficult to find the roots, and hence, the eigenvalues of the problem. Moreover, generally shooting methods are not able to determine the index of the approximated eigenvalue. However, these complications can be overcome by using the Prüfer transformations [61]

$$u = S^{-\frac{1}{2}} r \sin \theta, \quad pu' = S^{\frac{1}{2}} r \cos \theta \quad (1.7)$$

which reduce the Sturm-Liouville eigenvalue problem to an equivalent, nonlinear first order boundary value problems

$$2 \frac{r'}{r} = \left(\frac{S}{p} - \frac{\lambda w - q}{S} \right) \sin 2\theta - \frac{S'}{S} \cos 2\theta \quad (1.8)$$

$$\theta' = \frac{S}{p} \cos^2 \theta + \frac{\lambda w - q}{S} \sin^2 \theta + \frac{S'}{S} \sin \theta \cos \theta \quad (1.9)$$

for $r = r(x; \lambda)$ and $\theta = \theta(x; \lambda)$ which are known as the amplitude and Prüfer (or phase) angle, respectively. Here $S > 0$ is a scaling function which is introduced for numerical reasons. If $S = 1$, they are simply called Prüfer transformations, otherwise they take on the name scaled Prüfer transformations. Eigenvalue problem can be defined by the θ equation and once it

is solved, r can be obtained by a quadrature [61]. Boundary conditions in (1.3) lead to the conditions

$$\theta(a) = \gamma_a, \quad \theta(b) = \gamma_b \quad (1.10)$$

for θ , where

$$\tan \gamma_a = -\tan \alpha S(a), \quad \tan \gamma_b = -\tan \beta S(b) \quad (1.11)$$

which determine γ_a and γ_b only up to a constant multiple of π . The key point in Prüfer transformations is that each appropriate choice of this multiple specifies precisely one eigenvalue [61].

If the scaling function S is independent of λ at the matching point c and the end points a and b , then γ_a and γ_b are also independent of λ . In this case the scaled Prüfer mis-match function is defined as

$$D(\lambda) = \theta_a(c; \lambda) - \theta_b(c; \lambda) \quad (1.12)$$

where $\theta_a(x; \lambda)$ and $\theta_b(x; \lambda)$ are the solutions of (1.9) satisfying

$$\theta_a(a; \lambda) = \gamma_a \in [0, \pi), \quad \theta_b(b; \lambda) = \gamma_b \in (0, \pi]. \quad (1.13)$$

Then it is proved in [61] that the n th eigenvalue is the unique value such that

$$D(\lambda_n) = n\pi, \quad n = 0, 1, 2, \dots \quad (1.14)$$

Moreover, $D(\lambda)$ is strictly increasing on the real line and bounded below.

For each value of the mismatch function $D(\lambda)$ one needs to integrate (1.9). The numerical reason behind the scaling function S is to reduce the cost of integrations and allow the code to take as large step sizes as possible. Nevertheless, choosing an appropriate scaling function is not a trivial work. To this end, several researchers designed modified Prüfer transformations, for example, Bailey [4, 5] have chosen the scaling function as $S = n\pi/l$ where n is the eigenvalue index and l is approximately the length of interval on which $\lambda w - q$ is positive and implemented it in the code SLEIGN [7]. See also SLEIGN2 [6] which is based on the ideas and methods of the original SLEIGN code. Pryce [60] have chosen it as a piecewise linear function to keep some quantities in (1.9) such as $S/p - |q|/S$ and S'/S small and put it into practice in the NAG library codes D02KDF and D02KEF. Equation (1.9) becomes stiff at some parts of the interval (a, b) where $\lambda w - q \ll 0$ [61]. Both SLEIGN and NAG codes use explicit Runge-Kutta method to integrate (1.9) thus they suffer from stepsize restriction because of stiffness especially when solving for large eigenvalues [49].

Another subclass of shooting methods for numerical solution of the Sturm-Liouville eigenvalue problems is the coefficient approximation methods. Basic idea behind them is to replace the coefficients p , q and w of the equation by low degree polynomials and then solve the approximating problem. Pruess examined piecewise constant polynomial case and it is implemented in the code SLEDGE by Pruess and Fulton [59]. There is also another code, called SL02F, due to Marletta and Pryce [53, 54] which also uses Pruess method. The method relatively uninfluenced by the stiffness however it is difficult to obtain higher order methods [49].

Richardson extrapolation is natural if the coefficients are sufficiently smooth but for the piecewise perturbation methods higher order methods can easily be constructed. In these methods, like the coefficient approximation methods, coefficients are replaced by piecewise polynomials so that the resulting equation has closed form solution. The only difference is that they use perturbation theory to approximate the difference between the solution of the approximating and original problem [49]. However, they are designed for the numerical treatment of the regular Sturm-Liouville problems especially in the Schrödinger form [43, 44, 45]. Later on Ledoux et al. collected some higher order piecewise constant perturbation methods in a MATLAB package MATSLISE which also handles some singular cases such as the Schrödinger equation with distorted Coulomb potential [50]. This is done by truncating the infinite domain and adapting new boundary conditions. However, the process of choosing a suitable cutoff value is not straightforward and generally depends on the problem and index of the eigenvalue to be approximated. Moreover, boundary conditions are replaced by artificial ones which does not reflect the exact behavior of the eigenfunction.

Another important class of numerical methods for the approximation of differential equations includes the matrix methods. Main objective of these methods is to approximate the continuous derivative operator by its discrete analog on a certain set of points called grid, mesh or nodal points and then use it to solve differential equations approximately. Accordingly, equation (1.1) is reduces to a matrix eigenvalue problem

$$\mathbf{L}_N \mathbf{u}_N = \lambda \mathbf{u}_N \quad (1.15)$$

where the matrix \mathbf{L}_N and the vector \mathbf{u}_N are the discrete representation of the operator L and approximate solutions at the grid points, respectively. Here N is called approximation or truncation order. Discrete representation may differ from a matrix method to another depending

on the used basis functions and the choice of the grid points. The three main subclasses of matrix methods are finite difference, finite element and spectral methods. Most of the matrix methods available in the literature are belong to one of these three subclasses or to a combination of these subclasses.

In a finite difference method each derivative in L is replaced by a suitable difference operator. For instance, first derivative operator may be replaced by central differences

$$\frac{d}{dx}u(x) = \frac{f(x+h) - f(x-h)}{2h} \quad (1.16)$$

where h is a small spacing between the nodal points. This means that the interval (a, b) is divided into a finite number of equidistant mesh points. Alternatively, (1.16) may be derived in a different way [82]. First, one constructs the local interpolation polynomial

$$p_j(x) = u_{j-1}a_{-1}(x) + u_j a_0(x) + u_{j+1}a_1(x) \quad (1.17)$$

which is the unique polynomial of degree less than or equal to two with $p_j(x_{j-1}) = u_{j-1}$, $p_j(x_j) = u_j$ and $p_j(x_{j+1}) = u_{j+1}$ for fixed j . Here the coefficient functions are given by $a_{-1}(x) = (x - x_j)(x - x_{j+1})/2h^2$, $a_0(x) = -(x - x_{j-1})(x - x_{j+1})/h^2$ and $a_1(x) = (x - x_{j-1})(x - x_j)/2h^2$. Then differentiation and evaluation of (1.17) at the node $x = x_j$ leads to (1.16). As is seen the method approximates derivatives by low degree local polynomials, therefore they are exact for polynomials of low degree. They usually generate banded derivative matrices that are easy to implement but they are relatively low in accuracy especially for higher eigenvalues.

The idea behind the finite element methods is similar to that of finite differences. However, the approximations by piecewise polynomials of low degree are performed in subintervals which can easily be chosen to fit the geometry of the problem. Thus, they are useful for solving problems with complex geometry. Since a few number of basis functions are used in each subinterval their matrix representations are sparse. Similar to finite differences accuracy get worse for higher eigenvalues.

In spectral methods approximations are defined in terms of a truncated series expansion

$$u_N(x) = \sum_{k=0}^N u_k \phi_k(x) \quad (1.18)$$

where the trial or basis functions $\phi_k(x)$ are given and the expansion coefficients u_k must be determined. The chosen trial functions are orthogonal in the sense that

$$(\phi_k, \phi_l)_\rho = \int_a^b \phi_k(x)\phi_l(x)\rho(x)dx = h_k \delta_{kl}, \quad k, l = 0, 1, \dots, N \quad (1.19)$$

with respect to some positive weight function $\rho(x)$, where h_k is referred to as normalization constant and δ_{kl} is the Kronecker's delta. Now we introduce the residual

$$R_N = (L - \lambda)u_N \quad (1.20)$$

which should be forced to be zero in an approximate sense. This is done by setting the scalar product

$$(R_N, \psi_i)_{\bar{\rho}} = \int_a^b R_N(x) \psi_i(x) \bar{\rho}(x) dx = 0, \quad i = 0, 1, \dots, N \quad (1.21)$$

to zero, where $\psi_i(x)$ are called test functions and the weight $\rho(x)$ is associated with the method and trial functions $\phi_k(x)$ [14]. The choice of the test functions and the weight defines the method. For example, the Galerkin type method corresponds to the case where the test functions ψ_i are the same as the trial functions ϕ_i and $\bar{\rho}$ is the weight associated with the orthogonality of the trial functions, that is $\bar{\rho} = \rho$. The traditional Galerkin method applies when the trial functions ϕ_k in the expansion (1.18) satisfy the homogeneous boundary conditions.

Then, according to (1.21) the Galerkin equations are

$$(R_N, \phi_i)_{\rho} = (Lu_N - \lambda u_N, \phi_i)_{\rho} = 0, \quad i = 0, 1, \dots, N, \quad (1.22)$$

or else, replacing u_N by its expansion (1.18),

$$\sum_{k=0}^N (L\phi_k, \phi_i)_{\rho} u_k = \lambda \sum_{k=0}^N (\phi_k, \phi_i)_{\rho} u_k, \quad i = 0, \dots, N. \quad (1.23)$$

The scalar products $\mathbf{B} = (L\phi_k, \phi_i)_{\rho}$, $k = 0, 1, \dots, N$ are evaluated using the properties of the trial functions, in particular their orthogonality, leading to a square matrix of size $N + 1$. It is clear from (1.19) that the scalar product $\mathbf{D} = (\phi_k, \phi_i)_{\rho}$ on the right hand side produces diagonal matrix which becomes identity when the normalized trial functions $\frac{1}{\sqrt{h_k}}\phi_k$ are used. Therefore, the first $N + 1$ approximate eigenvalues of (1.1) are given by those of the matrix $\mathbf{L} = \mathbf{D}^{-1}\mathbf{B}$ where \mathbf{B} is full and \mathbf{D} is diagonal or even better, identity matrices. If the operator L is self adjoint then the resulting matrix \mathbf{B} , and hence \mathbf{L} , is symmetric. In this case, the Galerkin approach is conventionally called Rayleigh-Ritz method. If it is not possible to evaluate the inner product $(L\phi_k, \phi_i)_{\rho}$ in closed-form, one has to use numerical integration and this scheme is called the Galerkin with numerical integration.

Note in the above case that the number of Galerkin equations is exactly $N + 1$. This is because the boundary conditions are satisfied by the trial functions. When this is not the case, the method may be applied by constructing a new basis from the existing one satisfying the

boundary conditions. But the new basis may not be orthogonal, so that this approach is not much used and generally one prefers the so-called *tau method*. It is similar to Galerkin method but none of the test functions need to satisfy the boundary conditions. Therefore, a supplementary equations arising from boundary conditions are needed. For a detailed discussion see Gottlieb and Orszag [34] and Canuto et al. [14].

Another spectral type method is the collocation or pseudospectral method in which the test functions

$$\psi_i = \delta(x - x_i) \quad (1.24)$$

are shifted Dirac delta functions centered at the so-called collocation points $x_i \in [a, b]$ and the weight $\bar{\rho} = 1$ is chosen to be unity. From (1.21) and (1.24) we simply get

$$R_N(x_i) = 0 \quad (1.25)$$

by using the fundamental property

$$\int_a^b R_N(x) \delta(x - x_i) dx = R_N(x_i), \quad x_i \in (a, b) \quad (1.26)$$

of the Dirac delta function. Therefore, in the collocation method, the residual is exactly zero at certain points whereas in the Galerkin type method the residual is zero in the mean [14]. Among the spectral methods, pseudospectral methods are the easiest to implement [27].

Most spectral methods use classical orthogonal polynomials (COPs) as a basis set. Shizgal [68] introduced a relatively new spectral method called quadrature discretization method and later on authors [18, 51] use it to solve the Schrödinger equation for several potentials. The method may be seen as the generalization of the pseudospectral methods based on COPs. Main idea behind the method is to utilize a non-classical basis set to approximate the solution of differential equations. To this end, by using the well-known three term recurrence relation they construct new polynomials which are orthogonal with respect to some specific weight function. In order to determine the coefficients of the recursion numerically, they used discretized Stieltjes procedure which is proposed by Gautschi [30]. This procedure computes the coefficients by a quadrature. However, if the domain of integration is too large, to avoid numerical overflow, suitable cutoff is needed for accuracy and stability. Moreover, the choice of the weight function is very important so that the method converges rapidly which depends on the physical nature of the problem under consideration [17].

For a spectral method the error between the approximate and exact solution decrease very rapidly. This remarkable behavior is called spectral accuracy. However, in a finite difference scheme error decays algebraically. The reason is that, in contrast to local polynomial (low degree) basis of finite differences, spectral methods use global (high degree) basis. That is, to compute the derivative at a given point finite differences use information related to a small neighbourhood of the point whereas in spectral methods all collocation points are applied in the computation [82]. Consequently, resulting matrices are banded in finite difference schemes whereas they are full for spectral methods. Nevertheless, when the same accuracy is desired, matrix sizes of the former are larger when compared to the latter, or sometimes finite differences can not reach the desired accuracy at all.

One of the most attractive and interesting problem of physical and practical interest is the one dimensional time independent Schrödinger equation

$$\mathcal{H}\Psi(x) = E\Psi(x) \quad (1.27)$$

described by the Hamiltonian

$$\mathcal{H} = -\frac{d^2}{dx^2} + V(x), \quad x \in (\bar{a}, \bar{b}), \quad -\infty \leq \bar{a} < \bar{b} \leq \infty \quad (1.28)$$

where $V(x)$ is a quantum mechanical potential. Note that (1.28) is the special case of (1.2) with $p(x) = w(x) = 1$ and $q(x) = V(x)$. It is also possible to transform (1.1) having arbitrary coefficient functions $p > 0$, q , $w > 0$ into (1.27). This is done by the help of so-called Liouville's transformations [61] which reduce the classical Sturm-Liouville eigenvalue problems into the Schrödinger (or Liouville normal) form. In general, because of its simple structure, authors would rather approximate the Sturm-Liouville eigenvalue problems in the Schrödinger form. However, in this thesis we transform almost all, regular or singular, Sturm-Liouville problems in the Schrödinger form having square integrable solutions, into a more complicated but beneficial form

$$\sigma(\xi)y'' + \tau(\xi)y' + \nu(\xi)y = -\lambda r(\xi)y, \quad \xi \in (a, b) \subseteq \mathbb{R} \quad (1.29)$$

which will be called *the weighted equation of hypergeometric type with a perturbation* (WEHTP). Here, $\sigma(\xi)$ and $\tau(\xi)$ are polynomials of degrees at most two and one, respectively, and λ is a parameter. The form in (1.29) is closely related to the equation of hypergeometric type (EHT)

$$\sigma(\xi)y'' + \tau(\xi)y' = -\lambda^{(0)}y, \quad \xi \in (a, b) \subseteq \mathbb{R} \quad (1.30)$$

in which $v(\xi) \equiv 0$ and $r(\xi) \equiv 1$. The functions $v(\xi)$ and $r(\xi) > 0$ may, therefore, be regarded as a perturbation and weight, respectively. When $r(\xi) \equiv 1$ we might call (1.29) as an equation of hypergeometric type with a perturbation (EHTP).

It is known that the COPs are the solutions of EHT for specific values of $\lambda^{(0)}$, which form a basis for the Hilbert space $L^2_\rho(a, b)$ of square integrable functions [58]. Pseudospectral methods based on Jacobi (e.g. Chebyshev and Legendre) polynomials $P_n^{(\alpha, \beta)}(\xi)$ of degree n of order $\alpha > -1$, $\beta > -1$ are suitable for bounded domains and can not approximate the problem defined over an unbounded domain directly. Either they should use domain truncation followed by artificial boundary conditions [32, 66] or map the unbounded domain into a bounded one [13, 19] to handle the problem. Another alternative is the use of mapped Jacobi polynomials, see for example [37, 65, 67, 84]. Pseudospectral methods based on Hermite polynomials $H_n(\xi)$ of degree n and Laguerre polynomials $L_n^\gamma(\xi)$ of degree n and order $\gamma > -1$ are some of the natural choices for the problems over an unbounded domains.

The most widely used pseudospectral methods are Chebyshev ($\alpha = \beta = -\frac{1}{2}$) and Legendre ($\alpha = \beta = 0$) for bounded and Hermite and Laguerre ($\gamma = 0$) for unbounded domains. However, for specific problems some other choices of the parameters α , β , and γ may generate more accurate results and converge faster. The first advantage of new formulation (1.29) is that the WEHTP gives the possibility of deciding which polynomial class and the associated parameter(s) are the most suitable as a basis set for (1.27) with a prescribed potential $V(x)$ and an interval (a, b) .

Moreover, during the specific transformations on both independent and dependent variables, boundary conditions or asymptotic boundary conditions at infinity are automatically satisfied so that we don't have to impose any information related to boundary conditions as other methods do.

It is pointed out above that the COPs are the solutions of the EHT. Thus, they comprise the most natural expansion basis for the solution of the WEHTP since it can be seen as the perturbation over the EHT.

Therefore, the aim of the thesis is to construct unified pseudospectral formulation of the WEHTP, and hence the Schrödinger equation, in its full generality, based on any polynomial solutions of the EHT including every possible selection of $\sigma(\xi)$ and $\tau(\xi)$. This formulation leads to

a unified symmetric matrix representation of the Schrödinger equation defined over any subset of the real line for a variety of quantum mechanical potentials. Closed-form expression for the matrix elements are provided which only necessitates the knowledge of collocation points and the known coefficients $\sigma(\xi)$, $\tau(\xi)$ and $r(\xi)$ of the WEHTP.

Accordingly, in Chapter 2, we review some basic properties of polynomials of EHT. Chapter 3 is concerned with the construction of pseudospectral differentiation matrices, general pseudospectral formulation of the WEHTP and the review of some approximation results related to spectral methods. Chapter 4 contains the application of the pseudospectral formulation to mainly the Schrödinger type eigenvalue problems for numerical analysis. Finally, Chapter 5 concludes the thesis by discussing both the advantages and disadvantages of the method.

CHAPTER 2

POLYNOMIALS OF HYPERGEOMETRIC TYPE

In this chapter we review some basic and remarkable properties of the EHT that are necessary for the pseudospectral formulation of the WEHTP. Here, we present the results without their proofs and refer the reader to Nikiforov and Uvarov [58] for more about the special functions of mathematical physics.

2.1 Some basic properties of polynomials of hypergeometric type

Equation (1.30) can be written in the Sturm-Liouville or self adjoint form

$$\frac{d}{d\xi} \left[\sigma(\xi) \rho(\xi) \frac{dy}{d\xi} \right] + \lambda^{(0)} \rho(\xi) y = 0 \quad (2.1)$$

where ρ is a function satisfying the separable Pearson equation

$$\frac{d}{d\xi} [\sigma(\xi) \rho(\xi)] = \tau(\xi) \rho(\xi). \quad (2.2)$$

All derivatives of the functions of the hypergeometric type are also functions of the hypergeometric type which can easily be shown by differentiating (1.30) successively. This fact can be used to show that the EHT has polynomial solutions, say $y(\xi) = p_n(\xi)$, of degree n for specific values of $\lambda^{(0)}$ satisfying

$$\lambda^{(0)} := \lambda_n^{(0)} = -n \left[\tau' + \frac{1}{2}(n-1)\sigma'' \right], \quad n = 0, 1, \dots \quad (2.3)$$

These polynomial solutions are characterized by the celebrated Rodrigues formula

$$p_n(\xi) = \frac{K_n}{\rho(\xi)} \frac{d^n}{d\xi^n} [\sigma^n(\xi) \rho(\xi)] = k_n \xi^n + k'_n \xi^{n-1} + \dots \quad (2.4)$$

where k_n and k'_n are the coefficient of the leading and subleading terms, and K_n denotes a renormalization constant which depends on the standardization.

Orthogonality of the polynomials of the hypergeometric type may be summarized in the following theorem.

Theorem 2.1 *Let the coefficients of the EHT be such that*

$$\sigma(\xi)\rho(\xi)\xi^k \Big|_{\xi=a,b} = 0, \quad k = 0, 1, \dots \quad (2.5)$$

at the boundaries of interval (a, b) . Then the polynomials $p_n(x)$ of the hypergeometric type having the real argument ξ , corresponding to the different values of $\lambda^{(0)} = \lambda_n^{(0)}$ in (2.3) are orthogonal on (a, b) in the sense that

$$\int_a^b p_m(\xi)p_n(\xi)\rho(\xi)d\xi = h_n^2\delta_{mn} \quad (2.6)$$

where $\rho(\xi)$ is now called the weighting function, δ_{mn} is the Kronecker delta and

$$h_n = \left(\int_a^b p_n^2(\xi)\rho(\xi)d\xi \right)^{1/2} \quad (2.7)$$

is the normalization constant or L^2_ρ norm of the polynomial $p_n(\xi)$.

2.1.1 Zeros of polynomials of hypergeometric type

Moreover, $p_n(\xi)$ is orthogonal to every polynomial of lower degree [58] which can be used to prove the following theorem.

Theorem 2.2 *There exist exactly n real and distinct zeros ξ_i , $i = 1, 2, \dots, n$ of the polynomial $p_n(\xi)$ lying in the interval (a, b) .*

On the other hand, for each orthogonal polynomial there exist a finite sum

$$\sum_{k=0}^n \frac{1}{h_k^2} p_k(\xi)p_k(\eta) = \frac{1}{h_n^2} \frac{k_n}{k_{n+1}} \frac{1}{\xi - \eta} \begin{vmatrix} p_{n+1}(\xi) & p_{n+1}(\eta) \\ p_n(\xi) & p_n(\eta) \end{vmatrix} \quad (2.8)$$

which is known as Darboux-Christofel formula [58]. The following theorem, notifying the location of zeros of p_n , may be proved with the help of Darboux-Christofel formula.

Theorem 2.3 *The zeros of $p_n(\xi)$ and $p_{n+1}(\xi)$ are interlaced.*

This means that, the roots of p_{n+1} alternate with those of p_n , if they are sorted in ascending order. In another words, there exist a zero of p_n between two consecutive zeros of p_{n+1} , and vice-versa.

Under certain conditions any three functions of the hypergeometric type are connected by a linear relation [58]. Here we present two such relations. The first one is the recurrence relation for the three consecutive orthonormal polynomials $\psi_n(\xi) = \frac{1}{h_n} p_n(\xi)$ of hypergeometric type.

Theorem 2.4 [71, 3] *The following relation*

$$A_n \psi_{n+1}(\xi) + (B_n - \xi) \psi_n(\xi) + A_{n-1} \psi_{n-1}(\xi) = 0, \quad n = 1, 2, \dots \quad (2.9)$$

holds for any three consecutive orthonormal polynomials with $\psi_{-1}(\xi) = 0$, $\psi_0(\xi) = 1/h_0$, where the coefficients

$$A_n = \frac{k_n}{k_{n+1}} \frac{h_{n+1}}{h_n} \quad \text{and} \quad B_n = \frac{k'_n}{k_n} - \frac{k'_{n+1}}{k_{n+1}} := \eta_{n-1} - \eta_n \quad (2.10)$$

are given in terms of the normalization constant, leading and subleading terms of polynomials of hypergeometric type.

Actually, these coefficients can be identified completely by means of the coefficients in the EHT. Indeed, the ratios k_{n+1}/k_n and h_{n+1}/h_n are expressible as

$$\frac{k_{n+1}}{k_n} = -\frac{K_{n+1}}{K_n} \frac{\lambda_{2n}^{(0)} \lambda_{2n+1}^{(0)}}{2(2n+1) \lambda_n^{(0)}} \quad (2.11)$$

and

$$\left(\frac{h_{n+1}}{h_n} \right)^2 = 4 \left(\frac{k_{n+1}}{k_n} \right)^2 \frac{\lambda_n^{(0)}}{\lambda_{2n}^{(0)} \lambda_{2n+2}^{(0)}} \left[(n+1)^2 \sigma(0) - (n+1) \eta_n \sigma'(0) + \frac{1}{2} \eta_n^2 \sigma'' \right] \quad (2.12)$$

where the parameter η_n , that also appears in B_n , is given by

$$\frac{k'_n}{k_n} = \eta_{n-1} = n \left[\frac{\tau(0) + (n-1) \sigma'(0)}{\tau' + (n-1) \sigma''} \right] \quad (2.13)$$

whose proofs can be found in [71].

Actually, the recursions in (2.11) and (2.12) can be solved to obtain explicit representations for

$$k_n = (-1)^n 2K_n \frac{n!}{(2n)!} \prod_{m=n}^{2n-1} \lambda_m^{(0)}, \quad n = 1, 2, \dots \quad (2.14)$$

with $k_0 = 1$ and

$$h_n^2 = \frac{2\mu_0}{\lambda_{2n}^{(0)}} \left(\tau' h_0 2^n K_n \frac{n!}{(2n)!} \right)^2 \prod_{m=1}^{n-1} \frac{(\lambda_{2m+1}^{(0)})^2}{\lambda_m^{(0)}} \mu_m, \quad n = 1, 2, \dots \quad (2.15)$$

where $h_0^2 = \int_a^b \rho(\xi) d\xi$ and $\mu_m = \left[(m+1)^2 \sigma(0) - (m+1) \eta_m \sigma'(0) + \frac{1}{2} \eta_m^2 \sigma'' \right]$ for $m \in \mathbb{N}$. While solving for the leading coefficient k_n and normalization constant h_n^2 , a special care should be spent for $n = 0$ where the recursions are undetermined. Thus, one should remember (2.3) and look at the limiting case when $n \rightarrow 0$.

The second recurrence is known as the *differential-difference relation* relating the derivative of a polynomial of hypergeometric type with itself and that of degree one less. It is given in [58] for unnormalized polynomials but here we state the relation for orthonormal polynomials of hypergeometric type.

Theorem 2.5 *The relation*

$$\frac{1}{C_{2n}} \sigma(\xi) \psi_n'(\xi) = \left[B_n - \xi - \frac{C_n}{C_{2n} C_{2n+1}} (n \sigma'(\xi) + \tau(\xi)) \right] \psi_n(\xi) + A_{n-1} \psi_{n-1}(\xi) \quad (2.16)$$

$n = 1, 2, \dots$, holds for any two consecutive orthonormal polynomials where $\psi_{-1}(\xi) = 0$ and $\psi_0(\xi) = 1/h_0$. The coefficient $C_n = \frac{\lambda_n^{(0)}}{n}$, while A_n and B_n are as in the previous theorem.

On the other hand, recursion (2.9) may, possibly, be used to determine the zeros of $\psi_n(\xi)$ and therefore those of $p_n(\xi)$. Actually, running recursion (2.9) over the range $n = 0, 1, \dots, N$ we obtain an inhomogeneous linear algebraic system $(\mathbf{R} - \xi \mathbf{I})\mathbf{t} = \mathbf{b}$, or in matrix-vector form

$$\begin{bmatrix} B_0 - \xi & A_0 & & & 0 \\ A_0 & B_1 - \xi & A_1 & & \\ & A_1 & B_2 - \xi & \ddots & \\ & & \ddots & \ddots & A_{N-1} \\ 0 & & & A_{N-1} & B_N - \xi \end{bmatrix} \begin{bmatrix} \psi_0(\xi) \\ \psi_1(\xi) \\ \vdots \\ \psi_{N-1}(\xi) \\ \psi_N(\xi) \end{bmatrix} = \begin{bmatrix} 0 \\ 0 \\ \vdots \\ 0 \\ -A_N \psi_{N+1}(\xi) \end{bmatrix} \quad (2.17)$$

The right-hand side is a $N + 1$ vector with only one nonzero component. Therefore, if we require $\psi_{N+1}(\xi) = 0$ or, equivalently, $p_{N+1}(\xi) = 0$ then the system reduces to a standard eigenvalue problem $\mathbf{R}\mathbf{t} = \xi\mathbf{t}$ with the eigenvalue parameter ξ , which provides us the roots ξ_i , $i = 0, 1, \dots, N$ of $p_{N+1}(\xi)$ as required [3].

Since the eigenvector associated to each eigenvalue of \mathbf{R} is unique up to a constant factor, the m^{th} computed eigenvector $\mathbf{v}^m = [v_0^m, v_1^m, \dots, v_{N-1}^m, v_N^m]^T$ of the matrix \mathbf{R} associated to the

eigenvalue ξ_m is a constant multiple of $\mathbf{t}^m = [\psi_0(\xi_m), \psi_1(\xi_m), \dots, \psi_{N-1}(\xi_m), \psi_N(\xi_m)]^T$, that is $\mathbf{v}^m = a\mathbf{t}^m$. The value of a can be determined by considering the first entries v_0^m and $\psi_0(\xi_m)$ of the eigenvectors \mathbf{v}^m and \mathbf{t}^m , respectively, since $\psi_0(\xi) = 1/h_0$ is a constant polynomial and hence, we obtain $a = h_0 v_0^m$.

Therefore, the values $\{\psi_n(\xi_m)\}$ for $n = 0, 0, \dots, N$ of the orthonormal polynomials at the zeros of $\psi_{N+1}(\xi)$ may be computed as

$$\begin{bmatrix} \psi_0(\xi_m) \\ \psi_1(\xi_m) \\ \vdots \\ \psi_{N-1}(\xi_m) \\ \psi_N(\xi_m) \end{bmatrix} = \frac{1}{h_0 v_0^m} \begin{bmatrix} v_0^m \\ v_1^m \\ \vdots \\ v_{N-1}^m \\ v_N^m \end{bmatrix} \quad (2.18)$$

in terms of the computed eigenvector \mathbf{v}^m of tridiagonal symmetric matrix \mathbf{R} .

2.2 Classical orthogonal polynomials (COPs)

Excluding few degenerate cases every EHT can be put into three canonical forms in which $\sigma(\xi) = 1 - \xi^2$, ξ and 1 by linear and scaling transformations which lead to the well-known Jacobi, Laguerre and the Hermite polynomials, respectively. Keeping in mind that $\tau(\xi)$ is at most linear, solving (2.2), up to constant multiplier, we find that $\rho(\xi) = (1 - \xi)^\alpha(1 + \xi)^\beta$, $\xi^\gamma e^{-\xi}$ and $e^{-\xi^2}$, according to the descending degrees of $\sigma(\xi)$ [58]. In this section, some important and requisite properties of COPs will be outlined.

2.2.1 Jacobi polynomials

Let $\sigma(\xi) = 1 - \xi^2$ and $\rho_{\alpha,\beta}(\xi) = (1 - \xi)^\alpha(1 + \xi)^\beta$ in the differential equation (2.1). Then from (2.2), $\tau(x) = -(\alpha + \beta + 2)\xi + \beta - \alpha$ and from (2.3) $\lambda_n^{(0)} = n(n + \alpha + \beta + 1)$. The corresponding polynomials are denoted and defined by the Rodriguez formula in (2.4)

$$P_n^{(\alpha,\beta)}(\xi) = \frac{(-1)^n}{2^n n!} (1 - \xi)^{-\alpha} (1 + \xi)^{-\beta} \frac{d^n}{d\xi^n} [(1 - \xi)^{n+\alpha} (1 + \xi)^{n+\beta}] \quad (2.19)$$

where $K_n = \frac{(-1)^n}{2^n n!}$ is chosen for historical reasons. It is clear from (1.30) that Jacobi polynomials satisfy the differential equation

$$(1 - \xi^2)y'' + [\beta - \alpha - (\alpha + \beta + 2)\xi]y' + n(n + \alpha + \beta + 1)y = 0. \quad (2.20)$$

Orthogonality condition in (2.5) is satisfied when $a = -1$ and $b = 1$ provided $\alpha > -1$ and $\beta > -1$. Thus, the Jacobi polynomials are orthogonal over the interval $(-1, 1)$ in which the real and distinct zeros lie. The leading coefficient of the Jacobi polynomials

$$k_n = \frac{1}{2^n n!} (n + \alpha + \beta + 1)_n \quad (2.21)$$

may be computed from (2.14), where

$$(a)_m = a(a+1)\dots(a+m-1) = \frac{\Gamma(a+m)}{\Gamma(a)}, \quad (a)_0 = 1 \quad (2.22)$$

is the so called Pochhammer's symbol and can also be represented in terms of Euler gamma function. On the other hand, (2.15) leads to the normalization constant

$$h_n^2 = \frac{2^{\alpha+\beta+1}}{2n + \alpha + \beta + 1} \frac{\Gamma(n + \alpha + 1)\Gamma(n + \beta + 1)}{n!\Gamma(n + \alpha + \beta + 1)} \quad (2.23)$$

of the Jacobi polynomials. They satisfy the three-term recurrence relation in Theorem 2.4 with

$$A_n = \frac{2}{2n + \alpha + \beta + 2} \sqrt{\frac{(n+1)(n+\alpha+1)(n+\beta+1)(n+\alpha+\beta+1)}{(2n+\alpha+\beta+1)(2n+\alpha+\beta+3)}} \quad (2.24)$$

and

$$B_n = \frac{\beta^2 - \alpha^2}{(2n + \alpha + \beta)(2n + \alpha + \beta + 2)}. \quad (2.25)$$

It is worth noting that

$$A_0 = \frac{2}{\alpha + \beta + 2} \sqrt{\frac{(\alpha+1)(\beta+1)}{\alpha + \beta + 3}} \quad \text{and} \quad B_0 = \frac{\beta - \alpha}{\alpha + \beta + 2} \quad (2.26)$$

which can be obtained by simplifying the expressions in (2.24) and (2.25) when $n = 0$. Finally, the coefficient

$$C_n = n + \alpha + \beta + 1 \quad (2.27)$$

that appears in the differential-difference relation might easily be computed using the value $\lambda_n^{(0)} = n(n + \alpha + \beta + 1)$.

2.2.2 Laguerre polynomials

When $\sigma(\xi) = \xi$ and $\rho_\gamma(\xi) = \xi^\gamma e^{-\xi}$ we have, from (2.2) and (2.3) $\tau(\xi) = \gamma + 1 - \xi$ and $\lambda_n^{(0)} = n$, respectively. Corresponding polynomials defined by the Rodriguez formula in (2.4)

$$L_n^\gamma(\xi) = \frac{1}{n!} \xi^{-\gamma} e^\xi \frac{d^n}{d\xi^n} (\xi^{n+\gamma} e^{-\xi}) \quad (2.28)$$

are known as the associated Laguerre polynomials and they are solutions of the differential equation

$$\xi y'' + (\gamma + 1 - \xi)y' + ny = 0. \quad (2.29)$$

According to Theorem 2.1 they are orthogonal over the half line $(0, \infty)$ provided $\gamma > -1$. The coefficient of the leading order term

$$k_n = (-1)^n \frac{1}{n!} \quad (2.30)$$

and the normalization constant

$$h_n^2 = \frac{1}{n!} \Gamma(n + \gamma + 1) \quad (2.31)$$

can easily be obtained from (2.14) and (2.15), respectively. For the Laguerre polynomials, the coefficients

$$A_n = -\sqrt{(n+1)(n+\gamma+1)} \quad \text{and} \quad B_n = 2n + \gamma + 1 \quad (2.32)$$

of the recursion in (2.9) are derived from (2.10). In this case the coefficient emerging in (2.16) is equal to unity, i.e.,

$$C_n = 1. \quad (2.33)$$

2.2.3 Hermite polynomials

If $\sigma(\xi) = 1$ and $\rho(\xi) = e^{-\xi^2}$, then from (2.2) and (2.3) we obtain $\tau(\xi) = -2\xi$ and $\lambda_n^{(0)} = 2n$, respectively. Thus, the Hermite polynomials

$$H_n(\xi) = (-1)^n e^{\xi^2} \frac{d^n}{d\xi^n} (e^{-\xi^2}) \quad (2.34)$$

are solutions of the equation

$$y'' - 2\xi y' + 2ny = 0. \quad (2.35)$$

In the light of Theorem 2.1, they are orthogonal over the real line with the normalization constant

$$h_n^2 = 2^n n! \sqrt{\pi}. \quad (2.36)$$

The leading order term has the coefficient $k_n = 2^n$ and the polynomials satisfy the three term recursion in (2.9) with

$$A_n = \sqrt{\frac{n+1}{2}} \quad \text{and} \quad B_n = 0 \quad (2.37)$$

whereas the constant

$$C_n = 2 \tag{2.38}$$

that come out in the differential-difference relation in (2.16). Notice that, for the Hermite case the relation is so simple, i.e., $\psi'_n(\xi) = \sqrt{2n}\psi_{n-1}(\xi)$. On the other hand, it takes the form

$$H'_n(\xi) = 2nH_{n-1}(\xi), \quad n = 1, 2, \dots \tag{2.39}$$

for the unnormalized Hermite polynomials.

CHAPTER 3

PSEUDOSPECTRAL METHODS

In this chapter, we construct the so-called differentiation matrices which can be seen as discrete derivative operators. Then we develop pseudospectral formulation of the WEHTP. Finally, we review some approximation results related to pseudospectral methods.

3.1 Differentiation matrices

The use of pseudospectral methods as a tool for solving ordinary differential equations at least date backs to Frazer, Jones and Skan [28]. Then, in 1938, Lanczos showed that the choice of trial functions and the distribution of the nodal points are crucial to the accuracy of the solution [48]. Later on, in 1957, Clenshaw applied the Chebyshev polynomial expansion to initial value problems. Then, application to boundary value problems developed by Villadsen and Stewart in 1967 [83]. After 1970s it has been become a popular and powerful way of approximating ordinary and partial differential equations. One of the earliest application to partial differential equations published by Orszag who first used the term pseudospectral [15].

Roughly speaking, a pseudospectral method, also known as spectral collocation method, is based on the N th degree polynomial interpolation of a function $y(\xi)$ denoted by $I_N y(\xi)$,

$$I_N y(\xi) := P_N(\xi) = \sum_{n=0}^N \ell_n(\xi) y_n, \quad (3.1)$$

where the $y_n = y(\xi_n)$ are the actual values of the function $y(\xi)$ at the specified nodes $\xi = \xi_n$ for $n = 0, 1, \dots, N$ [29]. The set of Lagrange interpolating polynomials $\{\ell_n(\xi)\}$ of degree N is defined by

$$\ell_n(\xi) = \frac{\pi(\xi)}{(\xi - \xi_n)\pi'(\xi_n)} \quad (3.2)$$

for each $n = 0, 1, \dots, N$, in which

$$\pi(\xi) = \kappa \prod_{m=0}^N (\xi - \xi_m) \quad (3.3)$$

stands for a polynomial of degree $N + 1$ with the real and distinct roots at the nodes. The Lagrange polynomials have the very well-known cardinality property $\ell_n(\xi_m) = \delta_{mn}$ where δ_{mn} is Kronecker's delta. As a result, both the interpolant $P_N(\xi)$ and the function $y(\xi)$ agree, at least, at the nodes, $y(\xi_n) = P_N(\xi_n)$. Although the normalization constant κ is theoretically unnecessary, it plays a remarkable role in the numerical algorithm.

It is also possible to approximate the derivatives of the function $y(\xi)$ by differentiating the interpolant $P_N(\xi)$. Furthermore, the derivative values at the nodes ξ_n may be determined in terms of function values $y_n = P_N(\xi_n)$ by means of a *differentiation matrix* defined by

$$\mathbf{D}^{(k)} := [d_{mn}^{(k)}] = \left. \frac{d^k}{d\xi^k} [\ell_n(\xi)] \right|_{\xi=\xi_m}, \quad m, n, k = 1, 2, \dots, N \quad (3.4)$$

The approximate derivative values $\mathbf{y}^{(k)} = [P_N^{(k)}(\xi_0), P_N^{(k)}(\xi_1), \dots, P_N^{(k)}(\xi_N)]^T$ may therefore be written in matrix-vector form

$$\mathbf{y}^{(k)} = \mathbf{D}^{(k)} \mathbf{y} \quad (3.5)$$

where $\mathbf{y} = [y_0, y_1, \dots, y_N]^T$ is the vector of function values at the nodes. In particular, the entries of the first and the second order differentiation matrices are defined by

$$d_{mn}^{(1)} = \frac{1}{2} \begin{cases} \frac{2\pi'(\xi_m)}{(\xi_m - \xi_n)\pi'(\xi_n)} & \text{if } m \neq n \\ \frac{\pi''(\xi_n)}{\pi'(\xi_n)} & \text{if } m = n \end{cases} \quad (3.6)$$

and

$$d_{mn}^{(2)} = \frac{1}{3} \begin{cases} \frac{3}{\xi_m - \xi_n} \left[\frac{\pi''(\xi_m)}{\pi'(\xi_n)} - 2d_{mn}^{(1)} \right] & \text{if } m \neq n \\ \frac{\pi'''(\xi_n)}{\pi'(\xi_n)} & \text{if } m = n \end{cases} \quad (3.7)$$

respectively [29, 79]. Note that the entries of the above matrices are obtained first by differentiating the Lagrange polynomials $\ell_n(\xi)$ to a desired order $k = 1, 2, \dots$, and then, evaluating them at the nodal points ξ_m . In particular, diagonal entries are obtained from the derivatives of $\ell_n(\xi)$ by a limiting process when $\xi \rightarrow \xi_m$ since they are undetermined at the collocation points $\xi = \xi_m$.

3.2 Gauss quadrature rule of integration

In this section we derive the Gauss quadrature rule based on the zeros of normalized polynomial solutions $\psi_{N+1}(\xi) = \frac{1}{h_{N+1}} p_{N+1}(\xi)$ of EHT. Consider the integral

$$\int_a^b u(\xi)\rho(\xi)d\xi \quad (3.8)$$

where ρ is associated with the orthogonality of $p_{N+1}(\xi)$. It may be approximated by replacing the function u by its Lagrange interpolant $I_N u$ in (3.1) based on $\psi_{N+1}(\xi)$,

$$\int_a^b u(\xi)\rho(\xi)d\xi \approx \int_a^b I_N u(\xi)\rho(\xi)d\xi = \int_a^b \sum_{n=0}^N u_n \ell_n(\xi)\rho(\xi)d\xi = \sum_{n=0}^N u_n \omega_n \quad (3.9)$$

where $u_n = u(\xi_n)$ and the weights ω_n of Gaussian quadrature rule are given by

$$\omega_n = \int_a^b \ell_n(\xi)\rho(\xi)d\xi = \frac{1}{\psi'_{N+1}(\xi_n)} \int_a^b \frac{\psi_{N+1}(\xi)}{\xi - \xi_n} \rho(\xi)d\xi \quad (3.10)$$

which are called the Christoffel numbers. Now, letting $\eta = \xi_n$ and $p_{N+1}(\xi) = h_{N+1}\psi_{N+1}(\xi)$ in (2.8) we obtain

$$\sum_{k=0}^N \psi_k(\xi)\psi_k(\xi_n) = \frac{h_{N+1}}{h_N} \frac{k_N}{k_{N+1}} \frac{\psi_{N+1}(\xi)\psi_N(\xi_n)}{\xi - \xi_n} \quad (3.11)$$

since $\psi_{N+1}(\xi_n) = 0$. Then, multiplication of both sides of the last equation by $p_0(\xi)\rho(\xi)$ and integration from a to b lead to the equation

$$\int_a^b \frac{\psi_{N+1}(\xi)}{\xi - \xi_n} \rho(\xi)d\xi = \frac{h_N}{h_{N+1}} \frac{k_{N+1}}{k_N} \frac{1}{\psi_N(\xi_n)} \quad (3.12)$$

where we have used the fact that $\psi_0(\xi) = 1/h_0$ is orthogonal to all $p_k(\xi)$ for any $k = 1, 2, \dots, N$. Thus, inserting the last equation into (3.10) we get

$$\omega_n = \frac{h_N}{h_{N+1}} \frac{k_{N+1}}{k_N} \frac{1}{\psi'_{N+1}(\xi_n)\psi_N(\xi_n)} = \frac{1}{A_N} \frac{1}{\psi'_{N+1}(\xi_n)\psi_N(\xi_n)} \quad (3.13)$$

where A_N is one of the constants of the three term recursion in (2.10). Finally, (2.16) with $\xi = \xi_n$ and $n = N + 1$ implies that

$$\omega_n = \frac{1}{A_N^2 C_{2N+2}} \frac{\sigma(\xi_n)}{\psi_N^2(\xi_n)} \quad (3.14)$$

since $\psi_{N+1}(\xi_n) = 0$. Notice that everything is known, except $\psi_N(\xi_n)$. However, with a careful look, we see that it is no more than the last entry

$$\psi_N(\xi_n) = \frac{v_N^n}{h_0 v_0^n} \quad (3.15)$$

of the equation in (2.18). However, there exist an alternative way of computing the weights ω_n . The limiting case $\xi \rightarrow \xi_n$ of (3.11) leads to the equation

$$\sum_{k=0}^N \psi_k^2(\xi_n) = A_N \psi'_{N+1}(\xi_n) \psi_N(\xi_n) \quad (3.16)$$

or equivalently we have

$$\sum_{k=0}^N \psi_k^2(\xi_n) = A_N^2 C_{2N+2} \frac{\psi_N^2(\xi_n)}{\sigma(\xi_n)} = \frac{1}{\omega_n} \quad (3.17)$$

on using (2.16). Therefore, the weights ω_n of Gauss quadrature have another representation

$$\frac{1}{\omega_n} = \sum_{k=0}^N \psi_k^2(\xi_n) = \left(\frac{1}{h_0 v_0^n} \right)^2 \sum_{k=0}^N (v_k^n)^2 \quad (3.18)$$

where we have used (2.18). Note that the sum on the right hand side is the square of the Euclidean norm of the vector \mathbf{v}^n . Hence, we have

$$\omega_n = \frac{(h_0 v_0^n)^2}{\|\mathbf{v}^n\|^2}, n = 0, 1, \dots, N \quad (3.19)$$

which reduces to $\omega_n = (h_0 v_0^n)^2$ when the normalized eigenvectors are used. Actually, most of the linear algebra subroutines produce normalized eigenvectors together with the associated eigenvalues if the Euclidean norm is used.

Gaussian quadrature formula based on the zeros of $p_{N+1}(\xi)$ integrates polynomials of degree less than or equal to $2N + 1$ exactly. The two others, Gauss-Radau and Gauss-Lobatto quadratures, are exact for polynomials of degree less than or equal to $2N$ and $2N - 1$, respectively [29].

On the other hand, Gauss quadrature is exact for the integral

$$\int_a^b \ell_n(\xi) \ell_m(\xi) \rho(\xi) d\xi \quad (3.20)$$

since each Lagrange polynomial $\ell_n(\xi)$ is of degree N . Therefore, we have

$$\int_a^b \ell_n(\xi) \ell_m(\xi) \rho(\xi) d\xi = \sum_{k=0}^N \ell_n(\xi_k) \ell_m(\xi_k) \omega_k = \omega_n \delta_{mn} \quad (3.21)$$

on using the cardinality property $\ell_n(\xi_m) = \delta_{mn}$ of Lagrange polynomials.

3.3 Pseudospectral formulation of the WEHTP

In the previous chapter it is given that the each COP solution $y(\xi) = p_n(\xi)$ of the EHT has exactly n real and distinct zeros which are interlaced [58]: sorting all the roots in ascending order, the roots of $p_{n+1}(\xi)$ alternate with those of $p_n(\xi)$, so it obeys the definition of $\pi(\xi)$ in (3.3). Therefore, setting

$$\pi(\xi) = \kappa \prod_{m=0}^N (\xi - \xi_m) = \frac{1}{h_n} p_{N+1}(\xi) = \psi_{N+1}(\xi) \quad (3.22)$$

to be the polynomial solution $p_{N+1}(\xi)$ of the EHT, we define, from (3.6), the first order differentiation matrix

$$d_{mn}^{(1)} = \frac{1}{2} \begin{cases} \frac{2}{\xi_m - \xi_n} \frac{\psi'_{N+1}(\xi_m)}{\psi'_{N+1}(\xi_n)} & \text{if } m \neq n \\ -\frac{\tau(\xi_n)}{\sigma(\xi_n)} & \text{if } m = n \end{cases} \quad (3.23)$$

in which the main diagonal entries have been simplified by using the fact that $p_{N+1}(\xi)$ satisfies the EHT in (1.30). Similarly, after some algebra, the elements of the second order differentiation matrix in (3.7) take the form

$$d_{mn}^{(2)} = \frac{1}{3} \begin{cases} -\frac{3}{\xi_m - \xi_n} \left[\frac{\tau(\xi_m)}{\sigma(\xi_m)} + \frac{2}{\xi_m - \xi_n} \right] \frac{\psi'_{N+1}(\xi_m)}{\psi'_{N+1}(\xi_n)} & \text{if } m \neq n \\ \frac{1}{\sigma(\xi_n)} \left\{ \frac{\tau(\xi_n)}{\sigma(\xi_n)} [\sigma'(\xi_n) + \tau(\xi_n)] + N \left[\tau' + \frac{1}{2}(N+1)\sigma'' \right] \right\} & \text{if } m = n \end{cases} \quad (3.24)$$

with the help of (1.30) and (2.3) [3]. Higher order differentiation matrices may be obtained in a similar manner, however, first and second order differentiation matrices are sufficient for a treatment of a second order differential operator.

Now that the interpolant $P_N(\xi)$ in (3.1) is proposed to be an approximate solution of the EHTP, where N may be regarded as the approximation or truncation order. Therefore, we require that the EHTP is satisfied at the nodal points ξ_m

$$\sum_{n=0}^N [\sigma(\xi_m) \ell_n''(\xi_m) + \tau(\xi_m) \ell_n'(\xi_m) + \nu(\xi_m) \ell_n(\xi_m)] y_n = -\lambda r(\xi_m) \sum_{n=0}^N \ell_n(\xi_m) y_n \quad (3.25)$$

for $m = 0, 1, \dots, N$. This leads to the discrete representation

$$\widehat{\mathcal{B}} \mathbf{y} = -\lambda \mathbf{y} \quad (3.26)$$

of the WEHTP. Here, the vector $\mathbf{y}^i = [y_0^i, y_1^i, \dots, y_N^i]^T$ involves the values of the eigensolution associated with the eigenvalue λ_i at the nodal points, and the general entry $\widehat{\mathcal{B}}_{mn}$ of the resulting

matrix $\widehat{\mathcal{B}} = [\widehat{\mathcal{B}}_{mn}]$ is given by [3]

$$\widehat{\mathcal{B}}_{mn} = \frac{1}{r(\xi_m)} [\sigma(\xi_m)d_{mn}^{(2)} + \tau(\xi_m)d_{mn}^{(1)} + \nu(\xi_m)\delta_{mn}], \quad m, n = 0, 1, \dots, N. \quad (3.27)$$

By using (3.23) and (3.24) the first two terms in (3.27) can be incorporated to define

$$\widehat{\mathcal{K}}_{mn} = -\frac{1}{6r(\xi_m)} \begin{cases} \frac{12\sigma(\xi_m)}{(\xi_m - \xi_n)^2} \frac{\psi'_{N+1}(\xi_m)}{\psi'_{N+1}(\xi_n)} & \text{if } m \neq n \\ \frac{\tau(\xi_n)}{\sigma(\xi_n)} [\tau(\xi_n) - 2\sigma'(\xi_n)] - 2N \left[\tau' + \frac{1}{2}(N+1)\sigma'' \right] & \text{if } m = n \end{cases} \quad (3.28)$$

which represents the effect of kinetic energy terms independent of a specified potential [3].

It seems that the evaluation of $\widehat{\mathcal{K}}_{mn}$ requires the computation of the derivatives $p'_{N+1}(\xi_n)$ of the classical orthogonal polynomials at the nodes. Fortunately, a nice similarity transformation $\mathcal{B} = \mathcal{S}^{-1}\widehat{\mathcal{B}}\mathcal{S}$ in which $\mathcal{S} = \text{diag}\{s_0, s_1, \dots, s_m, \dots, s_N\}$ with

$$s_m = \sqrt{\frac{\sigma(\xi_m)}{r(\xi_m)}} \psi'_{N+1}(\xi_m), \quad m = 0, 1, \dots, N \quad (3.29)$$

makes it possible to get rid of such a cumbersome labor. Furthermore, the matrix in (3.26) reduces to a symmetric one, say $\mathcal{B} = \mathcal{S}^{-1}(\widehat{\mathcal{K}} + \mathcal{V})\mathcal{S}$, whose entries are given by

$$\mathcal{B}_{mn} = \mathcal{K}_{mn} + \mathcal{V}_m \delta_{mn} \quad (3.30)$$

where

$$\mathcal{K}_{mn} = -\frac{1}{6} \begin{cases} \frac{12}{(\xi_m - \xi_n)^2} \sqrt{\frac{\sigma(\xi_m)\sigma(\xi_n)}{r(\xi_m)r(\xi_n)}} & \text{if } m \neq n \\ \frac{1}{r(\xi_n)} \left\{ \frac{\tau(\xi_n)}{\sigma(\xi_n)} [\tau(\xi_n) - 2\sigma'(\xi_n)] - 2N \left[\tau' + \frac{1}{2}(N+1)\sigma'' \right] \right\} & \text{if } m = n \end{cases} \quad (3.31)$$

and $\mathcal{V} = [\mathcal{V}_m]$ with

$$\mathcal{V}_m = \frac{\nu(\xi_m)}{r(\xi_m)}. \quad (3.32)$$

Thus, the eigenvalues of (3.26), and, hence, the approximate eigenvalues of the EHTP can be determined by the symmetric matrix eigenvalue problem

$$\mathcal{B}u = -\lambda u \quad (3.33)$$

since the similar matrices share the same spectrum [3]. The construction of the resulting symmetric square matrix \mathcal{B} of size $N + 1$ can be accomplished by the calculation of the coefficient functions $\sigma(\xi)$, $\tau(\xi)$, $\nu(\xi)$ and $r(\xi)$ in EHTP (1.29) at the nodes which are the roots

ξ_m of the appropriate classical orthogonal polynomial $p_{N+1}(\xi)$ employed in the set up of the Lagrange interpolating polynomials. However, we have already found that the roots ξ_m of $p_{N+1}(\xi)$ are the eigenvalues of the symmetric tri-diagonal matrix \mathbf{R} in (2.17).

Therefore, the pseudospectral formulation of the EHTP leads to the symmetric matrix eigenvalue problem whose construction requires only the knowledge of the coefficient functions and the roots of the polynomial solution of the associated EHT.

On the other hand, the i -th eigenvector \mathbf{y}^i of (3.26) is given by the formula

$$\mathbf{y}^i = \mathbf{S}\mathbf{u}^i \quad (3.34)$$

in terms of the i -th eigenvector $\mathbf{u}^i = [u_0^i, u_1^i, \dots, u_N^i]^T$ of the symmetric matrix $\mathcal{B} = \mathbf{S}^{-1}\widehat{\mathcal{B}}\mathbf{S}$ since $\mathbf{S}^{-1}\widehat{\mathcal{B}}\mathbf{S}\mathbf{u} = -\lambda\mathbf{u}$ implies that $\widehat{\mathcal{B}}[\mathbf{S}\mathbf{u}] = -\lambda[\mathbf{S}\mathbf{u}]$. Thus, the m^{th} entry $y_m^i = y^i(\xi_m)$ of the i^{th} eigenvector \mathbf{y}^i may be written as $y_m^i = s_m u_m^i$, or in nodal notation

$$y^i(\xi_m) = \sqrt{\frac{\sigma(\xi_m)}{r(\xi_m)}} \psi'_{N+1}(\xi_m) u^i(\xi_m) \quad (3.35)$$

upon using (3.29). The only unknown value is $\psi'_{N+1}(\xi_m)$ to compute $\mathbf{y}^{(i)}(\xi_m)$. In order to determine it, the most primitive way is to construct the normalized polynomial with the roots ξ_m , differentiate it and evaluate at the node ξ_m which is not a practical idea for computer implementation. However, that value can be obtained in a beautiful manner. To this end, we first use Theorem 2.5 with n and ξ are replaced by $N + 1$ and ξ_m , respectively, to get

$$\psi'_{N+1}(\xi_m) = \frac{A_N C_{2N+2}}{\sigma(\xi_m)} \psi_N(\xi_m) \quad (3.36)$$

since $\psi_{N+1}(\xi_m) = 0$. Then, from (2.18) we see that $\psi_N(\xi_m)$ is related with the last entry of the computed eigenvector \mathbf{v}^m

$$\psi_N(\xi_m) = \frac{v_N^m}{h_0 v_0^m} \quad (3.37)$$

of the symmetric tridiagonal matrix \mathbf{R} in (2.17). Therefore, the i^{th} eigenvector of the wEHTP has the relation

$$y^i(\xi_m) = \frac{A_N C_{2N+2}}{\sqrt{\sigma(\xi_m) r(\xi_m)}} \frac{v_N^m}{h_0 v_0^m} u^i(\xi_m) \quad (3.38)$$

with the corresponding eigenvector \mathbf{u}^i of the symmetric matrix \mathcal{B} at a collocation point ξ_m .

Thus, in a constructive way, we proved the big part of the following proposition:

Proposition 3.1 *The approximate eigenvalues $-\lambda_i$ of the wEHTP in (1.29)*

$$\sigma(\xi)y'' + \tau(\xi)y' + \nu(\xi)y = -\lambda r(\xi)y, \quad \xi \in (a, b) \subseteq \mathbb{R}$$

are the eigenvalues of the linear system $\mathcal{B}\mathbf{u} = -\lambda\mathbf{u}$ in (3.33) where

$$\mathcal{B}_{mn} = -\frac{1}{6} \begin{cases} \frac{12}{(\xi_m - \xi_n)^2} \sqrt{\frac{\sigma(\xi_m)\sigma(\xi_n)}{r(\xi_m)r(\xi_n)}} & \text{if } m \neq n \\ \frac{1}{r(\xi_n)} \left\{ \frac{\tau(\xi_n)}{\sigma(\xi_n)} [\tau(\xi_n) - 2\sigma'(\xi_n)] - 2N \left[\tau' + \frac{1}{2}(N+1)\sigma'' \right] - 6\nu(\xi_n) \right\} & \text{if } m = n \end{cases} \quad (3.39)$$

and the values $y^i(\xi_m)$ of the corresponding normalized eigenfunctions (in L^2_ρ sense that is defined in (2.7)) at the nodes ξ_m are given by

$$y^i(\xi_m) = \frac{A_N \sqrt{C_{2N+2}}}{\sqrt{\sigma(\xi_m)r(\xi_m)}} \frac{v_N^m}{h_0 v_0^m} u^i(\xi_m) = \frac{u^i(\xi_m)}{\sqrt{\omega_m r(\xi_m)}} \quad (3.40)$$

whenever \mathbf{u}^i is the normalized (in Euclidean norm) eigenvector of \mathcal{B} .

Proof. Note that the equation (3.40) differs from (3.38) by the square root sign for the term C_{2N+2} . Now, let us show that (3.40) contains the values of the normalized eigenfunctions at the nodes. It is not difficult to see that if ρ is the weight function of the EHT in (2.1) then $\tilde{\rho} = r\rho$ is that of the WEHTP in (1.29). Thus, we have

$$\|y^i(\xi)\|_{L^2_{\tilde{\rho}}}^2 = \int_a^b [y^i(\xi)]^2 \tilde{\rho}(\xi) d\xi = \int_a^b [y^i(\xi)]^2 r(\xi) \rho(\xi) d\xi. \quad (3.41)$$

Applying the Gauss quadrature rule in (3.9) with $u(\xi) = [y^i(\xi)]^2 r(\xi)$ to the last integral we obtain

$$\|y^i(\xi)\|_{L^2_{\tilde{\rho}}}^2 = \int_a^b [y^i(\xi)]^2 r(\xi) \rho(\xi) d\xi = \sum_{m=0}^{\infty} [y^i(\xi_m)]^2 r(\xi_m) \omega_m \quad (3.42)$$

where the weights ω_m are defined in (3.14)-(3.15). Then, it reduces to

$$\|y^i(\xi)\|_{L^2_{\tilde{\rho}}}^2 = \sum_{m=0}^{\infty} [u^i(\xi_m)]^2 = 1 \quad (3.43)$$

upon using (3.40) which is equal to unity by assumption. □

3.4 Error estimates for spectral methods

In this section we summarize some results from the literature concerning the approximation errors for spectral methods.

For a numerical algorithm there are some important issues such as consistency, stability and convergence. When these conditions are fulfilled, the natural question arises: what is the rate of convergence? The rate depends on the regularity of the approximated function which might be a solution of a differential equation. That is, the smoother the function, the faster the convergence is. In the error analysis of spectral methods, smoothness of a function is measured in terms of its norm in an appropriate Sobolev space since it is more suitable for the analysis of differential equations [29].

There are numerous results on the analysis of polynomial methods in Sobolev spaces which starts with the paper of Canuto and Quarteroni [16] in 1982. Besides tens of papers on the subject, we have some good reference books such as [12, 13, 14, 15, 29, 35].

We start with the Hermite spectral approximations. The weighted space

$$L_\rho^2(\mathbb{R}) = \{u \mid \|u\|_{L_\rho^2(\mathbb{R})} < \infty\} \quad (3.44)$$

equipped with the inner product and norm

$$(u, v)_\rho = \int_{\mathbb{R}} u(\xi)v(\xi)e^{-\xi^2} d\xi, \quad \|u\|_{L_\rho^2(\mathbb{R})} = \left(\int_{\mathbb{R}} u^2(\xi)e^{-\xi^2} d\xi \right)^{\frac{1}{2}} \quad (3.45)$$

is known as the Hilbert space of square integrable functions over the real line. Then, It is possible to define the family of weighted Sobolev spaces

$$H_\rho^m(\mathbb{R}) = \{u \mid u^{(k)} \in L_\rho^2(\mathbb{R}), 0 \leq k \leq m\} \quad (3.46)$$

with the norm

$$\|u\|_{H_\rho^m(\mathbb{R})} = \left(\sum_{k=0}^m \|u^{(k)}\|_{L_\rho^2(\mathbb{R})}^2 \right)^{\frac{1}{2}} \quad (3.47)$$

where $u^{(k)}$ is the k -th derivative of the function u . We begin with the error analysis of the L_ρ^2 orthogonal projection $\Pi_N : L_\rho^2(\mathbb{R}) \rightarrow \mathbb{P}_N$, defined by

$$(u - \Pi_N u, v_N)_\rho = \int_{\mathbb{R}} (u - \Pi_N u)(\xi)v_N(\xi)e^{-\xi^2} d\xi = 0, \quad \forall v_N \in \mathbb{P}_N \quad (3.48)$$

since it will be used in the error analysis of pseudospectral approximation by Hermite polynomials or functions. Here, \mathbb{P}_N stands for the space of all polynomials degree $\leq N$ and

$$\Pi_N u(\xi) = \sum_{n=0}^N u_n H_n(\xi), \quad u_n = \frac{1}{h_n^2} \int_{\mathbb{R}} u(\xi)H_n(\xi)e^{-\xi^2} d\xi \quad (3.49)$$

is the truncated Fourier-Hermite expansion of $u(\xi)$ where h_n^2 is the normalization constant or the square of L_ρ^2 norm of H_n given by (2.36).

Theorem 3.2 For any $u \in H_\rho^m(\mathbb{R})$ with $m \geq 0$,

$$\|(u - \Pi_N u)^{(k)}\|_{L_\rho^2(\mathbb{R})} \leq CN^{(k-m)/2} \|u^{(m)}\|_{L_\rho^2(\mathbb{R})}, \quad 0 \leq k \leq m \quad (3.50)$$

where C is a constant independent of N .

Proof. For any $u \in L_\rho^2(\mathbb{R})$ (3.49) holds. Moreover, from (2.39) we have

$$H_n^{(k)}(\xi) = c_{n,k} H_{n-k}(\xi), \quad n \geq k. \quad (3.51)$$

with $c_{n,k} = \frac{2^k n!}{(n-k)!}$. Thus, for $k \leq m \leq N$, we have

$$\begin{aligned} \|(u - \Pi_N u)^{(k)}\|_{L_\rho^2(\mathbb{R})}^2 &= \left\| \sum_{n=N+1}^{\infty} u_n H_n^{(k)}(\xi) \right\|_{L_\rho^2(\mathbb{R})}^2 = \sum_{n=N+1}^{\infty} u_n^2 c_{n,k}^2 h_{n-k}^2 \\ &= \sum_{n=N+1}^{\infty} u_n^2 \frac{c_{n,k}^2 h_{n-k}^2}{c_{n,m}^2 h_{n-m}^2} c_{n,m}^2 h_{n-m}^2 \leq CN^{k-m} \sum_{n=N+1}^{\infty} u_n^2 c_{n,m}^2 h_{n-m}^2 \\ &= CN^{k-m} \|u^{(m)}\|_{L_\rho^2(\mathbb{R})}^2 \end{aligned}$$

which completes the proof. \square

Different versions, such as the ones in [29, 36], are available in the literature but here we followed the lines of [67] which is a good review article on spectral methods in unbounded domains.

Moreover, it is possible to show that

$$\|p^{(k)}\|_{L_\rho^2(\mathbb{R})} \leq CN^{k/2} \|p\|_{L_\rho^2(\mathbb{R})}, \quad \forall p \in \mathbb{P}_N \quad (3.52)$$

on expanding the polynomial p into Fourier-Hermite series and then using (3.51).

We now examine the error of interpolation operator $I_N : C(\mathbb{R}) \rightarrow \mathbb{P}_N$ defined by (3.1) for which we need to bound the quantity $\|I_N u\|_{L_\rho^2(\mathbb{R})}$. Actually, the norm $\|I_N u\|_{L_\rho^2(\mathbb{R})}$ of the interpolatory polynomial $I_N u$ constructed by Hermite polynomials $p_{N+1}(\xi) = H_{N+1}(\xi)$ becomes

$$\begin{aligned} \|I_N u\|_{L_\rho^2(\mathbb{R})} &= \int_a^b \left(\sum_{n=0}^N \ell_n(\xi) u_n \right)^2 \rho(\xi) d\xi \\ &= \sum_{n=0}^N \left(\int_a^b \ell_n^2(\xi) \rho(\xi) d\xi \right) u_n^2 + 2 \sum_{\substack{m=0 \\ m \neq n}}^N \sum_{n=0}^N \left(\int_a^b \ell_n(\xi) \ell_m(\xi) \rho(\xi) d\xi \right) u_n u_m \\ &= \sum_{n=0}^N u_n^2 \omega_n. \end{aligned}$$

with the help of (3.21). Therefore, an error estimate for the Hermite pseudospectral method (HPM) reduces to bounding the Christoffel numbers ω_n .

For the Hermite-Gauss quadrature, the weights in (3.14) becomes

$$\omega_n = \frac{1}{(N+1)\psi_N^2(\xi_n)} = \frac{2^N N! \sqrt{\pi}}{(N+1)H_N^2(\xi_n)}, \quad n = 0, 1, \dots, N \quad (3.53)$$

on using (2.36)–(2.39). In [2], Aguirre and Rivas give a bound

$$\omega_n \leq e^{\xi_n^2} \omega_n \leq CN^{-1/6}, \quad n = 0, 1, \dots, N \quad (3.54)$$

for (3.53), where C is independent of N . This is the sharpest bound for the Hermite-Gauss weights in the literature so far. Then, they use it to prove that

$$\|I_N u\|_{L_p^2(\mathbb{R})}^2 \leq CN^{1/3} \left(\|u\|_{L_p^2(\mathbb{R})}^2 + N^{-1} \|u'\|_{L_p^2(\mathbb{R})}^2 \right) \quad (3.55)$$

for any $u \in H_\rho^1(\mathbb{R})$. Consequently, we can prove the following theorem with the help of Theorem 3.2 and the last inequality in (3.55).

Theorem 3.3 [2] *For any $u \in H_\rho^m(\mathbb{R})$ with $m \geq 1$, there exists a constant $C > 0$ such that*

$$\|(u - I_N u)^{(k)}\|_{L_p^2(\mathbb{R})} \leq CN^{\frac{1}{6} + \frac{k-m}{2}} \|u^{(m)}\|_{L_p^2(\mathbb{R})} \quad (3.56)$$

with $0 \leq k \leq m$.

Proof. By triangle inequality

$$\begin{aligned} \|(u - I_N u)^{(k)}\|_{L_p^2(\mathbb{R})}^2 &\leq \left(\|(u - \Pi_N u)^{(k)}\|_{L_p^2(\mathbb{R})} + \|(\Pi_N u - I_N u)^{(k)}\|_{L_p^2(\mathbb{R})} \right)^2 \\ &\leq \|(u - \Pi_N u)^{(k)}\|_{L_p^2(\mathbb{R})}^2 + 2\|(u - \Pi_N u)^{(k)}\|_{L_p^2(\mathbb{R})} \|(I_N(\Pi_N u - u))^{(k)}\|_{L_p^2(\mathbb{R})} \\ &\quad + \|(I_N(\Pi_N u - u))^{(k)}\|_{L_p^2(\mathbb{R})}^2, \end{aligned}$$

since $\Pi_N u$ is a polynomial of degree N , thus $I_N \Pi_N u = \Pi_N u$. Moreover, Theorem 3.2 implies

$$\|(u - \Pi_N u)^{(k)}\|_{L_p^2(\mathbb{R})}^2 \leq CN^{k-m} \|u^{(m)}\|_{L_p^2(\mathbb{R})}^2. \quad (3.57)$$

Then, applying (3.52) with $p = I_N(\Pi_N u - u)$, (3.55) and (3.57) with $k = 0, 1$ we obtain

$$\begin{aligned} \|(I_N(\Pi_N u - u))^{(k)}\|_{L_p^2(\mathbb{R})}^2 &\leq CN^k \|I_N(\Pi_N u - u)\|_{L_p^2(\mathbb{R})}^2 \\ &\leq CN^{\frac{1}{3}+k} \left(\|\Pi_N u - u\|_{L_p^2(\mathbb{R})}^2 + N^{-1} \|(\Pi_N u - u)'\|_{L_p^2(\mathbb{R})}^2 \right) \\ &\leq CN^{\frac{1}{3}+k} \left(N^{-m} \|u^{(m)}\|_{L_p^2(\mathbb{R})}^2 + N^{-1} N^{1-m} \|u^{(m)}\|_{L_p^2(\mathbb{R})}^2 \right) \\ &\leq CN^{\frac{1}{3}+k-m} \|u^{(m)}\|_{L_p^2(\mathbb{R})}^2 \end{aligned}$$

Therefore, finally we have

$$\begin{aligned} \|(u - I_N u)^{(k)}\|_{L^2_\rho(\mathbb{R})}^2 &\leq CN^{k-m} \|u^{(m)}\|_{L^2_\rho(\mathbb{R})}^2 + 2CN^{\frac{1}{6}+k-m} \|u^{(m)}\|_{L^2_\rho(\mathbb{R})}^2 + CN^{\frac{1}{3}+k-m} \|u^{(m)}\|_{L^2_\rho(\mathbb{R})}^2 \\ &\leq CN^{\frac{1}{3}+k-m} \|u^{(m)}\|_{L^2_\rho(\mathbb{R})}^2 \end{aligned}$$

which completes the proof. \square

Similar results hold also for the Laguerre and Jacobi spectral approximations. For the Laguerre case, we define the non-uniformly weighted Sobolev space

$$H_\gamma^m(\mathbb{R}_+) = \{u \mid u^{(k)} \in L^2_{\rho_{\gamma+k}}(\mathbb{R}_+), 0 \leq k \leq m\} \quad (3.58)$$

of square integrable functions on the half line with the norm

$$\|u\|_{H_\gamma^m(\mathbb{R}_+)} = \left(\sum_{k=0}^m \|u^{(k)}\|_{L^2_{\rho_{\gamma+k}}(\mathbb{R}_+)}^2 \right)^{\frac{1}{2}}, \quad \|u^{(k)}\|_{L^2_{\rho_{\gamma+k}}(\mathbb{R}_+)} = \left(\int_{\mathbb{R}_+} u^{(k)}(\xi) \xi^{\gamma+k} e^{-\xi} d\xi \right)^{\frac{1}{2}}. \quad (3.59)$$

Now, the $L^2_{\rho_\gamma}$ orthogonal projection $\Pi_N^\gamma : L^2_{\rho_\gamma}(\mathbb{R}_+) \rightarrow \mathbb{P}_N$, defined by

$$(u - \Pi_N^\gamma u, v_N)_{\rho_\gamma} = \int_{\mathbb{R}_+} (u - \Pi_N^\gamma u)(\xi) v_N(\xi) \xi^\gamma e^{-\xi} d\xi = 0, \quad \forall v_N \in \mathbb{P}_N \quad (3.60)$$

where

$$\Pi_N^\gamma u(\xi) = \sum_{n=0}^N u_n^\gamma L_n^\gamma(\xi), \quad u_n = \frac{1}{h_n^2} \int_{\mathbb{R}_+} u(\xi) L_n^\gamma(\xi) \xi^\gamma e^{-\xi} d\xi \quad (3.61)$$

satisfies the following approximation result (see, for instance, [29, 67]).

Theorem 3.4 For any $u \in H_\gamma^m(\mathbb{R}_+)$ and $m \geq 0$,

$$\|(u - \Pi_N^\gamma u)^{(k)}\|_{L^2_{\rho_{\gamma+k}}(\mathbb{R}_+)} \leq CN^{(k-m)/2} \|u^{(m)}\|_{L^2_{\rho_{\gamma+m}}(\mathbb{R}_+)}, \quad 0 \leq k \leq m \quad (3.62)$$

where C is a constant independent of N .

Note here that, h_n^2 in (3.61) is the normalization constant of Laguerre polynomials given in (2.31).

Let I_N^γ be the interpolation operator $I_N^\gamma : C(\bar{\mathbb{R}}_+) \rightarrow \mathbb{P}_N$ defined by (3.1) based on the Laguerre-Gauss, i.e., zeros of $L_{N+1}^\gamma(\xi)$ or Laguerre-Radau, i.e., zeros of $\xi \frac{d}{d\xi} L_{N+1}^\gamma(\xi)$ interpolation points ξ_m so that $I_N^\gamma u(\xi_m) = u(\xi_m)$ $m = 0, 1, \dots, N$. Then the following result holds.

Theorem 3.5 Assuming $u \in C(\bar{\mathbb{R}}_+)$, $u \in H_\gamma^m(\mathbb{R}_+)$ and $u' \in H_\gamma^{m-1}(\mathbb{R}_+)$ with $m \geq 1$ we have

$$\|u - I_N^\gamma u\|_{L^2_{\rho_\gamma}(\mathbb{R}_+)} \leq CN^{(1-m)/2} \left(\|u^{(m)}\|_{L^2_{\rho_{\gamma+m-1}}(\mathbb{R}_+)} + (\ln N)^{1/2} \|u^{(m)}\|_{L^2_{\rho_{\gamma+m}}(\mathbb{R}_+)} \right) \quad (3.63)$$

where C is a constant independent of N [67].

The above theorem is proved in [39] which improves the results of [52, 56, 86].

Finally, using the Jacobi weight $\rho_{\alpha,\beta}(\xi) = (1 - \xi)^\alpha(1 + \xi)^\beta$, similar to the Laguerre case we define the non-uniformly weighted Sobolev space

$$H_{\alpha,\beta}^m(\mathbb{I}) = \{u \mid u^{(k)} \in L_{\rho_{\alpha+k,\beta+k}}^2(\mathbb{I}), 0 \leq k \leq m\} \quad (3.64)$$

on the interval $\mathbb{I} := (-1, 1)$ with the norm

$$\|u\|_{H_{\alpha,\beta}^m(\mathbb{I})} = \left(\sum_{k=0}^m \|u^{(k)}\|_{L_{\rho_{\alpha+k,\beta+k}}^2(\mathbb{I})}^2 \right)^{\frac{1}{2}}, \quad \|u^{(k)}\|_{L_{\rho_{\alpha+k,\beta+k}}^2(\mathbb{I})} = \left(\int_{\mathbb{I}} u^{(k)2}(\xi) \rho_{\alpha+k,\beta+k}(\xi) d\xi \right)^{\frac{1}{2}}. \quad (3.65)$$

Then the $L_{\rho_{\alpha,\beta}}^2(\mathbb{I})$ orthogonal projection $\Pi_N^{\alpha,\beta} : L_{\rho_{\alpha,\beta}}^2(\mathbb{I}) \rightarrow \mathbb{P}_N$ defined by

$$(u - \Pi_N^{\alpha,\beta} u, v_N)_{\rho_{\alpha,\beta}} = \int_{\mathbb{I}} (u - \Pi_N^{\alpha,\beta} u)(\xi) v_N(\xi) \rho_{\alpha,\beta} d\xi = 0, \quad \forall v_N \in \mathbb{P}_N \quad (3.66)$$

satisfies the following bound.

Theorem 3.6 *For any $u \in H_{\alpha,\beta}^m(\mathbb{I})$ and $0 \leq k \leq m$,*

$$\|(u - \Pi_N^{\alpha,\beta} u)^{(k)}\|_{L_{\rho_{\alpha+k,\beta+k}}^2(\mathbb{I})} \leq CN^{k-m} \|u^{(m)}\|_{L_{\rho_{\alpha+m,\beta+m}}^2(\mathbb{I})} \quad (3.67)$$

where C is a constant independent of N .

The proof can be found in [29, 38]. Let $I_N^{\alpha,\beta}$ be the interpolation operator based on Jacobi-Gauss nodes. Then the following result is established in [38].

Theorem 3.7 [38] *For any $u \in H_{\alpha,\beta}^m(\mathbb{I})$ with $m \geq 1$*

$$\|(u - I_N^{\alpha,\beta} u)'\|_{L_{\rho_{\alpha+1,\beta+1}}^2(\mathbb{I})} + N \|(u - I_N^{\alpha,\beta} u)\|_{L_{\rho_{\alpha,\beta}}^2(\mathbb{I})} \leq CN^{1-m} \|u^{(m)}\|_{L_{\rho_{\alpha+m,\beta+m}}^2(\mathbb{I})} \quad (3.68)$$

where C is a constant independent of N .

For a more general investigation of Jacobi approximation results see for example [12, 29, 38].

When we look at the Theorems 3.2, 3.4 and 3.6 concerning the L_p^2 - projections we observe that the convergence rate of Jacobi approximation is twice of those of Laguerre and Hermite cases. This is related to the eigenvalues $\lambda_n^{(0)}$ of the associated EHT in (1.30) leading to COPs. Notice the quadratic growth of the eigenvalues $\lambda_n^{(0)} = n(n + \alpha + \beta + 1)$ of Jacobi polynomials contrary to the linear growth of those of Laguerre $\lambda_n^{(0)} = n$ and Hermite $\lambda_n^{(0)} = 2n$ polynomials.

The interpolation results in Theorems 3.3 and 3.5 are suboptimal in the sense that the factors of $N^{-1/6}$ and $(N \ln N)^{-1/2}$ are lost when compared with the projection results in Theorems 3.2 and 3.4 (with $k = 0$), respectively.

It can be inferred from the above theorems on spectral (projection) and pseudospectral (interpolation) approximations that for smooth functions ($u^{(k)} \in L_\rho^2$ for any $k = 0, 1, \dots$) error decays faster than any power of N . This means that the exponential rate of convergence is achieved. On the other hand, for functions having singularities inside its domain ($u^{(i)} \in L_\rho^2$ for $i = 0, 1, \dots, k$ but $u^{(k+1)} \notin L_\rho^2$), the Jacobi methods converge at an optimal rate of k whereas the Laguerre and Hermite methods converge only at a rate of $\frac{1}{2}k$. Here it should be noted that we do not compare the methods for the same problem but for the problems that they can handle separately. More specifically, Jacobi spectral methods are suitable for problems over a finite domain while the other two are appropriate for infinite domains. Nevertheless, with a convenient transformation, Jacobi polynomials can be mapped onto infinite domains which allows one to compare the methods for the same problem. Approximation properties of mapped Jacobi spectral approximations can be found in [65, 67].

CHAPTER 4

APPLICATION TO THE SCHRÖDINGER EQUATION

In this chapter we show that the Schrödinger equation with a wide class of quantum mechanical potentials can indeed be converted to the WEHTP and then the pseudospectral algorithm suggested in the previous chapter is applied to approximate the eigenvalues of the problem.

4.1 The Schrödinger equation over the real line

The EHT in (1.30) has three canonical forms which are called Hermite, Laguerre and Jacobi differential equations. Accordingly, equation (1.29) with $\sigma(\xi) = 1, \xi$ and $1 - \xi^2$ will be called here the WEHTP of the first, second and the third kind, respectively.

As a first example falling into the first kind we deal with the one-dimensional Schrödinger equation in (1.27)

$$\left[-\frac{d^2}{dx^2} + V(x) \right] \Psi(x) = E\Psi(x), \quad x \in (-\infty, \infty), \quad \Psi \in L^2_\rho(-\infty, \infty) \quad (4.1)$$

over the real line for a variety of quantum mechanical potentials $V(x)$ [79]. We, first, scale the independent variable

$$\xi = cx, \quad c > 0, \quad \xi \in (-\infty, \infty), \quad (4.2)$$

by c , which transforms the Schrödinger equation (4.1) into the form

$$\left[-\frac{d^2}{d\xi^2} + c^{-2}V(c^{-1}\xi) \right] \Psi(\xi) = c^{-2}E\Psi(\xi), \quad \Psi \in L^2_\rho(-\infty, \infty) \quad (4.3)$$

whose eigenfunctions Ψ should be in the Hilbert space L^2_ρ of square integrable functions [79]. Then, proposing the solution of form

$$\Psi(\xi) = e^{-\xi^2/2}y(\xi), \quad (4.4)$$

we rewrite the Schrödinger equation (4.1) as

$$y'' - 2\xi y' + [\xi^2 - c^{-2}V(\xi/c)]y = (1 - c^{-2}E)y \quad (4.5)$$

which is an EHTP of the first kind [79, 3]. Clearly, the HPM is suitable for this problem since the unperturbed part of the last equation resembles the Hermite differential equation. This leads to the diagonalization of the matrix $\mathcal{B} = \mathcal{K} + \mathcal{V}$ in (3.33) by taking $\sigma(\xi) = 1$, $\tau(\xi) = -2\xi$, $\nu(\xi) = \xi^2 - c^{-2}V(\xi/c)$ and $r(\xi) = 1$. Therefore, the kinetic energy matrix \mathcal{K} takes the simple form

$$\mathcal{K}_{mn} = -\frac{2}{3} \begin{cases} \frac{3}{(\xi_m - \xi_n)^2} & \text{if } m \neq n \\ \xi_n^2 + N & \text{if } m = n \end{cases} \quad (4.6)$$

on replacing the coefficients σ , τ and r . Thus, the eigenvalues $-\lambda = 1 - c^{-2}E$ of (4.5), and hence the energies

$$E_n = c^2(1 + \lambda_n), \quad n = 0, 1, \dots \quad (4.7)$$

of the original equation (4.1) can be approximated by diagonalizing the symmetric matrix $\mathcal{B} = \mathcal{K} + \mathcal{V}$ where \mathcal{V} is the diagonal matrix

$$\mathcal{V}_{mn} = \nu(\xi_m)\delta_{mn} = [\xi_m^2 - c^{-2}V(\xi_m/c)]\delta_{mn} \quad (4.8)$$

composed of values of the perturbation term or modified potential at the nodal points. It is clear that the grid points ξ_m are the roots of Hermite polynomial $H_{N+1}(\xi)$ and can be computed as the eigenvalues of the symmetric tridiagonal matrix [79]

$$\mathbf{R} = \frac{1}{\sqrt{2}} \begin{bmatrix} 0 & \sqrt{1} & & & 0 \\ \sqrt{1} & 0 & \sqrt{2} & & \\ & \sqrt{2} & 0 & \ddots & \\ & & \ddots & \ddots & \sqrt{N} \\ 0 & & & \sqrt{N} & 0 \end{bmatrix} \quad (4.9)$$

in (2.17) where $A_{n-1} = \sqrt{n/2}$ and $B_n = 0$ are given in (2.37).

Notice that, an orthonormal eigenfunction $y(\xi)$ of (4.5) satisfies

$$1 = \int_{-\infty}^{\infty} y^2(\xi)e^{-\xi^2} d\xi = \int_{-\infty}^{\infty} \Psi^2(\xi)d\xi \quad (4.10)$$

on returning back to original dependent variable via (4.4). Now, replacing ξ by ξ/c in the last equation, we obtain

$$1 = \int_{-\infty}^{\infty} \Psi^2(\xi)d\xi = \int_{-\infty}^{\infty} \Psi^2(\xi/c)d(\xi/c) = \int_{-\infty}^{\infty} \frac{1}{c} \Psi^2(\xi/c)d\xi \quad (4.11)$$

which means that $\Psi(\xi/c) = \sqrt{c}\Psi(\xi)$. Thus, the values of the normalized wave function in original variable $x_m = \xi_m/c$ are given by $\Psi(x_m) = \sqrt{c}\Psi(\xi_m)$, that is,

$$\Psi^i(x_m) = \sqrt{c}\Psi^i(\xi_m) = \sqrt{c}e^{-\xi_m^2/2}y^i(\xi_m) = e^{-\xi_m^2/2} \frac{\sqrt{c(N+1)}v_N^m}{\pi^{1/4}} \frac{v_N^m}{v_0^m} u_m^i \quad (4.12)$$

where we have used (3.40) for $y^i(\xi_m)$.

On the other hand, if the potential function $V(x)$ is symmetric, i.e., $V(x) = V(-x)$, then equation (4.1) becomes reflection symmetric. For a reflection symmetric system, the potential may be regarded as a function of x^2 , i.e., $V(x^2)$, and hence the spectrum can be decomposed into two disjoint subsets containing solely the even and odd eigen-states, respectively. First of all, instead of linear scaling in (4.2), the symmetry of the potential function suggests the use of a quadratic transformation [78]

$$\xi = (cx)^2, \quad c > 0, \quad \xi \in (0, \infty), \quad (4.13)$$

which converts the Schrödinger equation (4.1) to the form

$$\left[\xi \frac{d^2}{d\xi^2} + \frac{1}{2} \frac{d}{d\xi} - \frac{1}{4c^2} V(\xi/c^2) \right] \Psi(\xi) = -\frac{E}{4c^2} \Psi(\xi) \quad (4.14)$$

where c is an optimization parameter [78]. Then, suggesting a solution of the type

$$\Psi(\xi) = \xi^p e^{-\xi/2} y(\xi), \quad p \in \mathbb{R} \quad (4.15)$$

satisfying the asymptotic boundary condition at infinity, where the factor ξ^p has been introduced to cope with the *artificial* singularity of (4.14) at $\xi = 0$. [78] Note that (4.1) is in fact regular everywhere except the ‘‘point at infinity’’, and the additional singularity of (4.14) at the origin has been resulted from using the quadratic transformation (4.13). Substitution of (4.15) into (4.14) leads to the equation that the new dependent variable $y(\xi)$ must satisfy

$$\xi y'' + (2p + \frac{1}{2} - \xi)y' + \frac{1}{4} \left[\xi - c^{-2}V(\xi/c^2) + \frac{2p(2p-1)}{\xi} \right] y = \frac{1}{4} [4p + 1 - c^{-2}E] y \quad (4.16)$$

implying that the unwelcome singularity located at the origin can be removed if p is either 0 or 1/2. Therefore, setting [78]

$$2p + \frac{1}{2} = \gamma + 1 \quad (4.17)$$

we then express (4.16) in the neater form

$$\xi y'' + (\gamma + 1 - \xi)y' + \frac{1}{4} \left[\xi - c^{-2}V(\xi/c^2) \right] y = \frac{1}{4} [2(\gamma + 1) - c^{-2}E] y \quad (4.18)$$

with $\gamma = \mp\frac{1}{2}$ [78]. Now it is clear that the solutions in (4.15) with $p = 0$ ($\gamma = -\frac{1}{2}$) and $p = \frac{1}{2}$ ($\gamma = \frac{1}{2}$) yield even and odd eigenfunctions, respectively, on returning back to the original variable x via (4.13). Accordingly the new set up of the problem in (4.18) allows us to determine symmetric (even) and antisymmetric (odd) states separately, for the two specific values of $\gamma = -\frac{1}{2}$ and $\gamma = \frac{1}{2}$ [78].

Obviously, the last equation is an EHTP of the second kind that suggests the use of Laguerre pseudospectral methods (LPM) with $\gamma = \mp\frac{1}{2}$. Therefore, the kinetic energy term in (3.31) reads as [78]

$$\mathcal{K}_{mn} = -\frac{1}{6} \begin{cases} \frac{12\sqrt{\xi_m\xi_n}}{(\xi_m - \xi_n)^2} & \text{if } m \neq n \\ 2N + \frac{1}{\xi_n}[(\gamma - \xi_n)^2 - 1] & \text{if } m = n \end{cases} \quad (4.19)$$

on replacing $\sigma(\xi) = \xi$, $\tau(\xi) = \gamma + 1 - \xi$ and $r(\xi) = 1$ and the potential energy matrix in (3.32) takes the form

$$\mathcal{V}_{mn} = v(\xi_m)\delta_{mn} = \frac{1}{4} [\xi - c^{-2}V(\xi/c^2)] \delta_{mn}. \quad (4.20)$$

The only absent data set is the nodal points ξ_m which are the roots of Laguerre polynomials $L_{N+1}^\gamma(\xi)$ of order $\gamma = \mp\frac{1}{2}$. It can be computed as the eigenvalues of the tridiagonal symmetric matrix \mathbf{R} in (2.17) with off-diagonal and diagonal entries $A_n = -\sqrt{(n+1)(n+\gamma+1)}$ and $B_n = 2n + \gamma + 1$, for $n = 0, 1, \dots, N$ respectively, which are given in (2.32).

Thus, the eigenvalues $-\lambda = \frac{1}{4} [2(\gamma + 1) - c^{-2}E]$ of the EHTP in (4.18) and, hence, the energies

$$E = c^2 [4\lambda + 2(\gamma + 1)], \quad \gamma = \mp\frac{1}{2}, \quad (4.21)$$

of the Schrödinger equation (4.1) with symmetric potentials over the real line can be approximated as the eigenvalues of the symmetric matrix $\mathcal{B} = \mathcal{K} + \mathcal{V}$ where the entries of \mathcal{K} and \mathcal{V} are specified in (4.19)-(4.20) [78]. Notice that, $\gamma = -\frac{1}{2}$ leads to the even states

$$E_{2k} = c^2 (1 + 4\lambda_k) \quad (4.22)$$

and $\gamma = \frac{1}{2}$ to the odd levels

$$E_{2k+1} = c^2 (3 + 4\lambda_k) \quad (4.23)$$

of the Schrödinger equation (4.1) [78]. Therefore, the eigenvalues of (4.1) with symmetric potentials can also be approximated by LPM which seem to be more advantageous in the numerical point of view. It is clear from the last two equations that two matrices of order N

is sufficient in the LPM whereas a matrix of order $2N$ should be diagonalized in the HPM to get the same number of approximate eigenvalues.

On the other hand, for an orthonormal eigenfunction $y(\xi)$ of (4.18) we have

$$1 = \int_0^\infty y^2(\xi) \xi^\gamma e^{-\xi} d\xi = \int_0^\infty y^2(\xi) \xi^{2p-\frac{1}{2}} e^{-\xi} d\xi = \int_0^\infty \Psi^2(\xi) \xi^{-\frac{1}{2}} d\xi. \quad (4.24)$$

upon using (4.17). However, letting $\xi = (cx)^2$ in original wave function, we obtain

$$\int_{-\infty}^\infty \Psi^2(x) dx = 2 \int_0^\infty \Psi^2(x) dx = \frac{1}{c} \int_0^\infty \Psi^2(\xi) \xi^{-\frac{1}{2}} d\xi = \frac{1}{c} \quad (4.25)$$

where we first made use of the evenness of the integrand. Thus, we must multiply the eigenfunction $\Psi(\xi)$ by \sqrt{c} so that L^2 -norm of the wave function $\Psi(x)$ in original variable x is equal to unity. Therefore, we may write

$$\Psi(x_m) = \sqrt{c} \Psi(\xi_m) = \sqrt{c} \xi_m^{p/2} e^{-\xi_m/2} y(\xi_m) = \sqrt{c} \xi_m^{\frac{1}{2}(\gamma+\frac{1}{2})} e^{-\xi_m/2} y(\xi_m). \quad (4.26)$$

Finally, using (3.40) for $y(\xi_m)$, we get

$$\Psi^i(x_m) = -\sqrt{\frac{c(N+1)(N+\gamma+1)}{\Gamma(\gamma+1)}} \frac{v_N^m}{v_0^m} \xi_m^{\frac{1}{2}(\gamma-\frac{1}{2})} e^{-\xi_m/2} u_m^i \quad (4.27)$$

Notice that, $x_m = \pm \sqrt{\xi_m}/c$. If $\gamma = -\frac{1}{2}$, then the values of the wave function at negative x values are the same as those at positive x values since eigenfunctions corresponding to even indexed eigenvalues are even functions of x . Similarly, when $\gamma = \frac{1}{2}$ the values at negative x values are the negatives of those at positive x values since eigenfunctions associated with odd indexed eigenvalues are odd functions of x .

For numerical illustrations, first, we consider an asymmetrical double well potential (ADWP)

$$V(x) = a_1 x^2 (x + a_2)(x - 1), \quad a_1 > 0, \quad 0 < a_2 < 1, \quad x \in (-\infty, \infty) \quad (4.28)$$

and a Morse potential (MP) of the form

$$V(x) = (e^{-ax} - 1)^2, \quad 0 < a < 2, \quad x \in (-\infty, \infty) \quad (4.29)$$

as typical examples of asymmetrical potentials.

Asymmetrical Double Well Potential

The ADWP has two minima located asymmetrically about the origin [73]. It is clear that the left hand limiting value of a_2 , $a_2 = 0$, does not represent a double well oscillator anymore

where the potential has an inflection point at $x = 0$ while $a_2 = 1$ corresponds to a symmetrical two well potential. These potentials are of practical interest for the protonic movement of hydrogen-bonded systems [69, 73, 89].

For the ADWP, potential energy matrix in (4.8) becomes

$$\mathcal{V}_{mn} = \left[\xi_m^2 - c^{-2} a_1 (c^{-1} \xi_m)^2 (c^{-1} \xi_m + a_2) (c^{-1} \xi_m - 1) \right] \delta_{mn}. \quad (4.30)$$

Thus the energy levels $E_n = c^2(1 + \lambda_n)$ of Schrödinger equation (4.1) with an ADWP are listed in Table 4.1, where the range of a_2 is covered by choosing $a_2 = 0.25$, $a_2 = 0.50$ and $a_2 = 0.75$.

Table 4.1: Several eigenvalues of ADWP for $a_1 = 100$, as a function of a_2 [3].

a_2	c_{opt}	N	n	E_n
0.25	4.4	69	0	-4.277 344 849 182 474 166 847 348 848 02
		69	1	7.080 517 391 364 158 656 090 710 350 21
		72	2	19.817 761 502 618 821 399 175 325 525 2
		73	3	36.209 337 296 287 706 584 558 242 608 6
	5.5	204	100	4591.756 700 061 399 687 274 143 286 5
0.50	4.4	58	0	-6.816 052 047 536 736 982 561 430 365 98
		58	1	4.675 693 930 558 290 057 997 135 848 24
		59	2	15.973 204 136 317 836 561 600 922 534 7
		62	3	31.505 546 630 519 551 260 800 075 872 1
	5.5	200	100	4549.714 975 331 339 127 227 825 899 0
0.75	4.4	57	0	-9.459 479 212 224 512 858 546 562 584 43
		57	1	0.010 560 072 717 619 621 379 801 416 92
		59	2	10.866 977 233 476 768 562 653 506 503 7
		61	3	24.888 991 175 519 381 797 134 001 071 9
	5.5	200	100	4492.595 909 516 835 740 641 080 843 6

Table 4.2: The effect of c on the accuracy E_0 of an ADWP with $a_1 = 100$ and $a_2 = 0.25$ when $N = 69$ [3].

c	E_0
1.1	-4.27
2.2	-4.277 344 849 182
3.3	-4.277 344 849 182 474 166 847 34
4.4	-4.277 344 849 182 474 166 847 348 848 02
5.5	-4.277 344 849 182 474 166 847 3
6.6	-4.277 344 84
7.7	-4.277

In all tables, n stands for the eigenvalue index, N truncation order for which the desired accuracy of the corresponding eigenvalue is obtained, and c denotes a scaling or an optimization

parameter which may be exploited to accelerate the convergence rate of the method. The effect of c on the accuracy of the ground state eigenvalue E_0 of an ADWP is displayed in Table 4.2. Note that we used quadruple precision arithmetic on a main frame computer with machine accuracy of about 32 digits, by truncating the results to 28-30 significant figures.

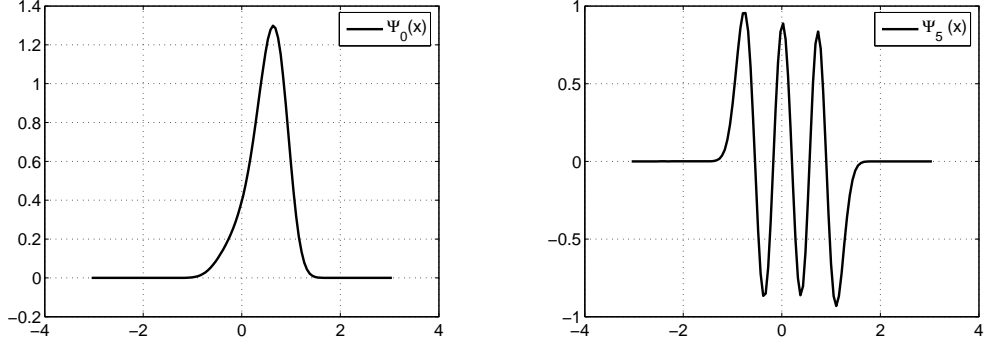


Figure 4.1: Ground state and fifth excited state eigenfunctions of the ADWP with $a_1 = 100$ and $a_2 = 0.5$.

In all figures we illustrate the normalized eigenfunctions of the corresponding problem which are obtained by using FORTRAN programming language and plotted in MATLAB. It is worth noting that, depending on the truncation size N , sometimes we obtain negative of the normalized eigenfunctions. Figure 4.1 illustrates the two eigenfunctions of the ADWP.

A Morse-Like Potential

The analytically solvable MP in (4.29) has a finite number of discrete spectral points lying between $0 < E_n < 1$ and a continuous spectrum for all $E \geq 1$ [76]. The discrete eigenvalues are expressible as

$$E_n = (n + \frac{1}{2})a \left[2 - (n + \frac{1}{2})a \right], \quad n = 0, 1, \dots, \llbracket \frac{1}{a} - \frac{1}{2} \rrbracket \quad (4.31)$$

where $\llbracket \cdot \rrbracket$ denotes the integer part of a real number. After adding potential matrix

$$\mathcal{V}_{mn} = (e^{-a\xi_m} - 1)^2 \delta_{mn} \quad (4.32)$$

to (4.6) we diagonalize the resulting algebraic system $\mathcal{B} = \mathcal{K} + \mathcal{V}$, to write down the energies of MP in Table 4.3. The lower states are obtained to the machine accuracy, but a considerable slowing down of the convergence rate occurs especially for higher energy levels that are very close to the border of the continuous spectrum, and hence, the method fails to give the desired

Table 4.4: First few nearly degenerate states of SDWP by using HPM with $N_{HPM} = 140$ and optimization parameter $c = 2.05$.

n	E_n	n	E_n
0	-149.219 456 142 190 888 029 163 966 538	8	-95.259 459 679 082 836 735 165 917 631
1	-149.219 456 142 190 888 029 163 958 974	9	-95.259 459 679 082 794 260 293 757 345
2	-135.324 512 011 840 858 579 892 393 334	10	-82.504 478 354 512 192 043 606 307 701
3	-135.324 512 011 840 858 579 887 397 260	11	-82.504 478 354 507 810 898 147 390 913
4	-121.688 950 604 621 648 258 910 138 759	12	-70.088 717 531 234 847 815 434 803 087
5	-121.688 950 604 621 648 257 347 725 677	13	-70.088 717 530 886 437 987 303 260 507
6	-108.328 000 567 332 309 875 230 475 701	14	-58.044 145 096 311 338 186 422 572 755
7	-108.328 000 567 332 309 568 103 879 703	15	-58.044 145 074 552 692 717 373 129 654

Table 4.5: First few nearly degenerate states of SDWP by using LPM with $N_{LPM} = 70$ and optimization parameter $c = 2.05$.

n	E_{2n}	E_{2n+1}
0	-149.219 456 142 190 888 029 163 966 538	-149.219 456 142 190 888 029 163 958 974
1	-135.324 512 011 840 858 579 892 393 334	-135.324 512 011 840 858 579 887 397 260
2	-121.688 950 604 621 648 258 910 138 759	-121.688 950 604 621 648 257 347 725 677
3	-108.328 000 567 332 309 875 230 475 701	-108.328 000 567 332 309 568 103 879 703
4	-95.259 459 679 082 836 735 165 917 631	-95.259 459 679 082 794 260 293 757 345
5	-82.504 478 354 512 192 043 606 307 701	-82.504 478 354 507 810 898 147 390 913
6	-70.088 717 531 234 847 815 434 803 087	-70.088 717 530 886 437 987 303 260 507
7	-58.044 145 096 311 338 186 422 572 755	-58.044 145 074 552 692 717 373 129 654

with SDWP, we list the lower energy eigenvalues in Tables 4.4 and 4.5.

Notice from the Tables 4.4 and 4.5 that, in order to calculate the first sixteen eigenvalues to 30-digits accuracy HPM needs a matrix of order $N_{HPM} = 140$. On the other hand, two matrices of dimension $N_{LPM} = 70$ is sufficient for LPM. For both methods the optimum value of the parameter c is the same ($c_{opt} = 2.05$). It is clear that the determination of the gaps requires indeed a high precision algorithm and both HPM and LPM are successful in separating the nearly degenerate states.

Table 4.6: Improvement of accuracy for E_{100} of the SDWP with respect to N , where $c = 2.6$ [3].

N_{HPM}	N_{LPM}	E_{100}
180	90	625.512 519 838 7
190	95	625.512 519 838 760 54
200	100	625.512 519 838 760 543 998
210	105	625.512 519 838 760 543 998 347 7
220	110	625.512 519 838 760 543 998 347 757 56
222	111	625.512 519 838 760 543 998 347 757 56
224	112	625.512 519 838 760 543 998 347 757 56

In addition, both methods gives not only satisfactory results for lower eigenvalues but also higher states. For instance, in Table 4.6 we illustrate the convergence rate of E_{100} as a function of the truncation size N . Observe that eigenvalue E_{100} stabilizes when $N_{HPM} = 220$ and $N_{LPM} = 110$, for HPM and LPM, respectively. In general, the accuracy of the results in all tables reported here has been checked similarly by inspecting the number of stable digits between two consecutive truncation orders.

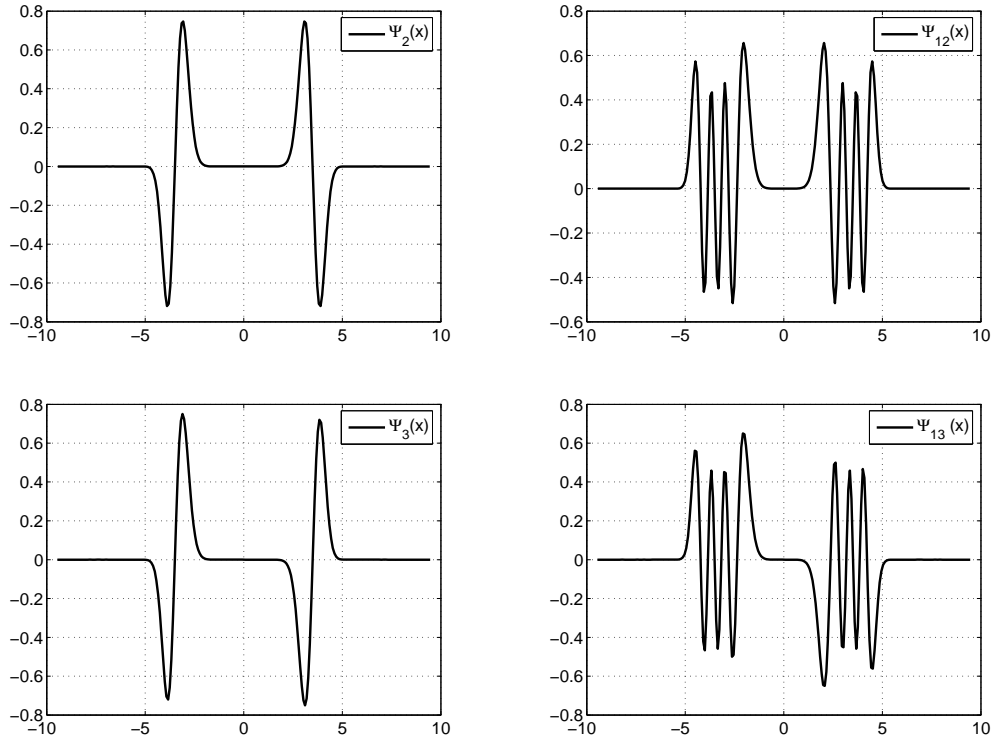


Figure 4.2: Several eigenfunctions of the SDWP by using LPM.

In Figure 4.2 we demonstrate several eigenfunctions of the SDWP by using LPM. However, it is not possible to obtain these eigenfunctions by making use of HPM because of numeric degeneracy in the lower eigenvalues. Thus, separation of even and odd states not only halves the truncation size but also leads to the correct values of the eigenfunctions at the nodes.

A Pöschl-Teller Type Potential

We, then consider the potential hole of modified Pöschl-Teller type (problem 39 of [26])

$$V(x) = -m(m + 1) \operatorname{sech}^2 x, \quad m > 0, \quad x \in (-\infty, \infty) \quad (4.34)$$

which has a finite number of discrete eigenvalues

$$E_n = -(m - n)^2, \quad n = 0, 1, \dots, \llbracket m \rrbracket \quad (4.35)$$

and a continuous spectrum for all $E > 0$ [26]. Tables 4.7 and 4.8 demonstrates the discrete states of (4.34) for $m = 10$ by using HPM and LPM, respectively.

Notice from (4.35) that for integer values of m there is always one eigenvalue lying at zero energy. As in the other algorithms, at the border of the continuous spectrum, both methods fail to give high accuracy and produce poor result correct only to two digits.

Moreover, the slowing down of convergence for the eigenvalues that are closer to zero can also be seen from Tables 4.7 and 4.8.

Table 4.7: Discrete states of modified Pöschl-Teller potential hole with $m = 10$ by using HPM where $N_{HPM} = 400$ and optimization parameter $c = 1.3$.

n	E_n	n	E_n
0	-99.999 999 999 999 999 999 999 999 999 87	5	-25.000 000 000 000 000 000 000 000 001
1	-81.000 000 000 000 000 000 000 000 004	6	-15.999 999 999 999 999 999 999 998
2	-63.999 999 999 999 999 999 999 997	7	-9.000 000 000 000 000 000 000 003
3	-49.000 000 000 000 000 000 000 000 1	8	-3.999 999 999 999 999 999 999 997
4	-35.999 999 999 999 999 999 999 999 6	9	-0.999 999 999 999 999 95

Table 4.8: Discrete states of modified Pöschl-Teller potential hole with $m = 10$ by using LPM where $N_{LPM} = 200$ and optimization parameter $c = 1.3$.

n	E_{2n}	E_{2n+1}
0	-100.000 000 000 000 000 000 000 000 002	-80.999 999 999 999 999 999 999 998
1	-63.999 999 999 999 999 999 999 998	-48.999 999 999 999 999 999 999 990
2	-35.999 999 999 999 999 999 999 999 6	-24.999 999 999 999 999 999 999 994
3	-15.999 999 999 999 999 999 999 998	-8.999 999 999 999 999 999 999 996
4	-3.999 999 999 999 999 999 999 997	-0.999 999 999 999 999 999 7

Generalized Anharmonic Oscillators

Next example is the generalized anharmonic oscillators (GAO) described by the potential

$$V(x) = x^2 + v_{2m}x^{2m}, \quad m = 2, 3, \dots, \quad v_{2m} > 0, \quad x \in (-\infty, \infty) \quad (4.36)$$

where v_{2m} is called the anharmonicity or coupling constant. It is directly related to the study of various atomic and molecular problems of quantum chemistry. Similar to the SDWP in

(4.33) several methods have consequently been applied to approximate the eigenvalues of GAO among which we can recall WKB methods [8], Rayleigh-Ritz variational method [72], Hill's determinant [24], Wronskian [23] and finite difference approaches [25].

Table 4.9: Ground state energies of the quartic oscillator $V(x) = x^2 + v_4 x^4$, as a function of v_4 [78].

v_4	E_0	N_{HPM}	N_{LPM}	c_{opt}
10^{-4}	1.000 074 986 880 200 111 122 834 155 30	15	8	1.0
10^{-2}	1.007 373 672 081 382 460 533 843 905 98	32	17	1.0
1	1.392 351 641 530 291 855 657 507 876 61	51	25	2.1
10	2.449 174 072 118 386 918 268 793 906 19	53	27	3.1
10^3	10.639 788 711 328 046 063 622 042 669 4	56	27	6.5
10^4	22.861 608 870 272 468 891 759 867 963 5	56	28	10.0
10^5	49.225 447 584 229 625 157 076 387 001 1	56	28	14.0

Typical computations for the ground state eigenvalues of the quartic and sextic oscillators as a function of the coupling constants v_4 and v_6 are displayed in Tables 4.9 and 4.10, respectively.

Table 4.10: Ground state energies of the sextic oscillator $V(x) = x^2 + v_6 x^6$, as a function of v_6 [78].

v_4	E_0	N_{HPM}	N_{LPM}	c_{opt}
10^{-4}	1.000 187 228 153 680 768 286 355 665 62	30	16	1.0
10^{-2}	1.016 741 363 754 732 031 671 817 981 51	70	34	1.8
1	1.435 624 619 003 392 315 761 272 220 54	78	38	3.2
10	2.205 723 269 595 632 351 009 973 387 17	78	40	4.2
10^3	6.492 350 132 329 671 550 549 557 845 34	80	42	7.0
10^4	11.478 798 042 264 543 961 289 816 038 6	78	40	9.5
10^5	20.375 098 656 309 660 844 567 287 513 5	81	41	12.0

In Table 4.11 we illustrate the minimum truncation size N needed to obtain the ground state energy of sextic oscillator to 30-digits accuracy. Note that the choice of optimum value c_{opt} for optimization parameter c is important. However, we don't need to determine the value of c_{opt} too sensitively. For instance, when $v_6 = 10^5$, any number between $11.5 < c_{opt} < 14.5$ can be chosen as an c_{opt} since it does not effect the truncation size considerably.

Notice that to obtain the ground state eigenvalue of quartic oscillator with $v_4 = 10^{-4}$ to 30-digits accuracy, both the HPM and LPM require only a matrix of order 15 and 8, respectively and the optimization parameter has no effect on the solution, i.e., $c_{opt} = 1$. This is because when v_4 is very small potential behaves like the harmonic oscillator. However, as v_4 grows that is, the system is in the pure anharmonic regime, the contribution of the parameter c becomes

Table 4.11: The effect of parameter c on the truncation size N to calculate the ground state eigenvalue of the sextic oscillator, as v_6 varies, within quadruple precision arithmetic.

$v_6 = 10^{-4}$			$v_6 = 1$			$v_6 = 10^5$		
c_{opt}	N_{HPM}	N_{LPM}	c_{opt}	N_{HPM}	N_{LPM}	c_{opt}	N_{HPM}	N_{LPM}
0.6	100	50	2.0	120	60	8.5	124	62
0.7	70	35	2.4	94	47	9.0	114	57
0.8	52	26	2.8	81	41	9.8	102	51
0.9	38	19	3.2	78	38	11.5	84	42
1.0	30	15	3.6	80	40	12.2	82	41
1.1	34	17	3.8	96	48	12.9	78	39
1.3	44	22	4.2	102	51	13.6	79	40
1.5	66	33	4.6	120	60	14.5	80	40

significant. For example, when $v_4 = 10^5$, c_{opt} becomes 14 for which the desired accuracy is reached with matrix sizes $N_{HPM} = 56$ and $N_{LPM} = 28$ for HPM and LPM, respectively.

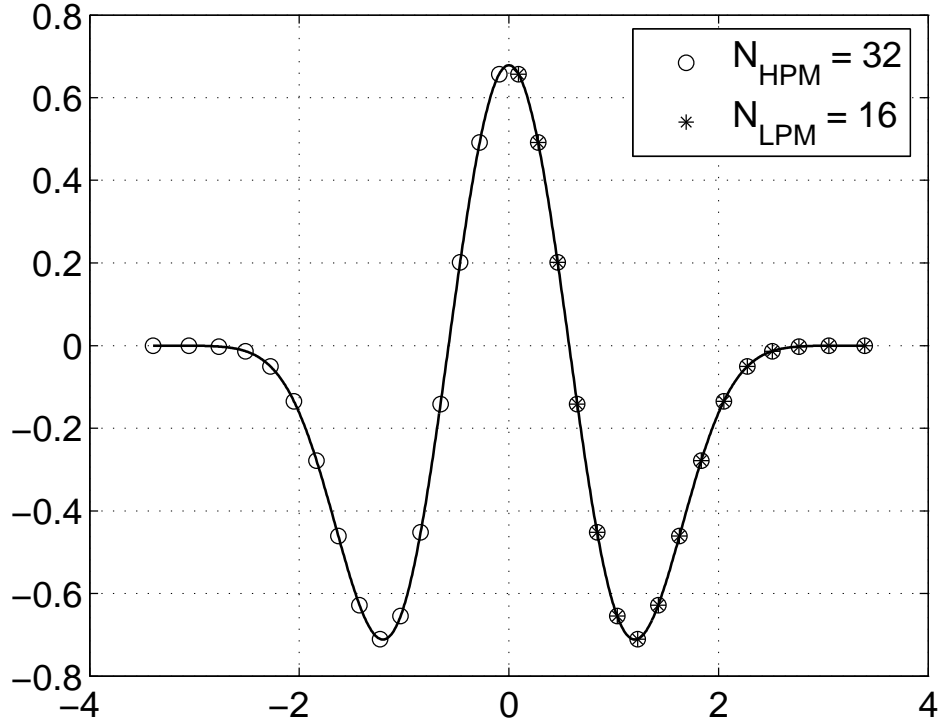


Figure 4.3: The eigenfunction $\Psi_2(x)$ of quartic anharmonic oscillator with $v_4 = 0.01$ and $c = 2.1$. Solid line is obtained by spline approximation.

Figure 4.3 shows the approximate values of the second excited state eigenfunction of quartic anharmonic oscillator with $v_4 = 0.01$ at the zeros of $H_{32}(x)$ and $L_{16}^{-1/2}(x)$. That is, the numerical values of $\Psi_2(x)$ obtained by using HPM and LPM, respectively. Notice that,

in LPM we reflect the solution with respect to y-axis to get the full picture since $\Psi_2(x)$ is even in x . The nodal sets $x_i = \xi_i/c$ and $x_i = \sqrt{\xi_i}/c$ for the HPM and LPM, respectively, coincide on the positive half line. This is not surprising because of the interrelations $H_{2n}(\xi) = (-1)^n 2^{2n} n! L_n^{-1/2}(\xi^2)$ and $H_{2n+1}(\xi) = (-1)^n 2^{2n+1} n! \xi L_n^{1/2}(\xi^2)$ between the Hermite and Laguerre polynomials. Therefore, we see that for symmetric potentials over the real line, use of the LPM in place of the HPM halves the truncation size N .

Gaussian Potential

Finally, in this section, we take into account the nonpolynomial Gaussian potential

$$V(x) = -e^{-\delta x^2}, \quad \delta > 0, \quad x \in (-\infty, \infty) \quad (4.37)$$

having a finite number of discrete eigenvalues located on the negative real axis together with a continuous spectrum over the entire positive real axis for small values of the parameter δ .

Table 4.12: Even discrete states of the Gaussian potential $V(x) = -e^{-\delta x^2}$ as δ varies.

δ	c	N_{LPM}	N_{HPM}	n	E_{2n}
0.001	0.2	200	400	0	-0.968 752 703 034 398 668 606 599 656 91
				1	-0.846 820 196 725 804 118 603 225 951 44
				2	-0.731 125 549 125 734 739 132 375 767 29
				3	-0.621 888 650 443 182 657 155 148 987 66
				4	-0.519 364 950 583 428 249 615 031 790 9
				5	-0.423 856 070 842 708 088 081 323 949 4
				6	-0.335 725 389 869 448 866 857 878 683 2
				7	-0.255 422 042 129 619 875 883 845 365 7
				8	-0.183 520 193 247 718 643 542 217 565 1
				9	-0.120 788 829 915 192 793 998 362 147 4
				10	-0.068 331 350 243 752 810 432 2
				11	-0.027 922 921 267 91
				12	-0.003 20
0.1	0.3	200	400	0	-0.721 530 628 487 107 638 685 036 884 81
				1	-0.007 927

There exist a threshold value δ_{thr} , of the parameter δ , for which the discrete negative spectral points can no longer survive and melt fully into the continuous spectrum. Taşeli and Erseçen [80] calculated the discrete states by using an appropriately scaled Hermite-Weber basis in the Rayleigh-Ritz variational picture.

Table 4.13: Odd discrete states of the Gaussian potential $V(x) = -e^{-\delta x^2}$ as δ varies.

δ	c	N_{LPM}	N_{HPM}	n	E_{2n+1}
0.001	0.2	200	400	0	-0.907 019 292 592 812 082 715 416 167 023
				1	-0.788 180 130 992 659 421 804 061 549 09
				2	-0.675 684 854 719 018 240 848 779 291 58
				3	-0.569 770 033 727 450 439 655 309 062 31
				4	-0.470 712 623 024 420 087 564 042 654 02
				5	-0.378 842 756 108 543 457 710 150 610 05
				6	-0.294 562 957 171 686 723 792 487 677 29
				7	-0.218 378 575 398 707 288 207 832 339 73
				8	-0.150 949 512 145 370 006 773 365 439 35
				9	-0.093 187 162 389 194 505 371 0045
				10	-0.046 464 865 007 120 74
				11	-0.013 208 449 9
0.1	0.3	200	400	0	-0.254 340 163 216 611 811 747 716 919

Tables 4.12 and 4.12 exhibit the fact that, as in the other methods [6, 50, 87], a noticeable slowing down of convergence is encountered for the discrete states just below zero, as δ approaches its threshold value δ_{thr} beyond which the discrete states can no longer survive.

Hence, the HPM and LPM stand for alternative numerical procedures of the problem. Evidently, we deduce from the numerical tables that $N_{HPM} = 2N_{LPM}$. Therefore, the most efficient pseudospectral discretization of the Schrödinger equation over $(-\infty, \infty)$ having a symmetric potential is not the HPM, and it is suggested by the LPM.

4.2 The Schrödinger equation over the half line

In this section we deal with the radial Schrödinger equation in M dimensions

$$\left[-\frac{d^2}{dr^2} - \frac{M-1}{r} \frac{d}{dr} + \frac{\ell(\ell+M-2)}{r^2} + V(r) \right] \mathcal{R}(r) = E\mathcal{R}(r), \quad r \in (0, \infty), \quad (4.38)$$

which is naturally defined over the half line so that $\mathcal{R}(r) \in L^2(0, \infty)$. Here, $M = 1, 2, \dots$ and $\ell = 0, 1, \dots$ are space dimension and angular quantum number, respectively, and $V(r)$ is an arbitrary continuous potential function. Notice that, the equation in (4.1), when considered over the half line, is the particular case of (4.38) with $M = 1$ and $\ell = 0$ or $\ell = 1$. Moreover, whenever $V(x)$ in (4.1) is even, the eigenvalues of (4.38) in the one dimensional case of $M = 1$ are the even and odd states of the system (4.1) if $\ell = 0$ and $\ell = 1$, respectively [74].

First introducing the scaled quadratic variable [3]

$$\xi = (cr)^2, \quad c > 0, \quad \xi \in (0, \infty) \quad (4.39)$$

we get the operational equivalences [3]

$$\frac{1}{r} \frac{d}{dr} \equiv 2c^2 \frac{d}{d\xi} \quad \text{and} \quad \frac{d^2}{dr^2} \equiv 4c^2 \xi \frac{d^2}{d\xi^2} + 2c^2 \frac{d}{d\xi} \quad (4.40)$$

for the first and second derivatives, respectively, so that the equation (4.38) reads as [3]

$$\left[-\xi \frac{d^2}{d\xi^2} - \frac{M}{2} \frac{d}{d\xi} + \frac{\ell(\ell + M - 2)}{4\xi} + \frac{1}{4c^2} V(c^{-1} \sqrt{\xi}) \right] \mathcal{R}(\xi) = \frac{E}{4c^2} \mathcal{R}(\xi). \quad (4.41)$$

Then, proposing a solution of the type

$$\mathcal{R}(\xi) = \xi^{\ell/2} e^{-\xi/2} y(\xi) \quad (4.42)$$

satisfying the asymptotic boundary condition at infinity and the regularity condition at the origin, we end up with an EHTP of the second kind ($\gamma = \ell + \frac{1}{2}M - 1$)

$$\xi y'' + \left(\ell + \frac{1}{2}M - \xi \right) y' + \frac{1}{4} \left[\xi - c^{-2} V(\sqrt{\xi}/c) \right] y = \frac{1}{4} (M + 2\ell - c^{-2} E) y \quad (4.43)$$

where $y(\xi)$ should be regular [3]. Alternatively, starting with the linear scaled variable

$$\xi = cr, \quad c > 0, \quad \xi \in (0, \infty) \quad (4.44)$$

we rewrite the equation (4.38) as

$$\left[-\frac{d^2}{d\xi^2} - \frac{M-1}{\xi} \frac{d}{d\xi} + \frac{\ell(\ell + M - 2)}{\xi^2} + \frac{V(\xi/c)}{c^2} \right] \mathcal{R}(\xi) = \frac{E}{c^2} \mathcal{R}(\xi). \quad (4.45)$$

Then, continuing with a solution of the type

$$\mathcal{R}(\xi) = \xi^\ell e^{-\xi/2} y(\xi) \quad (4.46)$$

we obtain a WEHTP of the second kind ($\gamma = 2\ell + M - 2$)

$$\xi y'' + (2\ell + M - 1 - \xi) y' - \left[\frac{1}{2}(2\ell + M - 1) + c^{-2} \xi V(\xi/c) \right] y = - \left(c^{-2} E + \frac{1}{4} \right) \xi y. \quad (4.47)$$

For the radial Schrödinger equation we have obtained two different EHTPs. The advantages and disadvantages of these formulations will be clear in the numerical examples. However, according to transformations, we expect that the former will produce good results for problems whose exact eigenfunctions decay at infinity like e^{-br^2} whereas the latter is assumed to produce good results for those behave like e^{-br} , where b is a positive constant.

The EHTPs in (4.43) and (4.47) recommend the use of LPM with the parameter values $\gamma = \ell + \frac{1}{2}M - 1$ and $\gamma = 2\ell + M - 2$, respectively. Hence, the kinetic energy matrix in (3.31) takes the form

$$\mathcal{K}_{mn} = -\frac{1}{6} \begin{cases} \frac{12\sqrt{\xi_m\xi_n}}{(\xi_m - \xi_n)^2} & \text{if } m \neq n \\ 2N + \frac{1}{\xi_n}[(\gamma - \xi_n)^2 - 1] & \text{if } m = n \end{cases} \quad (4.48)$$

when the equation (4.43) is used, i.e., $\sigma(\xi) = \xi$, $\tau(\xi) = \gamma + 1 - \xi = \ell + \frac{1}{2}M - \xi$ and $r(\xi) = 1$.

In this case the potential energy matrix becomes

$$\mathcal{V}_{mn} = \mathcal{V}_m \delta_{mn} = \frac{v(\xi_m)}{r(\xi_m)} \delta_{mn} = \frac{1}{4} [\xi_m - c^{-2}V(\sqrt{\xi_m}/c)] \delta_{mn}. \quad (4.49)$$

For the weighted EHTP in (4.47) we have

$$\mathcal{K}_{mn} = -\frac{1}{6} \begin{cases} \frac{12}{(\xi_m - \xi_n)^2} & \text{if } m \neq n \\ \frac{1}{\xi_n} \left\{ 2N + \frac{1}{\xi_n} [(\gamma - \xi_n)^2 - 1] \right\} & \text{if } m = n \end{cases} \quad (4.50)$$

on replacing the coefficients $\sigma(\xi) = r(\xi) = \xi$ and $\tau(\xi) = \gamma + 1 - \xi = 2\ell + M - 1 - \xi$. On the other hand, potential energy matrix reads as

$$\mathcal{V}_{mn} = \mathcal{V}_m \delta_{mn} = \frac{v(\xi_m)}{r(\xi_m)} \delta_{mn} = - \left[\frac{1}{2\xi_m} (\gamma + 1) + c^{-2}V(\xi_m/c) \right] \delta_{mn}. \quad (4.51)$$

The energies E_n of the original problem (4.38) can easily be obtained from both the eigenvalues $-\lambda_n^{EHTP} = \frac{1}{4} (M + 2\ell - c^{-2}E_n)$ and $-\lambda_n^{wEHTP} = -(c^{-2}E_n + \frac{1}{4})$ of (4.43) and (4.47), respectively. That is,

$$E_n = E_{n,\ell}^{(M)} = (M + 2\ell + 4\lambda_n^{EHTP})c^2 = \left(\lambda_n^{wEHTP} - \frac{1}{4} \right) c^2. \quad (4.52)$$

It can be seen from (4.43) and (4.47) that the spectrum of (4.38) remains invariant for a fixed value of the sum $2\ell + M$. Thus the eigenvalues $E_{n,\ell}^{(M)}$ in M dimension with the radial and angular quantum numbers n and ℓ , respectively, are degenerate in such a way that

$$\begin{aligned} E_{n,1}^{(2)} &\equiv E_{n,0}^{(4)} \\ E_{n,2}^{(2)} &\equiv E_{n,1}^{(4)} \equiv E_{n,0}^{(6)} \\ &\vdots \\ E_{n,\ell}^{(2)} &\equiv E_{n,\ell-1}^{(4)} \equiv E_{n,\ell-2}^{(6)} \equiv \dots \equiv E_{n,2}^{(2\ell-2)} \equiv E_{n,1}^{(2\ell)} \equiv E_{n,0}^{(2\ell+2)} \end{aligned} \quad (4.53)$$

for even values of space dimension M where $E_{n,0}^{(2)}$ is single in the system. Similarly,

$$\begin{aligned}
E_{n,1}^{(3)} &\equiv E_{n,0}^{(5)} \\
E_{n,2}^{(3)} &\equiv E_{n,1}^{(5)} \equiv E_{n,0}^{(7)} \\
&\vdots \\
E_{n,\ell}^{(3)} &\equiv E_{n,\ell-1}^{(5)} \equiv E_{n,\ell-2}^{(7)} \equiv \dots \equiv E_{n,2}^{(2\ell-1)} \equiv E_{n,1}^{(2\ell+1)} \equiv E_{n,0}^{(2\ell+3)}
\end{aligned} \tag{4.54}$$

if M is odd [74]. As it was explained above $E_{n,0}^{(3)}$ ($M = 3$, $\ell = 0$) corresponds to the odd states E_{2n+1} of (4.1) ($M = 1$, $\ell = 1$). Note also that $2\ell + M = 3$ for each case. The degeneracy in the spectrum suggests that we may consider only two- and three-dimensional cases, without any loss of generality.

On the other hand, for an orthonormal eigenfunction $y(\xi)$ of (4.43) we have

$$1 = \int_0^\infty y^2(\xi) \xi^\gamma e^{-\xi} d\xi = \int_0^\infty y^2(\xi) \xi^{\ell + \frac{M}{2} - 1} e^{-\xi} d\xi = \int_0^\infty \mathcal{R}^2(\xi) \xi^{\frac{M}{2} - 1} d\xi. \tag{4.55}$$

However, letting $\xi = (cr)^2$ in original wave function, we obtain

$$\int_0^\infty \mathcal{R}^2(r) r^{M-1} dr = \frac{1}{2c^M} \int_0^\infty \mathcal{R}^2(\xi) \xi^{\frac{M}{2} - 1} d\xi = \frac{1}{2c^M} \tag{4.56}$$

which means that $\mathcal{R}(r_m) = \sqrt{2c^M} \mathcal{R}(\xi_m)$ so that the L_p^2 -norm of the eigenfunction $\mathcal{R}(r)$ in original variable r is equal to one. Thus, we have

$$\mathcal{R}(r_m) = \sqrt{2c^M} \mathcal{R}(\xi_m) = \sqrt{2c^M} \xi_m^{\ell/2} e^{-\xi_m/2} y(\xi_m) \tag{4.57}$$

or equivalently we obtain

$$\mathcal{R}^i(r_m) = -\sqrt{\frac{2c^M(N+1)(N+\gamma+1)}{\Gamma(\gamma+1)}} \frac{v_N^m}{v_0^m} \xi_m^{\frac{\ell-1}{2}} e^{-\xi_m/2} u_m^i \tag{4.58}$$

upon using (3.40) where $\gamma = \ell + \frac{1}{2}M - 1$. Similar analysis shows that for (4.47) the values of the wave function at r_m is given by

$$\mathcal{R}^i(r_m) = -\sqrt{\frac{c^M(N+1)(N+\gamma+1)}{\Gamma(\gamma+1)}} \frac{v_N^m}{v_0^m} \xi_m^{\ell-1} e^{-\xi_m/2} u_m^i \tag{4.59}$$

where $\gamma = 2\ell + M - 2$.

For the radial Schrödinger equation, potential function $V(r)$ can be classified into two groups; the ones regular at the origin and the others that decay not faster than $1/r$ at the origin. The first group, for example, includes isotropic polynomial and Gaussian type potentials. On the

other hand, the latter includes mostly Coulomb-like potentials such as Yukawa, exponential cosine screened Coulomb potential and Hulthén screening potential. Now, we will test the two methods of this section for several potentials of these two classes. In order to avoid confusion, we call the methods as LPM and wLPM (LPM of weighted EHTP) based on the EHTPs in (4.43) and (4.47), respectively.

Isotropic Quartic Oscillator

The first example is the M-dimensional isotropic quartic oscillator

$$V(r) = r^2 + v_4 r^4, \quad v_4 > 0 \quad (4.60)$$

which is regular at $r = 0$. Taşeli and Zafer [81] expanded the wave function into a Fourier-Bessel series to solve the radial Schrödinger equation with isotropic polynomial potentials and Taşeli [74] proposed an alternative series solution to the isotropic quartic oscillator in M-dimensions. It seems that the unweighted EHTP in (4.43) is more suitable for quartic oscillator since it is even in r . Remember that we have used quadratic transformation (4.39) on the independent variable r to obtain (4.43). In Table 4.14 we present eigenvalues of isotropic quartic oscillator in 3-dimensions for some pairs of (n, l) .

Table 4.14: The energy eigenvalues $E_{n,\ell}^{(3)}$ of the potential, $V(r) = r^2 + v_4 r^4$, as a function of v_4 .

v_4	c	N_{LPM}	n	l	$E_{n,\ell}^{(3)}$
10^{-4}	1	8	0	0	3.000 374 896 936 121 098 337 846 829 9
	1	40	25	1	105.410 343 852 439 559 553 621 014 591 0
	1	66	50	5	214.674 964 990 804 822 025 570 511 216 2
	1	124	100	10	429.514 482 011 916 008 399 592 238 938
1	3	30	0	10	54.184 984 610 454 439 924 123 480 175 6
	3	65	25	5	483.022 207 413 394 709 428 608 270 729 1
	2.5	100	50	1	1062.889 853 853 655 671 834 975 735 691
	2	160	100	0	2604.432 485 714 639 307 459 405 681 55
10^4	9	30	0	0	81.903 316 953 284 467 567 471 308 555
	9	80	25	1	9253.923 499 415 499 714 821 586 373 98
	12	100	50	5	23756.533 983 690 976 108 458 514 955 3
	13	162	100	10	59302.060 313 455 515 491 294 154 604 9

It is also possible to use the weighted EHTP (4.47) for this potential. However, we observe the slowing down of convergence when compared to unweighted formulation (4.43). For instance, when $v_4 = 10^{-4}$, ground state energy $E_{0,0}^{(3)}$ is obtained to the same accuracy with

$N = 50$ and $c = 15$ when the weighted formulation is used. The reason for that the unweighted formulation imitates the true behaviour of the exact eigenfunctions good enough.

Gaussian Type Potential

Then, as a second example of the same type, we consider the Gaussian type potential [3]

$$V(r) = -e^{-\delta r^2}, \quad \delta > 0, \quad r \in (0, \infty) \quad (4.61)$$

having a finite number of negative discrete eigenvalues together with a continuous spectrum over the entire positive real axis for small values of the parameter δ .

Table 4.15: Discrete states of the Gaussian potential $V(x) = -e^{-\delta r^2}$ in three-dimension when $l = 0$ as δ varies.

δ	c	N_{wLPM}	n	$E_{n,0}^{(3)}$
0.001	1	100	0	-0.907 019 292 592 812 082 715 416 167 023
			1	-0.788 180 130 992 659 421 804 061 549 09
			2	-0.675 684 854 719 018 240 848 779 291 58
			3	-0.569 770 033 727 450 439 655 309 062 31
			4	-0.470 712 623 024 420 087 564 042 654 02
			5	-0.378 842 756 108 543 457 710 150 610 05
			6	-0.294 562 957 171 686 723 792 487 677 29
			7	-0.218 378 575 398 707 288 207 832 339 73
			8	-0.150 949 512 145 370 006 773 365 439 4
			9	-0.093 187 162 389 194 505 371 004 475 9
			10	-0.046 464 865 007 120 743 034 242 682 3
			11	-0.013 208 449 937 779 071 969 887 946 2
0.1	3	55	0	-0.254 340 163 216 611 811 747 716 919

The vibrational levels $\ell = 0$ of the Gaussian potential in three dimension $M = 3$ displayed in Table 4.15 as δ varies. Notice that the wLPM is used to approximate the eigenvalues of the problem. Nevertheless, it is also possible to use LPM instead. In this case, we obtained the same results as Table 4.13 with a slight differences in the last digits of some eigenvalues, with the same truncation sizes N and optimization parameter c . This is not surprising since $E_{n,0}^{(3)} = E_{2n+1}$ where E_{2n+1} is the odd states of (4.1). On the other hand, wLPM yields better results for higher states which are just below zero with a smaller truncation size of $N_{wLPM} = 100$. It is reported that $N_{LPM} = 200$ for the LPM of the present and the previous sections. The reason behind this difference is that the exact eigenfunction of the Gaussian potential behaves like $e^{-\sqrt{-E}r}$ which is reflected by wLPM (see (4.44) and (4.46)). However, LPM suggests a

solution decaying at infinity like $e^{-c^2 r^2/2}$ (see (4.39) and (4.42)). This somehow explains why the optimization parameter $0 < c < 1$ in LPM for the Gaussian potential (see Table 4.13).

Airy Equation

The third example of regular potentials at the origin is

$$V(r) = r, \quad r \in (0, \infty) \quad (4.62)$$

which is known as Airy equation in one dimension $M = 1$ and $\ell = 0$ or $\ell = 1$. Several eigenvalues are reported in Table 4.16 by using wLPM for illustration. On the other hand, LPM does not produce any satisfactory results. This is because the formulation in (4.41) uses even transformation on the independent variable whereas the potential in (4.62) is odd. To obtain the first eleven eigenvalues to approximately 30-digits accuracy $N_{wLPM} = 66$ is enough together with optimization parameter $c = 6$. Eigenvalues are given implicitly by $\text{Ai}(-E) = 0$ where $\text{Ai}(x)$ is the Airy function [26]. Properties of Airy functions can be found in [1, 26].

Table 4.16: Several eigenvalues of the Airy equation. The last column includes the negatives of first ten zeros of Airy function $\text{Ai}(x)$.

c	N_{wLPM}	n	$E_n = E_{n,1}^{(1)}$	Reference [1]
6	66	0	2.338 107 410 459 767 038 489 197 252 4	2.338 107 41
		1	4.087 949 444 130 970 616 636 988 701 4	4.087 949 44
		2	5.520 559 828 095 551 059 129 855 512 9	5.520 559 83
		3	6.786 708 090 071 758 998 780 246 384 5	6.786 708 09
		4	7.944 133 587 120 853 123 138 280 555 8	7.944 133 59
		5	9.022 650 853 340 980 380 158 190 839 9	9.022 650 85
		6	10.040 174 341 558 085 930 594 556 737 3	10.040 174 34
		7	11.008 524 303 733 262 893 235 439 649 6	11.008 524 30
		8	11.936 015 563 236 262 517 006 364 902 9	11.936 015 56
		9	12.828 776 752 865 757 200 406 729 407 2	12.828 776 75
6	66	10	13.691 489 035 210 717 928 295 696 779 4	
6	70	20	21.224 829 943 642 095 368 459 920 359 3	
8	110	30	27.588 387 809 882 444 811 950 364 414 1	
9	135	40	33.284 884 681 901 401 879 619 739 896 0	
10	155	50	38.528 808 305 094 248 822 629 896 744 7	
15	280	100	60.858 931 764 608 923 795 521 455 753 8	

Woods-Saxon Potential

Then, we take into account the Woods-Saxon potential defined by

$$V(r) = -\frac{50}{1+t} \left[1 - \frac{5t}{3(1+t)} \right] \quad (4.63)$$

where $t = e^{\frac{3}{5}(r-7)}$, $r \in (0, \infty)$. The problem has been considered by several authors, for instance, Zakrzewski [88] used a power series method, Lo and Shizgal [51] applied quadrature discretization method, Shao and Wang [64] considered Obrechhoff one-step method to approximate the eigenvalues of the problem.

Bound states $E_{n,0}^{(3)}$, which is equal to those $E_{n,1}^{(1)}$ of corresponding one-dimensional problem with $\ell = 1$, are presented in Table 4.17. In this case, there exist 14 discrete states before the start of continuous spectrum over the entire positive real axis. The truncation size of $N_{wLPM} = 200$ is enough to obtain the bound states of Woods-Saxon potential whereas with the same truncation order of $N_{LPM} = 200$ and an appropriately chosen parameter $c = 2$, LPM produces results correct only to 7-10 digits.

Table 4.17: Bound states $E_{n,0}^{(3)}$ of Woods-Saxon potential in 3-dimensions when $\ell = 0$ with $N_{wLPM} = 200$ and $c = 30$.

n	$E_{n,0}^{(3)} = E_{n,1}^{(1)}$
0	-49.457 788 728 082 579 670 330 458 705
1	-48.148 430 420 006 361 035 971 245 463
2	-46.290 753 954 466 087 580 582 890 228
3	-43.968 318 431 814 233 002 577 289 234
4	-41.232 607 772 180 218 479 078 577 843
5	-38.122 785 096 727 919 755 861 765 839
6	-34.672 313 205 699 650 691 489 091 456
7	-30.912 247 487 908 848 263 645 899 252
8	-26.873 448 916 059 872 462 417 069 632
9	-22.588 602 257 693 219 572 212 411 689
10	-18.094 688 282 124 421 158 056 170 233
11	-13.436 869 040 250 076 995 975 578 733
12	-8.676 081 670 736 545 808 091 349 527
13	-3.908 232 481 206 230 174 049 698 348

Figure 4.4 shows $\mathcal{R}_1(r)$ of woods-Saxon potential at $N = 120$ points for different values of the optimization parameter c . At this truncation order, the optimum c value is $c_{\text{opt}} = 45$. Notice that, c_{opt} collects the grid points to the region where the eigenfunction is nonzero. Neither the points are wasted in the region where the wavefunction is too close to zero (machine epsilon),

nor they are insufficient to recover the shape of the eigenfunction. In this way, it reduces the number N of collocation points used to get the desired accuracy. Here, for $c = 15$ and $c = 45$, the energy E_1 is correct to 20 and 27 digits respectively, but no convergence occurs when $c = 100$ for the same truncation order of $N = 120$.

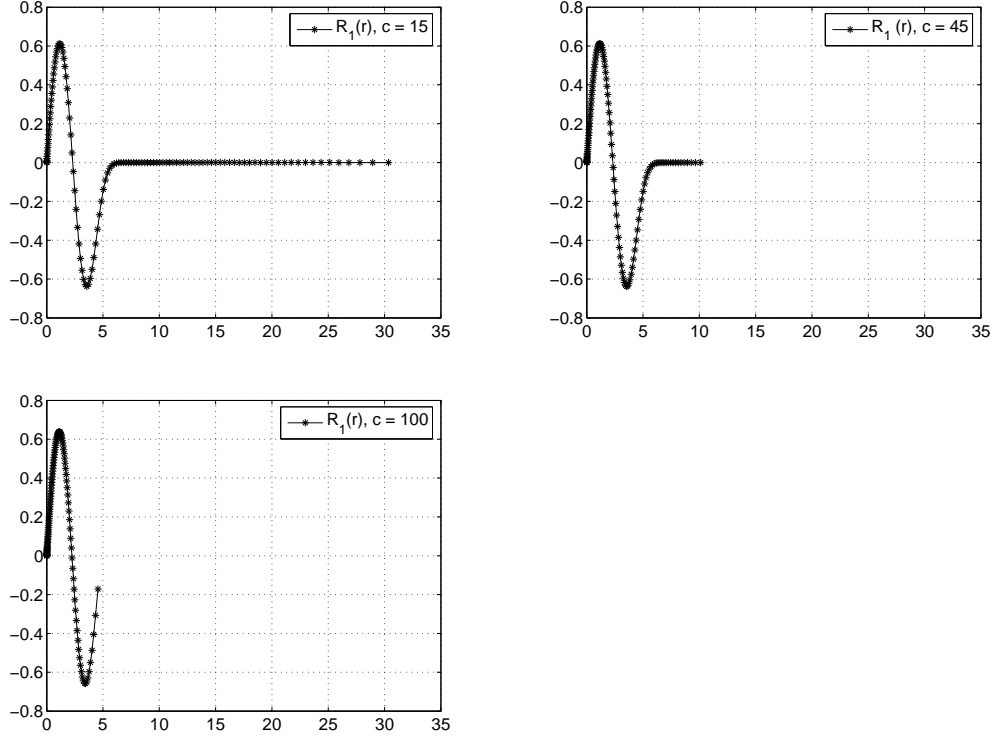


Figure 4.4: The eigenfunction $\mathcal{R}_1(r)$ of woods-Saxon potential computed by using $N = 120$ collocation points with several c values.

Exponential Cosine Partially Screened Coulomb Potential

The first example of Coulomb-like potentials is the exponential cosine partially screened Coulomb potential (ECPSC)

$$V(r) = -2ZV_{ec}(r, \lambda, \mu) - 2Z_{as} \left[\frac{1}{r} - V_{ec}(r, \lambda, \mu) \right], \quad Z > 0, \quad Z_{as} > 0 \quad (4.64)$$

where

$$V_{ec}(r, \lambda, \mu) = \frac{1}{r} e^{-\lambda r} \cos(\mu r) \quad (4.65)$$

with the two screening parameters λ and μ [46]. In particular, when $Z_{as} = 0$ the potential reduces to the exponential cosine screened Coulomb potential (ECSC). If further, $\mu = 0$ at the

same time, it is known as the Yukawa potential. On the other hand, $Z_{as} = Z$ corresponds to the pure attractive Coulomb potential which has countably many discrete states given by

$$E_{n,\ell}^{(M)} = \frac{-4Z^2}{(2n + 2\ell + M - 1)^2}, \quad n = 0, 1, \dots \quad (4.66)$$

together with the continuous spectrum over the entire positive real axis. Moreover, in this case $Z = Z_{as} = \frac{1}{2}$ leads to the hydrogen atom problem.

These potentials have been subject of several studies. Here we remember some of them; Lai [47] determined several states of ECSC within the framework of the hypervirial Padé scheme. Taşeli [75] used modified Laguerre basis for the ECSC and Yukawa potentials. Ixaru, De Meyer and Vanden Berghe [46] developed accurate, robust and safe approach for ECPSC. Ikhdaïr and Sever [42] applied a new perturbative formalism for the ECSC.

Several eigenvalues of the ECPSC potential in three-dimensions are reported in Table 4.18 for the parameter values $Z = 50$, $Z_{as} = 1$ and $\lambda = \mu = 0.025$ when $\ell = 0, 10$. The results are satisfactory, but higher levels become expensive to obtain. On the other hand, the LPM of this section does not lead any accurate results for Coulomb-like potentials being considered here. The reason for this is that the transformations do not reflect or not able to imitate the true behaviour of the exact eigenfunctions.

Table 4.18: Several states of the ECPSC potential in three-dimensions when $Z = 50$, $Z_{as} = 1$ and $\lambda = \mu = 0.025$ as ℓ varies.

c	N_{wLPM}	n	ℓ	$E_{n,\ell}^{(3)}$
90	20	0	0	-2497.550 000 612 117 302 611 999 477 0
60	20	1		-622.550 008 558 171 072 433 651 132 85
30	20	2		-275.327 819 864 885 534 764 663 309 750
8	30	10		-18.218 254 864 529 448 891 256 063 943 9
5	40	20		-3.301 293 923 744 987 946 825 007 566 6
3	62	30		-0.477 979 395 108 803 362 523 577 038 9
.5	325	50		-0.001 531 833 374 319 363 664 975 806 4
8	25	0	10	-18.214 451 240 408 459 529 166 833 611 8
8	25	1		-14.916 599 484 348 635 959 872 635 251 2
8	25	2		-12.351 299 229 508 114 531 034 516 078 1
5	40	10		-3.289 943 284 017 899 997 236 108 480 7
4	80	20		-0.460 117 420 637 774 647 219 316 169 8
.7	200	30		-0.003 368 086 423 513 184 468 068 809 9
.3	355	50		-0.000 699 631 092 664 645 508

Table 4.19 illustrates the discrete states of the ECSC as a function of the parameter μ when

Table 4.19: Bound energy eigenvalues of the ECSC potential in three-dimensions when $Z = 1$ and $\lambda = 0.05$, as μ varies. The case, $\mu = 0$ corresponds to the Yukawa potential.

μ	c	N_{wLPM}	n	ℓ	$E_{n,\ell}^{(3)}$			
0	0.6	65	0	0	-0.903 632 857 049 011 087 712 434 151 5			
			1		-0.163 542 391 590 506 248 346 978 827 5			
			2		-0.038 705 109 629 504 684 590 795 993 6			
			3		-0.006 183 319 800 322 642 969 317 900 6			
		0.08	250	4		-0.000 003 138 989 336 707 735 885		
	0.4	56	0	0	1	-0.161 480 774 075 569 219 424 205 487 2		
				1		-0.037 115 503 766 811 993 209 787 987 8		
				2		-0.005 196 117 705 143 707 930 522 382 5		
		51	0	0	2	-0.033 831 141 139 631 685 772 229 516 5		
				1		-0.003 161 743 253 742 009 905 767 896 1		
	0.05	1	55	0	0	-0.900 234 932 841 375 336 090 552 641 8		
1					-0.152 899 192 500 495 488 768 133 761 7			
2					-0.023 151 128 414 121 591 695 111 322 3			
55			0	0	1	-0.152 118 024 883 462 094 709 873 149 7		
				1		-0.021 858 659 645 112 322 497 129 462 4		
55			0	0	2	-0.019 109 758 645 475 738 881 842 814 0		

$\lambda = 0.05$. Due to the nonexistence of the contributions coming from the continuous spectrum, the method can not obtain the further states as other methods do.

Table 4.20: Several states of the pure attractive Coulomb potential in three-dimensions when $Z = Z_{as} = 1$ as ℓ varies.

c	N_{wLPM}	n	ℓ	$E_{n,\ell}^{(3)}$
2	2	0	0	-1.000 000 000 000 000 000 000 000 0
0.08	40	25		-0.001 479 289 940 828 402 366 863 905 3
0.04	80	50		-0.000 384 467 512 495 194 156 093 810 1
0.02	130	100		-0.000 098 029 604 940 692 089 010 881 3
0.3	15	0	5	-0.027 777 777 777 777 777 777 777 8
0.06	50	25		-0.001 040 582 726 326 742 976 066 597 3
0.04	80	50		-0.000 318 877 551 020 408 163 265 306 1
0.02	130	100		-0.000 088 999 644 001 423 994 304 022 8

In Table 4.20 we illustrate several eigenvalues of the pure attractive Coulomb potential when $Z = Z_{as} = 1$ for the two values $\ell = 0$ and $\ell = 5$ of ℓ . For this potential the choice of c becomes more important. Small changes in c has big effects on the accuracy.

Partially Screening Hulthén Potential

The last potential that we consider in this section is the partially screening Hulthén potential

$$V(r) = -2ZV_H(r, \lambda) - 2Z_{as} \left[\frac{1}{r} - V_H(r, \lambda) \right], \quad Z > 0, \quad Z_{as} > 0 \quad (4.67)$$

where

$$V_H(r, \lambda) = \frac{\lambda e^{-\lambda r}}{1 - e^{-\lambda r}} \quad (4.68)$$

in which λ is the screening parameter. The potential behaves as a pure Coulomb potential with charges Z and Z_{as} at small and large distances r , respectively [46]. It reduces to the Hulthén screening potential [41] when $Z_{as} = 0$ which is exactly solvable when $M = \ell = 1$ in (4.38).

In this case, bound states are given by

$$E_{n,1}^{(1)} = E_{n,0}^{(3)} = - \left(\frac{Z}{n+1} - \frac{(n+1)\lambda}{2} \right)^2, \quad n = 0, 1, \dots, k \quad (4.69)$$

where $k = \llbracket \sqrt{2Z/\lambda} \rrbracket - 1$ [26].

The partially screening Hulthén potential is considered by Ixaru, De Meyer and Vanden Berghe [46]. Hulthén potential is studied by many authors. For instance Roy [62] applied the generalized pseudospectral approach to approximate the bound states, Stubbins [70] used the generalized variational method to compute the eigenvalues for $n \leq 6$, Bayrak and Boztosun [11] used asymptotic iteration method for any ℓ state and Gönül and co-workers [33] considered the potential in the Hamiltonian hierarchy picture to approximate the eigenvalues when $\ell \neq 0$.

The wLPM works exactly as in the case of ECPS potential for the partially screening Hulthén potential. We numerically analyzed the method with the Hulthén screening potential for $Z = 50$, $Z_{as} = 1$ and $\lambda = 0.025$ and obtained the similar results for the truncation size and optimization parameter as in Table 4.19. Again the high energy levels ($n > 100$) become expensive to compute within the 30-digits accuracy.

Table 4.21 illustrates the bound states of the Hulthén screening potential in three-dimensions when $Z = 50$ and $\lambda = 0.025$, for the values of $\ell = 0, 10$. The exact eigenvalues in (4.69) for $\ell = 0$ provide the possibility of comparison with the results of the wLPM which are in excellent agreement. However, The LPM of this section is unsuccessful for this potential, too.

Table 4.21: Bound states of the Hulthén screening potential in three-dimensions when $Z = 50$ and $\lambda = 0.025$, as ℓ varies.

c	N_{wLPM}	n	ℓ	$E_{n,\ell}^{(3)}$
60	60	0	0	-2498.750 156 250 000 000 000 000 000 019 8
		1		-623.750 625 000 000 000 000 000 000 000 7
		2		-276.529 184 027 777 777 777 777 779 5
		3		-155.002 500 000 000 000 000 000 000 001 6
0.5	350	59		-0.006 944 444 444 444 444 444 444 4
		60		-0.003 268 652 579 951 625 907 014 243 5
		61		-0.000 989 203 954 214 360 041 623 309 1
		62		-0.000 037 832 262 534 6
8	30	0	10	-19.424 335 304 526 595 443 026 049 233 6
		1		-16.127 883 961 903 674 884 056 154 659 1
		2		-13.563 579 616 949 111 137 705 699 537 1
		3		-11.530 002 448 250 049 695 932 487 845 2
1	250	47		-0.015 675 609 084 845 879 723 414 562 8
		48		-0.009 260 969 711 122 159 378 014 469 3
		49		-0.004 448 783 837 632 467 073 719 998 2
		50		-0.001 188 166 258 891 096 462 375 433 4

In this section, we developed two different pseudospectral approximations LPM and wLPM of the radial Schrödinger equation. The numerical results show that the former works better mainly for isotropic polynomial oscillators whereas the latter is much more suitable for non-polynomial and Coulomb-like potentials.

4.3 The Schrödinger equation over a finite interval

In this section, we examine several regular and singular problems over a finite interval. The first one is the angular part

$$\mathcal{T}\Theta(\theta; m) = E\Theta(\theta; m), \quad \theta \in \left(-\frac{1}{2}\pi, \frac{1}{2}\pi\right), \quad \Theta(\theta; m) \in L^2\left(-\frac{1}{2}\pi, \frac{1}{2}\pi\right) \quad (4.70)$$

of the internal amplitude function described by the trigonometric Hamiltonian

$$\mathcal{T} = -\frac{1}{\cos\theta} \frac{d}{d\theta} \left(\cos\theta \frac{d}{d\theta} \right) + \frac{m^2}{\cos^2\theta} + V(\sin^2\theta), \quad m = 0, 1, \dots \quad (4.71)$$

where m stands for the magnetic quantum number. This problem results in a Schrödinger equation of a two-particle system by separation of variables under the assumption that the potential energy of the system is to be the sum of a central potential depending only on r and an angular potential which is a polynomial in even powers of $\sin\theta$ [57]. Singularities

of (4.70) as well as the unboundedness of the trigonometric potential at $\theta = \pm\frac{1}{2}\pi$ implies that the eigenfunction Θ must vanish at the boundaries. Clearly, such an eigenfunction will be in the space $L^2(-\frac{1}{2}\pi, \frac{1}{2}\pi)$ of the square integrable functions which suggests the use of the Dirichlet conditions $\Theta(\pm\frac{1}{2}\pi; m) = 0$ at the boundaries. Furthermore, the reflection symmetry of the system under the replacement of θ by $-\theta$, implies that the spectrum can be decomposed into two subsets containing solely the even and the odd states such that the corresponding eigenfunctions are even and odd functions of θ , respectively. For even states, introduction of the mapping

$$\xi = \cos 2\theta, \quad \xi \in (-1, 1) \quad (4.72)$$

which is not one-to-one, leads to the operational equivalences

$$\tan \theta \frac{d}{d\theta} \equiv -2(1 - \xi) \frac{d}{d\xi} \quad \text{and} \quad \frac{d^2}{d\theta^2} \equiv 4(1 - \xi^2) \frac{d^2}{d\xi^2} - 4\xi \frac{d}{d\xi} \quad (4.73)$$

which transforms (4.70) into the form

$$\left[(1 - \xi^2) \frac{d^2}{d\xi^2} + \left(\frac{1}{2} - \frac{3}{2}\xi \right) \frac{d}{d\xi} - \frac{m^2}{2(1 + \xi)} - \frac{1}{4}V\left(\frac{1}{2}(1 - \xi)\right) \right] \Theta_e(\xi; m) = -\frac{1}{4}E\Theta_e(\xi; m) \quad (4.74)$$

subject to the condition $\Theta_e(-1; m) = 0$ for all m , where $\Theta_e(\xi; m)$ stands for an even eigenfunction in the original variable θ when ξ is replaced by $\cos 2\theta$. Next, to avoid the use of the term proportional to $(1 + \xi)^{-1}$, we suggest an eigenfunction of the type

$$\Theta_e(\xi; m) = (1 + \xi)^{m/2} y(\xi) \quad (4.75)$$

satisfying the above boundary condition as long as the new dependent variable y remains bounded at $\xi = -1$, to arrive at the EHTP of the third kind

$$(1 - \xi^2)y'' + \left[m + \frac{1}{2} - \left(m + \frac{3}{2} \right) \xi \right] y' - \frac{1}{4}V\left(\frac{1}{2}(1 - \xi)\right)y = \frac{1}{4}[m(m + 1) - E]y \quad (4.76)$$

with $\alpha = -\frac{1}{2}$ and $\beta = m$. It is not difficult to see that the last equation yields even states of (4.70) on returning back to the original variable θ via (4.75) and (4.72). On the other hand, odd state eigenfunctions can be expressed in the form

$$\Theta_o(\theta; m) = \sin \theta \Phi(\theta; m) \quad (4.77)$$

where Φ is necessarily an even function of θ . After straightforward manipulations, we see that Φ satisfies the boundary value problem

$$\left[-\frac{d^2}{d\theta^2} + (\tan \theta - 2 \cot \theta) \frac{d}{d\theta} + \frac{m^2}{\cos^2 \theta} + 2 + V(\sin^2 \theta) \right] \Phi(\theta; m) = E\Phi(\theta; m), \quad \Phi\left(\pm\frac{1}{2}\pi\right) = 0. \quad (4.78)$$

The evenness of Φ implies the application of the same transformations (4.72) and (4.75), that is, $\xi = \cos 2\theta$ and $\Phi(\xi; m) = (1 + \xi)^{m/2}y(\xi)$ which have been used for even states. Thus, we again reach at the EHTP of the third kind

$$(1 - \xi^2)y'' + \left[m - \frac{1}{2} - \left(m + \frac{5}{2}\right)\xi\right]y' - \frac{1}{4}V\left(\frac{1}{2}(1 - \xi)\right)y = \frac{1}{4}[(m + 1)(m + 2) - E]y \quad (4.79)$$

but this time with $\alpha = \frac{1}{2}$ and $\beta = m$ which gives rise to odd states of (4.70).

It is clear from (4.76) and (4.79) that the Jacobi pseudospectral method (JPM) is suitable for the example. Hence, the diagonalization of the final matrix \mathcal{B} in (3.30) with $\sigma(\xi) = 1 - \xi^2$, $\tau(\xi) = \left[m + \frac{1}{2} - \left(m + \frac{3}{2}\right)\xi\right]$, (i.e., $\alpha = -\frac{1}{2}$ and $\beta = m$) and $r(\xi) = 1$ leads to the even states

$$E_{2n} = m(m + 1) + 4\lambda_n, \quad (4.80)$$

whereas a slightly different $\tau(\xi) = \left[m - \frac{1}{2} - \left(m + \frac{5}{2}\right)\xi\right]$, (i.e., $\alpha = \frac{1}{2}$ and $\beta = m$) with the same σ and r produces the odd states

$$E_{2n+1} = (m + 1)(m + 2) + 4\lambda_n \quad (4.81)$$

of the problem in which λ_n are the eigenvalues of the transformed equation in (4.79). For this problem it can be seen from (4.76) and (4.79) that the potential energy matrix in (3.32) reads as

$$\mathcal{V}_{mn} = \mathcal{V}_m \delta_{mn} = \frac{v(\xi_m)}{r(\xi_m)} \delta_{mn} = -\frac{1}{4}V\left(\frac{1}{2}(1 - \xi_m)\right) \delta_{mn}. \quad (4.82)$$

It is clear that an orthonormal eigenfunction $y(\xi)$ of (4.76) satisfies

$$1 = \int_{-1}^1 y^2(\xi)(1 - \xi)^{-\frac{1}{2}}(1 + \xi)^m d\xi = \int_{-1}^1 \Theta_e^2(\xi; m)(1 - \xi)^{\frac{1}{2}} d\xi \quad (4.83)$$

in which the last equality is obtained on using (4.75). On the other hand, the weight function for (4.70) is $\rho(\theta) = \cos \theta$ which can be seen by writing it in the Sturm-Liouville form. Thus, for an eigenfunction of (4.70) we write

$$\int_{-\frac{\pi}{2}}^{\frac{\pi}{2}} \Theta_e^2(\theta; m) \cos \theta d\theta = 2 \int_0^{\frac{\pi}{2}} \Theta_e^2(\theta; m) \cos \theta d\theta = \frac{1}{\sqrt{2}} \int_{-1}^1 \Theta_e^2(\xi; m)(1 - \xi)^{\frac{1}{2}} d\xi \quad (4.84)$$

where, in the last equality, we have used (4.72). Therefore, comparing the last two equations we see that the values of normalized even eigenfunctions in original variable have values at $\theta = \theta_j$ as

$$\Theta_e(\theta_j; m) = 2^{1/4} \Theta_e(\xi_j; m) \quad (4.85)$$

in terms of the normalized eigenfunctions in ξ_j which are the roots of the Jacobi polynomial $P_{N+1}^{(-\frac{1}{2}, m)}(\xi)$. Therefore, we have

$$\Theta_e^i(\theta_j; m) = 2^{1/4}(1 + \xi_j)^{m/2}y^i(\xi_j) \quad (4.86)$$

where $y(\xi_j)$ is described in (3.40). Notice that, $\theta_j = \frac{1}{2} \arccos(\xi_j) \in (0, \frac{1}{2}\pi)$. The values of an eigenfunction at negative values of θ are the same as those at positive θ values since even indexed eigenfunctions are even functions of θ .

For odd state eigenfunctions from (4.79) we get

$$1 = \int_{-1}^1 y^2(\xi)(1 - \xi)^{\frac{1}{2}}(1 + \xi)^m d\xi = \int_{-1}^1 \Phi^2(\xi; m)(1 - \xi)^{\frac{1}{2}} d\xi. \quad (4.87)$$

Writing (4.78) in the self adjoint form, we see that the weight function is $\rho(\theta) = \sin^2 \theta \cos \theta$ and we write

$$\int_{-\frac{\pi}{2}}^{\frac{\pi}{2}} \Phi^2(\theta; m)\rho(\theta)d\theta = 2 \int_0^{\frac{\pi}{2}} \Phi^2(\theta; m)\rho(\theta)d\theta = \frac{1}{2\sqrt{2}} \int_{-1}^1 \Phi^2(\xi; m)(1 - \xi)^{\frac{1}{2}} d\xi. \quad (4.88)$$

Here, first we have made use of the evenness of the integrand and then apply the transformation in (4.72). Thus, we may write

$$\Phi(\theta_j; m) = 2^{3/4}\Phi(\xi_j; m) \quad (4.89)$$

so that $\Phi(\theta; m)$ is normalized in L^2 -norm, which implies

$$\Theta_o^i(\theta_j; m) = 2^{1/4}(1 - \xi_j)^{1/2}\Phi(\xi_j; m) = 2^{1/4}(1 - \xi_j)^{1/2}(1 + \xi_j)^{m/2}y^i(\xi_j) \quad (4.90)$$

since $\Theta_o(\theta; m) = \sin \theta \Phi(\theta; m)$ and $\Phi(\xi; m) = (1 + \xi)^{m/2}y(\xi)$. It is clear that the values of eigenfunction at negative values of θ are the negatives of those at positive values of θ since odd indexed eigenfunctions are odd functions of θ .

Notice that when the potential V is a function of $\sin \theta$ instead of $\sin^2 \theta$ the system (4.70) is no more symmetric. Thus, it is not possible to separate the even and odd states. In this case, the transformations $\xi = \sin \theta$ and $\Theta(\xi; m) = (1 - \xi^2)^{m/2}y(\xi)$ takes the equation into an EHTP of the third kind

$$(1 - \xi^2)y'' - 2(m + 1)\xi y' - V(\xi)y = -[m(m + 1) + E]y \quad (4.91)$$

with $\alpha = \beta = m$. Therefore, the energy eigenvalues E_n of (4.70) with potential function of the form $V(\sin \theta)$ has the connection formula

$$E_n = \lambda_n - m(m + 1) \quad (4.92)$$

with those of (4.91). Further, the values of the normalized eigenfunctions at $\theta_j = \arcsin \xi_j$ satisfies

$$\Theta(\theta_j; m) = \Theta(\xi_j; m) = (1 - \xi_j^2)^{m/2} y(\xi_j) \quad (4.93)$$

since

$$\int_{-\pi/2}^{\pi/2} \Theta^2(\theta_j; m) \cos \theta d\theta = \int_{-1}^1 \Theta^2(\xi_j; m) d\xi = \int_{-1}^1 y^2(\xi) (1 - \xi^2)^m d\xi = 1. \quad (4.94)$$

Spheroidal Wave Equation

We now consider the angular spheroidal wave equation

$$\left\{ -\frac{d}{dt} \left[(1 - t^2) \frac{d}{dt} \right] + C^2 t^2 + \frac{m^2}{1 - t^2} \right\} \Theta(t) = E \Theta(t), \quad \Theta(t) \in L^2(-1, 1) \quad (4.95)$$

where the angular momentum m is integer and the parameter C is real, which results from the Helmholtz equation by separation of variables in the prolate spheroidal coordinates. It arises in different areas of physics such as atomic and molecular physics, light scattering in optics and the nuclear shell model [10].

Actually, the spheroidal wave equation is no more than system (4.70) with the potential function $V(\sin^2 \theta) = C^2 \sin^2 \theta$, whenever the inverse substitution

$$\theta = \arcsin t, \quad \theta \in \left(-\frac{1}{2}\pi, \frac{1}{2}\pi\right) \quad (4.96)$$

is applied to the spheroidal wave equation in (4.95). Thus, the EHTPs corresponding to the even and odd states of (4.95) are (4.76) and (4.79) with $V(\sqrt{(1 - \xi)/2}) = C^2(1 - \xi)/2$, respectively, which suggest the use of the Jacobi pseudospectral methods having the parameter sets $\{\alpha, \beta\} = \{-\frac{1}{2}, m\}$ and $\{\frac{1}{2}, m\}$.

At the numerical side of the present example we compute the eigenvalues $E_{2n}(m, C^2) = m(m + 1) + 4\lambda_n$ and $E_{2n+1}(m, C^2) = (m + 1)(m + 2) + 4\lambda_n$ of the spheroidal wave equation for several values of m and C^2 . Table 4.22 demonstrates the convergence rates of several states with $m = 0$ and $C^2 = 10$. Extremely fast convergence rate of the method for an arbitrary state number n is quite impressive [3].

Notice that $m \neq 0$ leads to an extra term proportional to $1/(1 - t^2)$ which is singular at the end points $t = \pm 1$. We also test the method with nonzero m and do not encounter any difficulties. Still we have the same convergence rate as that of $m = 0$. The results are listed in Table 4.23.

Table 4.22: Convergence rate of eigenvalues $E_{2n}(0, 10)$ of spheroidal wave equation as n varies [3].

N	$E_0(0, 10)$	N	$E_{100}(0, 10)$
5	2.305 040 10	51	10105.0
6	2.305 040 107 940	52	10105.000 433
7	2.305 040 107 940 431 6	53	10105.000 433 246 48
8	2.305 040 107 940 431 635 6	54	10105.000 433 246 482 907 99
9	2.305 040 107 940 431 635 679 732	55	10105.000 433 246 482 907 993 562 45
10	2.305 040 107 940 431 635 679 732 102 9	56	10105.000 433 246 482 907 993 562 450
11	2.305 040 107 940 431 635 679 732 102 9	57	10105.000 433 246 482 907 993 562 450
N	$E_{200}(0, 10)$	N	$E_{400}(0, 10)$
101	40205.00	201	160405.00
102	40205.000 108 8	202	160405.000 027 2
103	40205.000 108 835 777	203	160405.000 027 275 870 8
104	40205.000 108 835 777 578 646 2	204	160405.000 027 275 870 838 131 19
105	40205.000 108 835 777 578 646 209 290	205	160405.000 027 275 870 838 131 198 65
106	40205.000 108 835 777 578 646 209 290	206	160405.000 027 275 870 838 131 198 65

Separation of even and odd states halves the truncation size N , moreover, because of the fast convergence rate higher states are not expensive to compute.

On the other hand, the values of the normalized eigenfunctions $\Theta(t_j)$ are given by

$$\Theta_{e,o}^i(t_j) = \Theta_{e,o}^i(\theta_j; m) \quad (4.97)$$

where $\Theta_{e,o}^i(\theta_j; m)$ are the values of the normalized even and odd eigenfunction values of (4.70) described in (4.86) and (4.90), respectively. This is true since the back transformation in (4.96) does not change the value of L^2 norm, i.e.,

$$\|\Theta\|_{L^2(-1,1)} = \int_{-1}^1 \Theta^2(t) dt = \int_{-\frac{\pi}{2}}^{\frac{\pi}{2}} \Theta(\theta; m) \cos \theta d\theta = \|\Theta\|_{L^2_{\cos \theta}(-\frac{\pi}{2}, \frac{\pi}{2})} = 1. \quad (4.98)$$

Here, notice that $t_j = \xi_j$ are the roots of Jacobi polynomial $P_{N+1}^{(\alpha, \beta)}$ where $\{\alpha, \beta\} = \{-\frac{1}{2}, m\}$ and $\{\frac{1}{2}, m\}$ for even and odd states respectively.

A Singular Trigonometric Potential

The number of singular examples over a finite interval can be further increased. For instance, the equation

$$\left[-\frac{d^2}{d\theta^2} + \frac{\mu(\mu+1)}{2(1+\cos\theta)} + V(\cos\theta) \right] \Theta(\theta; \mu) = E\Theta(\theta; \mu), \quad \mu > 0, \quad \theta \in (-\pi, \pi) \quad (4.99)$$

whose square integrable exact solutions $\Theta(\theta; \mu)$ have been examined by Marmorino [55] and Taşeli [77] when the regular part $V(\cos\theta)$ of the total potential is zero. Both the singularities

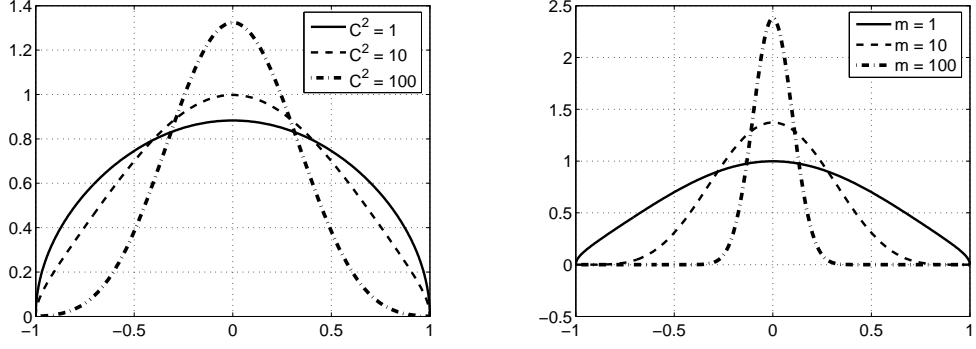


Figure 4.5: ground state eigenfunction of spheroidal wave equation while $m = 1$ and C^2 varies (left) and $C^2 = 10$ and m varies (right).

Table 4.23: Eigenvalue $E_{101}(m, C^2)$ of spheroidal wave equation while m and C^2 vary.

N_{JPM}	m	C^2	$E_{101}(m, C^2)$
55	1	1	10506.499 967 276 991 055 248 535 475 4
56		10	10510.999 940 378 439 800 892 978 058 2
59		100	10556.026 164 644 165 409 866 045 980 98
55	10	1	12432.495 990 327 209 846 178 706 135 98
56		10	12436.960 118 690 265 202 384 215 515 24
58		100	12481.622 725 202 337 649 507 963 187 86
54	100	1	40602.376 854 026 563 733 225 382 621 98
55		10	40605.768 528 171 499 786 758 027 566 70
57		100	40639.684 067 938 101 256 176 692 086 07

and reflection symmetric structure of the system suggest the use of similar procedure to that of (4.70). Thus, the mapping

$$\xi = \cos \theta, \quad \xi \in (-1, 1) \quad (4.100)$$

transforms (4.99) to the form

$$\left[(1 - \xi^2) \frac{d^2}{d\xi^2} - \xi \frac{d}{d\xi} - \frac{\mu(\mu + 1)}{2(1 + \xi)} - V(\xi) \right] \Theta_e(\xi; m) = -E \Theta_e(\xi; m) \quad (4.101)$$

subject to $\Theta_e(-1; m) = 0$ for all μ , where $\Theta_e(\xi; m)$ denotes the even wavefunction in θ . Then proposing an eigenfunction of the type

$$\Theta_e(\xi; m) = (1 + \xi)^{(\mu+1)/2} y(\xi) \quad (4.102)$$

we eliminate the term proportional to $1/(1 + \xi)$ and obtain the equation

$$(1 - \xi^2)y'' + [\mu + 1 - (\mu + 2)\xi]y' - V(\xi)y = \lambda y, \quad \lambda = \left[\frac{1}{4}(\mu + 1)^2 - E \right] \quad (4.103)$$

which is an EHTP of the third kind with $\alpha = -\frac{1}{2}$ and $\beta = \mu + \frac{1}{2}$. On the other hand, we transform the dependent variable

$$\Theta_o(\theta; \mu) = \sin \theta \Phi(\theta; \mu) \quad (4.104)$$

for the treatment of the odd eigenfunctions $\Theta_o(\theta; \mu)$, where $\Phi(\theta; \mu)$ is an even function of θ . It is not difficult to see that $\Phi(\theta; \mu)$ satisfies the differential equation

$$\left[-\frac{d^2}{d\theta^2} + -2 \cot \theta \frac{d}{d\theta} + \frac{\mu(\mu+1)}{2(1+\cos\theta)} + 1 + V(\cos\theta) \right] \Phi(\theta; m) = E\Phi(\theta; m). \quad (4.105)$$

Note from (4.104) that Φ should remain bounded at the end points $\theta = \pm\pi$. Now we may apply the similar transformations $\xi = \cos \theta$ and $\Phi(\xi; m) = (1+\xi)^{\mu/2} y(\xi)$ as in the case of even states to the last equation since Φ is an even function of θ . After a little algebra we obtain the following EHTP

$$(1-\xi^2)y'' + [\mu - (\mu+3)\xi]y' - V(\xi)y = \lambda y, \quad \lambda = \left[\frac{1}{4}(\mu+2)^2 - E \right] \quad (4.106)$$

of the third kind with $\alpha = \frac{1}{2}$, $\beta = \mu + \frac{1}{2}$.

Clearly the JPM with $\{\alpha, \beta\} = \left\{ -\frac{1}{2}, \mu + \frac{1}{2} \right\}$ and $\left\{ \frac{1}{2}, \mu + \frac{1}{2} \right\}$ is suitable for the approximation of the even $E_{2n}(\mu) = \frac{1}{4}(\mu+1)^2 + \lambda_n$ and odd $E_{2n+1}(\mu) = \frac{1}{4}(\mu+2)^2 + \lambda_n$ eigenvalues of (4.99), respectively. Some even eigenvalues of (4.99) are presented in Table 4.24 as μ varies. The method works well as in the previous example, that is convergence is fast and higher states are easy to obtain.

Table 4.24: Several even states of (4.99) as a function of μ .

N_{JPM}	μ	n	$E_{2n}(\mu)$
60	1	50	2601.506 544 844 102 970 540 696 378
108		100	10201.501 669 363 103 674 040 898 605
158		150	22801.500 746 911 100 904 849 561 472
208		200	40401.500 421 542 164 630 013 676 820
59	10	50	3080.834 369 480 225 070 383 654 415
108		100	11130.773 358 739 547 778 888 712 073
158		150	24180.760 753 055 598 522 425 650 152
208		200	42230.756 157 197 094 103 036 476 394
58	100	50	10103.093 627 746 026 304 033 361 397
108		100	22651.772 216 169 967 820 190 466 299
158		150	40201.321 434 408 931 753 789 841 423
208		200	62751.114 741 143 703 969 271 611 335

On the other hand, the normalized eigenfunctions are given by

$$\Theta(\theta_m) = 2^{-1/2}(1 - \xi_m)^{\frac{1}{2}(\alpha + \frac{1}{2})}(1 + \xi_m)^{\frac{\mu+1}{2}} y(\xi_m) \quad (4.107)$$

where $\alpha = -\frac{1}{2}$ leads to the even $\Theta_e(\theta)$ and $\alpha = \frac{1}{2}$ to the odd states $\Theta_o(\theta)$. The last formula can be obtained by a similar analysis to that of the previous problem.

Mathieu and Coffey-Evans Equations

Another example is the Schrödinger equation with a periodic potential

$$\left[-\frac{d^2}{d\zeta^2} + V(\cos 2\zeta) \right] \Theta(\zeta) = E\Theta(\zeta), \quad \zeta \in \left(-\frac{1}{2}\pi, \frac{1}{2}\pi \right) \quad (4.108)$$

subject to the conditions $\Theta\left(\pm\frac{\pi}{2}\right) = 0$ [3]. Rescaling the independent variable by putting $\theta = 2\zeta$, we obtain an equivalent equation

$$\left[-\frac{d^2}{d\theta^2} + \frac{1}{4}V(\cos \theta) \right] \Theta(\theta) = \frac{1}{4}E\Theta(\theta), \quad \Theta(\pm\pi) = 0 \quad (4.109)$$

which is the limiting case of (4.70) when $\mu \rightarrow 0^+$ with $V(\cos \theta)$ and E scaled by $\frac{1}{4}$. Therefore, the EHTPs of the third kind corresponding to even and odd states are written from (4.103) and (4.106),

$$(1 - \xi^2)y'' + (1 - 2\xi)y' - \frac{1}{4}V(\xi)y = -\lambda y, \quad E_{2n} = 1 + 4\lambda_n \quad (4.110)$$

and

$$(1 - \xi^2)y'' - 3\xi y' - \frac{1}{4}V(\xi)y = -\lambda y, \quad E_{2n+1} = 4(1 + \lambda_n) \quad (4.111)$$

respectively, where $\{\alpha, \beta\} = \{-\frac{1}{2}, \frac{1}{2}\}$ and $\{\frac{1}{2}, \frac{1}{2}\}$ [3]. In this case the normalized eigenfunctions have the expression

$$\Theta(\zeta_m) = 2^{\frac{1}{2}}\Theta(\theta_m) = 2^{\frac{1}{2}}(1 - \xi_m)^{\frac{1}{2}(\alpha + \frac{1}{2})}(1 + \xi_m)^{\frac{1}{2}} y(\xi_m) \quad (4.112)$$

where $\Theta(\theta_m)$ is given by (4.107).

Well known particular cases of (4.108) are the Mathieu and Coffey-Evans equations, if

$$V(\cos 2\zeta) = -2q \cos 2\zeta \quad (4.113)$$

and

$$V(\cos 2\zeta) = \nu^2 \sin^2 2\zeta - 2\nu \cos 2\zeta, \quad (4.114)$$

Table 4.25: Several eigenvalues of Mathieu differential equation with $q = 1$ [3].

n	N	E_n
0	9	-0.110 248 816 992 095 169 906 547 85
100	55	10201.000 049 019 607 990 453 093 342 0
200	105	40401.000 012 376 237 626 132 297 845 2
300	154	90601.000 005 518 763 797 119 609 337
400	204	160801.000 003 109 452 736 355 989 67
500	254	251001.000 001 992 031 872 519 841 33
1000	504	1002001.000 000 499 001 996 008 139 4

respectively, where q and ν denote real parameters [3]. The parameter ν in the Coffey-Evans equation controls the depth of the well potential under consideration. As ν increases, nearly degenerate triple states may occur.

From (4.110) and (4.111), several eigenvalues of the Schrödinger equation in (4.108) with Mathieu and Coffey-Evans potentials are reported in Tables 4.25 and 4.26, respectively, only for the parameter values of $q = 1$ and $\nu = 50$ in order not to overfill the content of the section with tabular material anymore. In fact, the convergence properties of the algorithm in the Mathieu case are typically the same for all q although a slight slowing down of convergence is observed as q increases [3].

Table 4.26: Triple eigenvalues of Coffey-Evans equation with $\nu = 50$, $N = 72$ [3].

n	E_n	n	E_n
0	0.000 000 000 000 000 000 000 000 0	9	947.047 491 585 860 179 592 142 658 2
1	197.968 726 516 507 291 450 189 104 5	10	1122.762 920 067 901 205 616 045 550 3
2	391.808 191 489 053 841 050 234 434 6	11	1122.762 920 071 056 526 891 891 942 2
3	391.808 191 489 053 841 832 241 249 9	12	1122.762 920 074 211 848 168 115 209 4
4	391.808 191 489 053 842 614 248 065 8	13	1293.423 567 331 707 081 413 958 872 2
5	581.377 109 231 579 654 864 715 898 8	14	1458.746 557 025 357 659 317 371 063 0
6	766.516 827 285 532 616 579 817 794 1	15	1458.746 558 472 128 708 810 534 887 1
7	766.516 827 285 535 505 431 430 237 3	16	1458.746 559 918 899 832 786 248 167 6
8	766.516 827 285 538 394 283 042 681 3	17	1618.391 008 042 643 345 932 885 816 0

A truncation order of $N = 72$ suffices to get the reported accuracy in Table 4.26 for the low lying states of the Coffey-Evans equation. It is shown that, as for the symmetric double well oscillator over the real line, the method is capable of determining the gaps between the nearly degenerate triple states of the Coffey-Evans equation successfully. Clustering of the eigenvalues does not seem to cause any difficulties in computations which is a serious troublesome for many other methods especially when high accuracy is required [50, 59, 61].

Figure 4.6 illustrates the eight eigenfunction of Coffey-Evans equation when $\nu = 50$. The

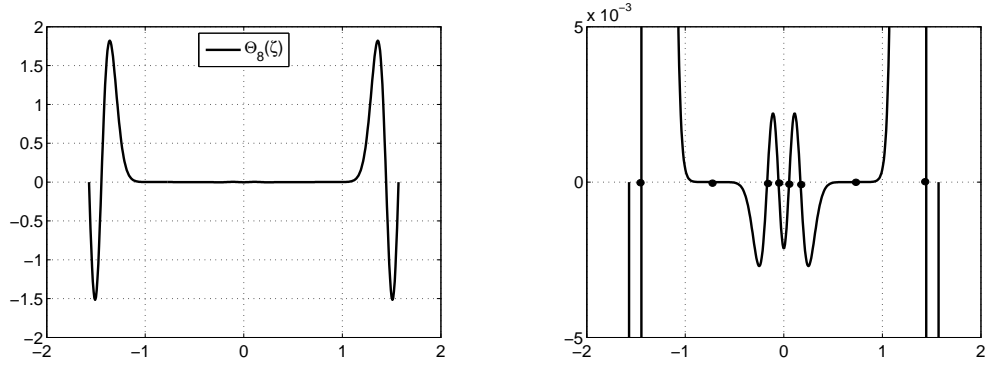


Figure 4.6: Eight eigenfunction of Coffey-Evans equation when $\nu = 50$.

well-known theory of Sturm-Liouville equations tells that it must have eight zeros in the interval $(-\pi/2, \pi/2)$. All the eighth roots are become clearer when we rescale the y-axis as shown on the right in figure 4.6.

A Weighted Example: Collatz Equation

Our final example is the Sturm-Liouville equation

$$-u'' = w(x)Eu, \quad u(\pm\pi) = 0 \quad (4.115)$$

in which $p(x) = 1$, $q(x) = 0$. When the coefficient $w(x) = 3 + \cos x$ we have a regular system [21]. On the other hand, with a small change in w , $w(x) = 1 + \cos x$ it is possible to make (4.115) into a singular one since the strictly positive term $w(x)$ becomes zero at both ends $x = \pm\pi$ of the interval.

Notice that (4.115) is reflection symmetric so that the even and odd states can be seperated. To this end, first letting $\xi = \cos x$, $\xi \in (-1, 1)$ we transform (4.115) into the form

$$(1 - \xi^2)u'' - \xi u' = -w(\xi)\lambda u, \quad y(-1) = 0. \quad (4.116)$$

Then transforming the dependent variable from y to u by setting $u(\xi) = (1 + \xi)^{1/2}y(\xi)$ we get a WEHTP of the third kind

$$(1 - \xi^2)y'' + (1 - 2\xi)y' - \frac{1}{4}y = -w(\xi)\lambda y, \quad E_{2n} = -\lambda_n \quad (4.117)$$

which is now free of boundary conditions where $u(\xi)$ is a bounded function. It is clear from the transformations that the last equation leads to the even states of (4.115). On the other

hand, the WEHTP for odd states

$$(1 - \xi^2)y'' - 3\xi y' - y = -w(\xi)\lambda y, \quad E_{2n+1} = -\lambda_n \quad (4.118)$$

maybe obtained by first letting $u(x) = \sin(x/2)v(x)$ and then using the same transformations as for the even states i.e., $\xi = \cos x$ and $v(\xi) = (1 + \xi)^{1/2}y(\xi)$ since v is an even function in x .

Table 4.27: Several eigenvalues of (4.115) when $w(x) = 3 + \cos x$.

n	N	E_n
0	7	0. 071 250 472 415 618 892 696 004 740 92
1	8	0. 330 308 392 380 975 379 846 094 175 87
2	11	0. 757 841 875 998 001 890 142 105 823 14
3	12	1. 352 122 184 297 188 245 943 947 217 42
100	80	862. 345 846 467 178 750 914 982 497
200	180	3415. 311 685 171 409 374 506 960 299
300	250	7658. 983 377 523 340 639 510 297 020

Last two equations suggest the use of weighted JPM (wJPM) with the parameter values $\{\alpha, \beta\} = \{-\frac{1}{2}, \frac{1}{2}\}$ and $\{\frac{1}{2}, \frac{1}{2}\}$ to approximate the even and odd eigenvalues of (4.115), respectively. Hence, having found the zeros of the Jacobi polynomials with the specified parameter sets $\{\alpha, \beta\}$ by means of (2.17), we diagonalize (3.30) with $\sigma(\xi) = (1 - \xi^2)$, $\tau(\xi) = 1 - 2\xi$, $r(\xi) = w(\xi)$ and $\nu(\xi) = -1/4$ to obtain the even states. On the other hand, $\tau(\xi) = -3\xi$ and $\nu(\xi) = -1$ with the same σ and r leads to the odd states. The results are tabulated in Tables 4.27 and 4.28 for two different choices of the function $w(x)$: one for

Table 4.28: Several eigenvalues of (4.115) when $w(x) = 1 + \cos x$.

n	N	E_n
0	7	0.164 502 863 913 457 323 306 759 241 01
1	10	0.929 105 845 742 146 673 250 363 316 7
2	12	2.313 475 399 952 284 033 850 395 403 8
3	13	4.315 804 581 299 675 265 350 877 278 4
100	110	3130.641 475 953 241 379 041 372 622
200	200	12429.653 986 476 452 664 627 738 315
300	290	27897.171 475 839 285 438 047 623 167

Compared to previous examples in this section, slowing down of convergence is observed especially for the singular one where $w(x) = 1 + \cos x$. However, it is still possible to reach the machine accuracy by increasing the truncation size N .

Figure 4.7 illustrates the first two normalized eigenfunctions $u_0(x)$ and $u_1(x)$ of (4.115) for

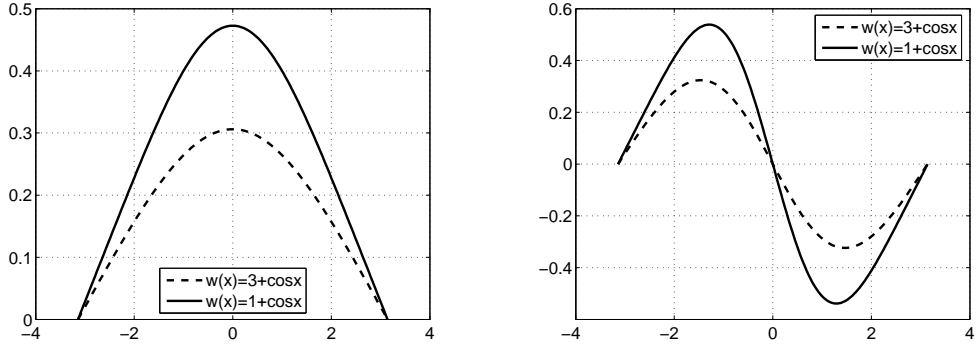


Figure 4.7: First two eigenfunctions of the Collatz equation in (4.115).

two different coefficient functions $w(x)$. In this case, we have the connection

$$u(x_m) = 2^{-\frac{1}{2}} u(\xi_m) = 2^{-\frac{1}{2}} (1 - \xi_m)^{\frac{1}{2}(\alpha + \frac{1}{2})} (1 + \xi_m)^{\frac{1}{2}} y(\xi_m) \quad (4.119)$$

between the eigenfunction $y(\xi)$ of the WEHTPs in (4.117) and (4.118) and the eigenfunction $u(x)$ of the Collatz equation in (4.115). Notice that, $\alpha = -\frac{1}{2}$ and $\alpha = \frac{1}{2}$ lead to the even and odd state eigenfunctions, respectively.

In this chapter, we have seen that a numerous Sturm-Liouville and Schrödinger equations can be converted into a WEHTP, and hence, the eigenvalues of the original problem are approximated by means of our general pseudospectral formulation. In the next chapter, we conclude the thesis by discussing the advantages and disadvantages of the proposed formulation.

CHAPTER 5

CONCLUSION

In this thesis, we present a unified pseudospectral framework based on the classical orthogonal polynomials for computing the eigenvalues of a wide class of physical problems, which can be transformed into a WEHTP. A symmetric matrix representation of the differential eigenvalue problem is formulated, where the matrix elements are determined using simple and elegant analytical expressions. In this setting the collocation points are also computed numerically to an arbitrary precision as the eigenvalues of a tridiagonal symmetric matrix.

Computer programs are written in FORTRAN programming language. We used quadruple-precision arithmetic on a main frame computer with machine accuracy of about 32 digits, by truncating the results to 25-31 significant figures.

We have taken advantage of the Hermite, Laguerre and the Jacobi pseudospectral methods for the problems over the real line, half-line and finite intervals, respectively. Numerical results verify the exponential rate of convergence, as expected theoretically for spectral methods. On the other hand, we do not have an explicit error bounds for eigenvalues for a specified truncation order N . Hence, the accuracy of the results in all tables reported here has been checked by inspecting the number of stable digits between two consecutive truncation orders [3].

The convergence of the Hermite and Laguerre pseudospectral methods may be accelerated by a scaling transformation. There exists an optimum value of the scaling factor c for which the desired accuracy is achieved at the smallest possible matrix size N . From Table 4.2 we notice that at a fixed truncation size of $N = 69$, E_0 converges to 30 digits when $c = 4.4$ whereas at the same truncation size we get merely three or four correct digits when $c = 1.1$ and $c = 7.7$, respectively. Indeed, an analytical treatment of an optimum value for c , c_{opt} , is very difficult

since it depends on several parameters such as the potential function V , quantum number n , truncation size N and even the required accuracy. For instance, the connection between c and the quantum number n is shown clearly in Tables 4.4 and 4.7. For lower states of SDWP $c_{opt} = 2.05$ whereas it is $c_{opt} = 2.6$ for E_{100} . From Table 4.2, we infer that if we require, for example, only 8 digits accuracy for E_0 we are free to choose any real number between $2.2 \leq c \leq 6.6$ which indicates how c_{opt} depends on the required accuracy. Nevertheless, such an 8 digits accuracy is obtainable when $N = 56$, $N = 28$ and $N = 69$ for $c = 2.2$, $c = 4.4$ and $c = 6.6$, respectively [3].

In fact, c_{opt} is related to a large extent the asymptotic behavior of the solution of the problem for a definite potential function in question. For example, the values of c_{opt} have been reported to be $c_{opt} = 4.4$ in Table 4.1 and $c_{opt} = 0.15$ in Table 5 for the low lying states of an ADWP in equation (4.28), and for a Gaussian type potential in (4.37), respectively. It is possible to find out that the exact eigenfunctions of an ADWP and a Gaussian potential behave like $e^{-\sqrt{a_1}|x|^3/3}$ and $e^{-\sqrt{-E}x}$ at infinity, respectively. On the other hand, the trial solutions we propose decay like $e^{-c^2x^2/2}$ for the ADWP and the Gaussian potential. This suggests that we must use an optimization parameter $c > 1$ and $0 < c < 1$ for the ADWP and the Gaussian potential, respectively, in order to imitate the true asymptotic behavior of the exact eigenfunctions. On the other hand, $c_{opt} = 1$ for the lower states of the Gaussian type potential over the half line since the alternative transformations in (4.44) and (4.46) reflects the correct behavior of the eigenfunctions.

Hence, we have seen that the optimum value of c can be estimated by inspecting the actual solution or, at least, its asymptotic behavior if it is known in advance. Otherwise it can be determined roughly by numerical experiments, i.e., by the trial and error technique. In this process, if a user takes a “bad” value for c then either the algorithm diverges or the convergence is reached at the cost of employing very high truncation orders N . In fact, a scaling transformation maps unbounded intervals onto themselves by solely rescaling the location of the points in the interval, whereas it is useless for the finite interval problems since it just shrinks or stretches the whole picture. In spite of the existence of such scaling parameter in the Hermite and Laguerre methods the convergence is still slower when compared to the Jacobi pseudospectral methods. In figure 5.1, we demonstrate how quickly the accuracy is improved as N increases in a typical Jacobi and a Laguerre method [3].

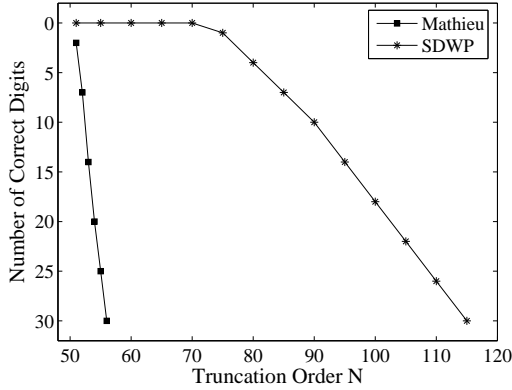


Figure 5.1: Number of correct digits versus matrix size N for E_{100} of Mathieu potential in (4.113) with $q=1$, and SDWP in (4.33) [3].

One of the most commonly used methods in literature is the Chebyshev pseudospectral method (CPM), which has two main practical advantages. First the zeros of the Chebyshev polynomials are expressible in closed form, and the second k th differentiation matrix $\mathbf{D}^{(k)}$ can be obtained from $\mathbf{D}^{(1)}$ by taking its k th power. Nevertheless, our approach enables to work automatically with the best appropriate classical orthogonal polynomial in the construction of the Lagrange interpolation, depending on the specific structure of the problem in question. For example, our algorithm suggests the use of the Jacobi polynomial $P_{N+1}^{(-\frac{1}{2}, \frac{1}{2})}(\xi)$ for the even states of the Mathieu equation.

Table 5.1: Comparison with standard CPM for the first eigenvalue of Mathieu equation with $q = 1$ [3].

N_{CPM}	E_0	N	E_0
7	-0.10	2	-0.10
14	-0.110 248 4	3	-0.110 248 4
20	-0.110 248 817 3	4	-0.110 248 816 9
27	-0.110 248 816 991 9	5	-0.110 248 816 992 08

If the standard Chebyshev method ($\alpha = \beta = -\frac{1}{2}$) were used directly to the original Mathieu equation, then the loss of accuracy is illustrated in Table 5.1. To be specific, to compute the ground state of the Mathieu equation accurate approximately to 10 digits the standard Chebyshev method requires the diagonalization of a matrix of order $N_{CPM} = 27$ whereas the same accuracy is reached at $N = 5$ in our algorithm. Actually, this is typical for all finite interval problems considered in this study [3].

Actually, in Chapter 4 we have not considered all potentials that the method can handle, instead we have exemplified some potentials that have different characteristic properties. On the other hand, this does not mean that the method works for all potentials. However, the general pseudospectral formulation proposed in this thesis is a powerful means of approximating the Schrödinger type eigenvalue problems for a wide range of potential functions as is seen from the tables.

REFERENCES

- [1] ABRAMOWITZ, M., AND STEGUN, I. A. *Handbook of Mathematical Functions with Formulas, Graphs, and Mathematical Tables*. Dover, New York, 1970.
- [2] AGUIRRE, J., AND RIVAS, J. Hermite pseudospectral approximations. An error estimate. *J. Math. Anal. Appl.* **304** (2005), 189–197.
- [3] ALICI, H., AND TAŞELI, H. Pseudospectral methods for an equation of hypergeometric type with a perturbation. *J. Comput. Appl. Math.* **234**, 1140–1152.
- [4] BAILEY, P. B. Sturm-Liouville eigenvalues via a phase function. *SIAM J. Appl. Math.* **14** (1966), 242–249.
- [5] BAILEY, P. B. Modified Prüfer transformations. *J. Comp. Phys.* **29** (1978), 306–310.
- [6] BAILEY, P. B., EVERITT, W., AND ZETTL, A. The SLEIGN2 Sturm-Liouville code. *ACM Trans. Math. Software* **21** (2001), 143–192.
- [7] BAILEY, P. B., GORDON, M. K., AND SHAMPINE, L. F. Automatic solution of the Sturm-Liouville problem. *ACM Trans. Math. Software* **4** (1978), 193–207.
- [8] BANERJEE, K. General anharmonic oscillators. *Proc. R. Soc. Lond. A* **364** (1978), 4767.
- [9] BANERJEE, K., AND BHATNAGAR, S. P. Two well oscillator. *Phys. Rev.* **D18** (1978), 4767–4769.
- [10] BARAKAT, T. ABODAYEH, K. M. A. The asymptotic iteration method for the angular spheroidal eigenvalues. *J. Phys. A: Math. Gen.* **38** (2005), 1299–1304.
- [11] BAYRAK, O. BOZTOSUN, I. Bound state solutions of the Hulthén potential by using the asymptotic iteration method. *Phys. Scr.* **76** (2007), 92–96.
- [12] BERNARDI, C., AND MADAY, Y. *Spectral Methods*. Handbook of Numerical Analysis. Elsevier, Netherlands, 1997.
- [13] BOYD, J. P. *Chebyshev and Fourier Spectral Methods*, 2nd ed. Dover Publications Inc., Mineola, NY, 2001.
- [14] CANUTO, C., HUSSAINI, M. Y., QUARTERONI, A., AND ZANG, T. A. *Spectral Methods in Fluid Dynamics*. Springer-Verlag, Berlin, 1988.
- [15] CANUTO, C., HUSSAINI, M. Y., QUARTERONI, A., AND ZANG, T. A. *Spectral Methods Fundamentals in Single Domains*. Springer, Berlin Heidelberg, 2006.
- [16] CANUTO, C., AND QUARTERONI, A. Approximation results for orthogonal polynomials in Sobolev spaces. *Math. Comp.* **38** (1982), 67–86.
- [17] CHEN, H. *The quadrature discretization method and its applications*. PhD thesis, Dept. of Math., The University of British Columbia, 1998.

- [18] CHEN, H., AND SHIZGAL, B. D. The quadrature discretization method (QDM) in the solution of the Schrödinger equation. *J. Math. Chem.* **24** (1998), 321–343.
- [19] CLOOT, A., AND WEIDEMAN, J. A. C. An adaptive algorithm for spectral computations on un-bounded domains. *J. Comput. Phys.* **102** (2) (1992), 398–406.
- [20] CODDINGTON, E. A., AND LEVINSON, N. *Theory of Ordinary Differential Equations*. McGraw-Hill, New York, 1955.
- [21] COLLATZ, L. *Differential Equations: An Introduction with Applications*. Wiley, Chichester, 1986.
- [22] DASHEN, R. F., HASSLACHER, B., AND NEVEU, A. Nonperturbative methods and extended-hadron models in field theory. i. semiclassical functional methods. *Phys. Rev.* **D10** (1974), 4114–4129.
- [23] DEMIRALP, M. A new algebraic approach to the eigenvalue problems of linear differential operators without integrations. *Int. J. Quantum Chem.* **29** (1986), 221.
- [24] DROZDOV, A. N. On the improvement of convergence of Hill determinants. *J. Phys. A: Math. Gen.* **28** (1995), 445.
- [25] FACK, V., AND VANDEN BERGHE, G. A finite difference approach for the calculation of perturbed oscillator energies. *J. Phys. A: Math. Gen.* **18** (1985), 3355.
- [26] FLÜGGE, S. *Practical Quantum Mechanics*. Classics in mathematics. Springer-Verlag, Berlin Heidelberg, 1999. Reprint of the 1994 edition.
- [27] FORNBERG, B. *A Practical Guide to Pseudospectral Methods*. Cambridge university press, 1996.
- [28] FRAZER, R. A., JONES, W. P., AND SKAN, S. W. Approximations to functions and to the solution of differential equations. *Rep. and Mem.* (1937), 1799.
- [29] FUNARO, D. *Polynomial Approximation of Differential Equations*. Lecture Notes in Physics. Springer-Verlag, Berlin Heidelberg, 1992.
- [30] GAUTSCHI, W. Orthogonal polynomials-Constructive theory and applications. *J. Comput. Appl. Math.* **12** (1985), 61–76.
- [31] GILDENER, E., AND PATRASCIOUI, A. Pseudo particle contributions to the energy spectrum of a one dimensional system. *Phys. Rev.* **D16** (1977), 423–430.
- [32] GIVOLI, D. *Numerical Methods for Problems in Infinite Domains*. Elsevier, Amsterdam, 1992.
- [33] GÖNÜL, B., ÖZER, O., CAŇCELİK, Y., AND KOÇAK, M. Hamiltonian hierarchy end the Hulthén potential. *Phys. Lett. A* **275** (2000), 238–243.
- [34] GOTTLIEB, D., AND ORSZAG, S. A. *Numerical Analysis of Spectral Methods: Theory and Applications*. SIAM, Philadelphia, 1977.
- [35] GUO, B. Y. *Spectral Methods and Their Applications*. World Scientific, River Edge, NJ, 1998.

- [36] GUO, B. Y. Error estimation of Hermite spectral method for nonlinear partial differential equations. *Math. Comp.* **68** (227) (1999), 1067–1078.
- [37] GUO, B. Y., SHEN, J., AND WANG, Z. Q. A rational approximation and its applications to differential equations on the half line. *J. Sci. Comp.* **15** (2000), 117–147.
- [38] GUO, B. Y., AND WANG, L. L. Jacobi approximations in non-uniformly Jacobi-weighted Sobolev spaces. *J. Approx. Theory* **128** (1) (2004), 1–41.
- [39] GUO, B. Y., WANG, L. L., AND WANG, Z. Q. Generalized Laguerre interpolation and pseudospectral method for unbounded domains. *SIAM J. Numer. Anal.* **43** (6) (2006), 2567–2589.
- [40] HSUE, C. S., AND CHERN, J. L. Two step approach to one-dimensional anharmonic oscillators. *Phys. Rev.* **D29** (1984), 643–647.
- [41] HULTHEN, L. *Ark. Mat. Astron. Fys. A* **28** (1942), 5.
- [42] IKHDAIR, S. M., AND SEVER, R. Bound energy for the exponential-cosine-screened Coulomb potential. *J. Math. Chem.* **41** (2007), 329–341.
- [43] IXARU, L. G. *Numerical Methods for Differential Equations and Applications*. Reidel, 1984.
- [44] IXARU, L. G., DE MEYER, H., AND VANDEN BERGHE, G. CP methods for the Schrödinger equation, revisited. *J. Comput. Appl. Math.* **88** (1997), 289–314.
- [45] IXARU, L. G., DE MEYER, H., AND VANDEN BERGHE, G. SLCPM12 - A program for solving regular Sturm-Liouville problems. *Comput. Phys. Commun.* **118** (1999), 259–277.
- [46] IXARU, L. G., DE MEYER, H., AND VANDEN BERGHE, G. Highly accurate eigenvalues for the distorted coulomb potential. *Phys. Rev. E* **61** (2000), 3151–3159.
- [47] LAI, C. S. Energies of the exponential cosine screened Coulomb potential. *Phys. Rev. A* **26** (1982), 2245–2248.
- [48] LANCZOS, C. Trigonometric interpolation of empirical and analytical functions. *J. Math. Phys.* **17** (1938), 123–199.
- [49] LEDOUX, V. *Study of Special Algorithms for Solving Sturm-Liouville and Schrödinger Equations*. PhD thesis, Dept. of Appl. Math. and Comp. Sci., Ghent University, 2007.
- [50] LEDOUX, V., VAN DAELE, M., AND VANDEN BERGHE, G. MATSLISE: A matlab package for the numerical solution of sturm-liouville and schrödinger equations. *ACM Trans. Math. Software* **31** (2005), 532–554.
- [51] LO, J. Q. W., AND SHIZGAL, B. D. Pseudospectral methods of solution of the Schrödinger equation. *J. Math. Chem.* **44** (2008), 787–801.
- [52] MADAY, Y., PERNAUD-THOMAS, B., AND VANDEVEN, H. Reappraisal of Laguerre type spectral methods. *La Recherche Aérospatiale* **6** (1985), 13–35.
- [53] MARLETTA, M., AND PRYCE, J. D. A new multipurpose software package for Schrödinger and Sturm-Liouville computations. *Comput. Phys. Commun.* **62** (1991), 42–52.

- [54] MARLETTA, M., AND PRYCE, J. D. Automatic solution of Sturm-Liouville problems using the Pruess method. *J. Comput. Appl. Math.* **39** (1992), 57–78.
- [55] MARMORINO, M. G. Exactly soluble hamiltonian with a squared cotangent potential. *J. Math. Chem.* **32** (2002), 303–308.
- [56] MASTROIANNI, G., AND OCCORSIO, D. Lagrange interpolation at Laguerre zeros in some weighted uniform spaces. *Acta Math. Hungar.* **91** (1-2) (2001), 27–52.
- [57] MICHAEL, G. On a singular Sturm-Liouville problem in the theory of molecular vibrations. *J. Math. Chem.* **39** (2006), 523–539.
- [58] NIKIFOROV, A., AND UVAROV, V. *Special Functions of Mathematical Physics*. Birkhäuser, Basel, 1988.
- [59] PRUESS, S., AND FULTON, C. T. Mathematical software for Sturm-Liouville problems. *ACM Trans. Math. Software* **19** (1993), 360–376.
- [60] PRYCE, J. D. Error control of phase function shooting methods for Sturm-Liouville problems. *IMA J. Numer. Anal.* **6** (1986), 103–123.
- [61] PRYCE, J. D. *Numerical Solution of Sturm-Liouville Problems*. Oxford University Press, 1993.
- [62] ROY, A. K. The generalized pseudospectral approach to the bound states of the Hulthén and the Yukawa potentials. *Pramana - J. Phys.* **65** (2005), 1–15.
- [63] SANCHES, A. M., AND BEJARANO, J. D. Quantum anharmonic symmetrical oscillators using elliptic functions. *J. Phys. A: Math. Gen.* **19** (1986), 887–902.
- [64] SHAO, H., AND WANG, Z. Arbitrarily precise numerical solutions of the one-dimensional Schrödinger equation. *Comput. Phys. Commun.* **180** (2009), 1–7.
- [65] SHEN, J., AND LI-LIAN, W. Error analysis for mapped Jacobi spectral methods. *J. Sci. Comput.* **24**, 2 (2005), 183–218.
- [66] SHEN, J., AND LI-LIAN, W. Analysis of a spectral-Galerkin approximation to the Helmholtz equation in exterior domains. *SIAM J. Numer. Anal.* **45** (2007), 1954–1978.
- [67] SHEN, J., AND LI-LIAN, W. Some recent advances on spectral methods for unbounded domains. *Commun. Comput. Phys.* **5** (2009), 195–241.
- [68] SHIZGAL, B. D. Eigenvalues of the Lorentz Fokker-Planck equation. *J. Chem. Phys.* **70** (1979), 1948–1951.
- [69] SOMORJAI, R. L., AND HORNIG, D. F. Double-minimum potentials in hydrogen-bonded solids. *J. Chem. Phys.* **36** (1962), 1980–1987.
- [70] STUBBINS, C. Bound states of the Hulthén and the Yukawa potentials. *Phys. Rev. A* **48** (1993), 220–227.
- [71] TAŞELI, H. A unification of recursions for functions of the hypergeometric type. to be submitted.
- [72] TAŞELI, H. The influence of the boundedness of polynomial potentials on the spectrum of the Schrödinger equation. *J. Comp. Phys.* **101** (1992), 252–255.

- [73] TAŞELI, H. Accurate lower and upper bounds of the energy spectrum for the asymmetrical two-well potentials. *Int. J. Quantum Chem.* **60** (1996), 641–648.
- [74] TAŞELI, H. An alternative series solution to the isotropic quartic oscillator in n dimensions. *J. Math. Chem.* **20** (1996), 235–245.
- [75] TAŞELI, H. Modified laguerre basis for hydrogen-like systems. *Int. J. Quantum Chem.* **63** (1997), 949–959.
- [76] TAŞELI, H. Accurate numerical bounds for the spectral points of the singular Sturm-Liouville problems over $-\infty < x < \infty$. *J. Comput. Appl. Math.* **115** (2000), 535–546.
- [77] TAŞELI, H. Exact analytical solutions of the hamiltonian with a squared tangent potential. *J. Math. Chem.* **34** (2003), 243–251.
- [78] TAŞELI, H., AND ALICI, H. The Laguerre pseudospectral method for the reflection symmetric Hamiltonians on the real line. *J. Math. Chem.* **41**, 407–416.
- [79] TAŞELI, H., AND ALICI, H. The scaled Hermite-Weber basis in the spectral and pseudospectral pictures. *J. Math. Chem.* **38** (2005), 367–378.
- [80] TAŞELI, H., AND ERSEÇEN, M. B. The scaled Hermite-Weber basis still highly competitive. *J. Math. Chem.* **34** (2003), 177–188.
- [81] TAŞELI, H., AND ZAFER, A. Bessel basis with applications: N-dimensional isotropic polynomial oscillators. *Int. J. Quant. Chem* **63** (1997), 935–947.
- [82] TREFETHEN, L. N. *Spectral Methods in MATLAB*. SIAM, Philadelphia, 2000.
- [83] VILLADSEN, J. V., AND STEWART, W. E. Solution of boundary value problems by orthogonal collocation. *Chem. Eng. Sci.* **22** (1967), 1483–1501.
- [84] WANG, Z. Q., AND GUO, B. Y. A rational approximation and its applications to nonlinear partial differential equations on the whole line. *J. Math. Anal. Appl.* **274** (1) (2002), 374–403.
- [85] WITWIT, M. R. M. Finite difference calculations of eigenvalues of various potentials. *J. Phys. A: Math. Gen.* **25** (1992), 503–512.
- [86] XU, C. L., AND GUO, B. Y. Mixed Laguerre-Legendre spectral method for incompressible flow in an infinite strip. *Adv. Comput. Math.* **16** (1) (2002), 77–96.
- [87] ZAFER, A., AND TAŞELI, H. Two-sided eigenvalue bounds for the spherically symmetric states of the Schrödinger equation. *J. Comput. Appl. Math.* **95** (1998), 83–100.
- [88] ZAKRZEWSKI, A. J. Highly precise solutions of the one-dimensional Schrödinger equation with an arbitrary potential. *Comput. Phys. Commun.* **175** (2006), 397–403.
- [89] ZNOJIL, M. Asymmetric anharmonic oscillators in the Hill determinant picture. *J. Math. Phys.* **33** (1992), 213–221.

VITAE

PERSONAL INFORMATION

Surname, Name: ALICI, Haydar

Nationality: Turkish (T.C.)

Date and Place of Birth: 28 June 1979, Hekimhan

Marital Status: Married

Phone: +90 505 242 63 08

email: haydaralici@gmail.com

EDUCATION

Degree	Institution	Year of Graduation
MS	METU, Mathematics	2003
BS	METU, Mathematics Education	2001
Double Major	METU, Mathematics	2001
High School	Cumhuriyet High Sc., İskenderun	1996

WORK EXPERIENCE

Year	Place	Enrollment
2005-2010	METU Mathematics	Research Assistant
2002-2005	Turkish Ministry of eEducation	High School Mathematics Teacher

FOREIGN LANGUAGE

English

PARTICIPATED SCIENTIFIC ACTIVITIES

1. 13th International Congress on Computational and Applied Mathematics, July 7-11, 2008, University of Ghent, Ghent, BELGIUM.

REFEREEING FOR INTERNATIONAL JOURNALS

1. Journal of Computational and Applied Mathematics

PUBLICATIONS

3. **H. Alici** and H. Taşeli *Pseudospectral methods for the equation of hypergeometric type with a perturbation*, J. Comput. Appl. Math., **234**, (2010) 1140-1152.
2. H. Taşeli and **H. Alici**, *The Laguerre pseudospectral method for the reflection symmetric Hamiltonians on the real line*, J. Math. Chem., **41**, (2007) 407-416.
1. H. Taşeli and **H. Alici**, *The scaled Hermite-Weber basis in the spectral and pseudospectral pictures*, J. Math. Chem., **38**, (2005) 367-378.

FIELD OF STUDY

Major Field: Computational Methods for ODE's and Eigenvalue Problems, Spectral Methods, Special Functions and Their Applications.